A PREDICTION MODEL FOR THE RESIDUAL FLEXURAL STRENGTH OF CORRODED REINFORCED CONCRETE BEAMS

BY

SYED AYUB AZHER

A Thesis Presented to the
DEANSHIP OF GRADUATE STUDIES

KING FAHD UNIVERSITY OF PETROLEUM & MINERALS

DHAHRAN, SAUDI ARABIA

In Partial Fulfillment of the
Requirements for the Degree of

MASTER OF SCIENCE

In

CIVIL ENGINEERING

JANUARY 2005

KING FAHD UNIVERSITY OF PETROLEUM AND MINERALS
DHAHRAN 31261, SAUDI ARABIA

DEANSHIP OF GRADUATE STUDIES

This thesis, written by **SYED AYUB AZHER** under the direction of his Thesis Advisor and approved by his Thesis Committee, has been presented to and accepted by the Dean of Graduate Studies, in partial fulfillment of the requirements for the degree of **MASTER OF SCIENCE IN CIVIL ENGINEERING**.

Thesis Committee

Prof. Abul Kalam Azad (Advisor)

Dr. Shamsad Ahmad (Co-Advisor)

Dr. Mohammed Maslehuddin (Member)

Dr. Ahmad Saad Al-Gahtani (Member)

Dr. Mesfer M. Al-Zahrani (Member)

Prof. Hamad I. Al-Abdul Wahhab
Department Chairman

Dr. Mohammad Abdul Aziz Al-Ohali
Dean of Graduate Studies

١٤٢٧/٥/١٠

Date 22-6-2005

DEDICATED TO

MY BELOVED PARENTS

AND

MY BROTHERS & SISTERS

ACKNOWLEDGEMENTS

First and foremost, I thank Allah (subhana wa taala) for bestowing me with health, patience, and knowledge to complete this work.

Acknowledgement is due to the King Fahd University of Petroleum & Minerals for the support given to this research through its excellent facilities and for granting me the opportunity to pursue my graduate studies with financial support.

I acknowledge, with deep gratitude and appreciation, the inspiration, encouragement, valuable time and guidance given to me by Prof. Abul Kalam Azad, who served as my major advisor. Thereafter, I am deeply indebted and grateful to Dr. Shamsad Ahmad, my co-advisor, and Dr. Mohammed Maslehuddin, my committee member, for their extensive guidance, continuous support, and personal involvement in all phases of this research. I am also grateful to my other committee members, Dr. Ahmad S. Al-Gahtani and Dr. Mesfer M. Al-Zahrani for their constructive guidance, valuable advices and cooperation.

I also acknowledge the sincere and untiring efforts of Engr. Mukarram Khan and Mr. Hassan Zakaria who assisted me during all stages of my experiments and also helped me in preparing the experimental set-up utilized in this study. Thanks are due to the laboratory personnel Mr. Omer, Mr. Essa, Mr. Saleem and Mr. Abdullah for their substantial assistance in the experimental work, and also to the department secretaries, Mr. Mumtaz and Mr. Solano for their help and assistance. I am also indebted to the department chairman, H.I.Al-Abdul Wahhab and other faculty members for their support.

Special thanks are due to my brothers Syed Idris Azher and Syed Ilyas Azher for their moral support and encouragement throughout this work.

Thanks are due to my senior colleagues at the University, Mr. Shameem, Mr. Ibrahim, Mr. Rizwan, Mr. Ghulam Akber and Mr. Imran Ali for their valuable advices. I would also like to thank my friends Baqtiar, Imran Quadri, Siraj, Yousuf, Khaja, Mazher, Kashif, Anees, Ismail, Jaffer, Muqtader, Asif, Obaid, Farooq, Rizwan, Riyaz, Sajeed and Atif for their friendly environment during my graduate studies. Special thanks are due to Hameed, Qaiyum and Adil, who were always there to help me in my work and my sincere appreciation is due to all other North Compound friends who provided wonderful company and some memories that will last a lifetime.

Finally, I would like to express my deepest gratitude to my mother, father, sisters, younger brother, and all other relatives, for their emotional and moral support throughout my academic career and also for their love, patience, encouragement and prayers.

TABLE OF CONTENTS

LIST OF TABLES

LIST OF FIGURES

THESIS ABSTRACT

Full Name	**SYED AYUB AZHER**
Title of Study	**A PREDICTION MODEL FOR THE RESIDUAL FLEXURAL STRENGTH OF CORRODED REINFORCED CONCRETE BEAMS**
Major Field	**CIVIL ENGINEERING (Structures)**
Date of Degree	**JANUARY 2005**

Corrosion of reinforcing steel and subsequent concrete deterioration is a major problem faced by the construction industry. However, limited work is available for the estimation of the flexural strength of corrosion-damaged members. In the present work, an effort has been made to develop a model to predict the residual flexural strength of reinforced concrete beams with varying degree of reinforcement corrosion. The experimental variables included: applied corrosion current density, corrosion duration, rebar diameter, and thickness of concrete cover.

A total of 56 reinforced concrete beams (150 × 150 × 1100 mm) were cast using a common concrete mix, out of which 8 beams were earmarked as control beams that were not subjected to corrosion and the remaining 48 beams were subjected to corrosion by impressed current. All beams were tested in flexure in four-point bend tests. After testing in flexure the beams were broken to retrieve the reinforcing steel. The steel bars were cleaned to assess the gravimetric weight loss.

Results indicate that the product of corrosion current density and corrosion period, $I_{corr}T$, is the most significant factor affecting the flexural strength of a corroded beam. Diameter of steel bars also affected the extent of metal loss for identical $I_{corr}T$. The effect of cover thickness on the loss of flexural strength was found to be insignificant for a given beam at constant $I_{corr}T$.

Based on the experimental data, a two-step approach to predict the residual flexural strength of a corroded beam has been proposed. The usefulness of the proposed approach for prediction of the residual strength of the corroded beams for which information on corrosion current density, corrosion period, beam cross-section, and strength of materials are available has been illustrated through numerical examples. The accuracy of the proposed method has been verified by comparing the results with the test data available in the literature.

MASTER OF SCIENCE
KING FAHD UNIVERSITY OF PETROLEUM AND MINERALS
Dhahran, Saudi Arabia
January 2005

THESIS ABSTRACT (ARABIC)

ملخص الرسالة

الاسم : سيد ايوب أزهر

عنوان الرسالة: تقدير مقاومةالآنحناء المتبقية للجسور الخرسانية المسلحة المعرضة للصدا

التخصص : الهندسة المدنية " الانشاءات"

تاريخ التخرج : يناير 2005

يعتبر صدأ حديد التسليح والتدهور في الخرسانة الناتج عنها المشكلة الرئيسية التي تواجه صناعة التشييد, وبالرغم من ذلك لايوجد الى الأن طريقة تحليلة لتقدير مقاومة النحناء المتبقية للجسور المعرضة للضرر . في هذه الدراسة , تم تطوير طريقة لتقدير مقاومة الانحناء المتبقية للجسور الخرسانية المسلحة المعلرضة لدرجات مختلفة من صدا حديد التسليح.العناصر المتغيرة في هذه الدراسة هي : كثافة تيار الصدأ المستخدم , مدة الصدأ, قطر حديد التسليح وسمك غطاء الخرسانة.

تم صب 56 جسر من الخرسانة المسلحة الشائعة والابعاد 150 x150x 1100 مم , 8 من هذه الجسور لم يحدث فيها صدأ , وماتبقى من الجسور تعرضت لصدأ حديد التسليح بعد التعرض للتيار الانودي .كل الجسور أختبرت لمقاومة الأنحناء وبعد الأختيار تم تكسير الجسور لاستخراج حديد التسليح وتنضيفه وقياس فقد الوزن فيه.

أوضحت النتائج أن حاصل ضرب كثافة تيار الصدأ ومدة الصدأ تؤثر بشكل رئيسي على مقاومة الانحناء للجسور المعرضة للصدأ, كذلك تبين أن عند قيمة محددة $I_{corr}T$ قطر حديد التسليح يؤثر مباشرة على مدى الفقد في المعدن .كذلك عند ثبات قيمة $I_{corr}T$ تبين أن سمك غطاء الخرسانة لايؤثر على نقصان مقاومة الانحناء.

باستخدام النتائج المعملية , ثم استخدام طريقة من خطوتين لتقدير مقاومة الانحناء للجسور المعرضة للصدأ. وتم اثبات فائدة هذه الطريقة المقترحة وذلك باستخدام الامثلة العددية وذلك لتقدير مقاومة الانحناء للجسور المعرضة للأنحناء وذلك بتوفر معلومات عن كثافة تيار الصدأ , مدة الصدأ,أبعاد قطاع الجسر وكذلك مقاومة المواد .وقد تم التحقق من دقة الطريقة بمقارنة النتائج مع النتائج المتوفرة في دراسات أخرى.

MASTER OF SCIENCE
KING FAHD UNIVERSITY OF PETROLEUM AND MINERALS
Dhahran, Saudi Arabia
January 2005

CHAPTER 1

INTRODUCTION

1.1 REINFORCEMENT CORROSION

Corrosion of reinforcing steel is one of the major worldwide deterioration problems for the reinforced concrete structures. Research in Saudi Arabia and elsewhere in the Middle East indicated that the service life of buildings in the Arabian Gulf is between 10 and 15 years [1]. What could be more frustrating than knowing that corrosion was, in some cases, so severe that concrete damage occurred even before the completion of construction? [2]. While corrosion of the reinforcing steel is not the sole cause of all structural deficiencies, it is a significant contributor and has therefore become a matter of major concern.

The highly alkaline environment of good quality concrete leads to the formation of a passive film on the surface of the embedded steel, which protects it from corrosion [3]. In addition, well-consolidated and properly cured concrete with a low water to cement ratio has a low permeability, which minimizes

diffusion of corrosion inducing agents, such as chloride, carbon dioxide, moisture, etc. to the steel surface. Further, the high electrical resistivity of concrete restricts the rate of corrosion by reducing the flow of hydroxyl ions from anode to cathode. At the outset, it must be mentioned that, usually in a properly designed, constructed and maintained structure, there should be little or no problem of steel corrosion during its design life.

Not all reinforced concrete structures have performed so well, however. There have been numerous examples of durability problems arising from the corrosion of reinforcement in concrete structures, mostly due to poor quality concrete, inadequate cover over reinforcing steel, chlorides in the concrete or combinations of these. These have led to various forms of corrosion-induced damages, such as cracking and spalling and reduction in the load carrying capacity of the structure. Indeed the scale of the problem can be judged from the size of the concrete repair industry and the number of technical publications on the topic [4].

The basic problem associated with the deterioration of reinforced concrete, due to reinforcement corrosion is not that the reinforcing steel itself is reduced in mechanical strength, but rather that the products of corrosion exert stresses within the concrete which cannot be supported by the limited tensile strength of concrete, and therefore it cracks. This leads to a weakening of the bond and anchorage between concrete and reinforcement which directly affects the serviceability and ultimate strength of concrete elements within a structure [5].

When reinforcement corrodes, the strength of a reinforced concrete member is undermined in several ways. Since corrosion products have a greater volume than the parent steel, internal tensile stresses will develop in the concrete at the steel/concrete interface. As a result, the surrounding concrete cracks and will eventually spall away, as corrosion advances. In addition, under tensile stresses developed during corrosion, existing fine cracks and microcracks in the surrounding concrete tend to enlarge and form a network of interconnected cracks, providing increased ionic transport between the surface of the concrete and the surface of the reinforcing steel, effectively promoting the corrosion process. Crack growth decreases concrete stiffness and tensile strength, while the formation of a network of cracks increases concrete permeability. Thus, the structural integrity of the reinforced concrete member is increasingly compromised as cracking progresses. As steel is progressively lost to corrosion, its cross-section is reduced, causing a decrease in the member's flexural strength. Furthermore, as corrosion advances, the bond between the steel and surrounding concrete is weakened, adversely affecting the load transfer between the two materials. To ensure that reinforced concrete members perform according to their design capacity and design service life, it is important to prevent or delay the occurance of corrosion [6].

1.2 EFFECT OF REINFORCEMENT CORROSION ON THE PERFORMANCE OF REINFORCED CONCRETE ELEMENTS

Where concrete has been carbonated to the depth of the steel reinforcement and a small but uniform amount of moisture is present, the steel is likely to corrode fairly uniformly. This deterioration is often indicated by fine hairline cracking parallel to the direction of the reinforcement throughout the length of the structural component. Fortunately, because corrosion is fairly uniform, cracking of the concrete cover in normally reinforced or pre-tensioned solid components usually occurs before the steel becomes excessively weak, so giving early visual warning of the deterioration.

If chlorides are concentrated near the surface of the steel or access of water and oxygen is restricted to a single location on the steel, severe pitting corrosion may occur. This reduces considerably the cross-sectional area of the bars at these locations, while the remainder of the bar may be left uncorroded. Structural cracking, or honeycombing, can also create conditions favorable to pitting corrosion by allowing the localized ingress of aggressive agents.

The reinforcement corrosion and concrete spalling cause a reduction in the ultimate capacity, and more significantly, a reduction in the stiffness and ductility of the R.C section primarily due to the loss or breakdown of the steel/concrete

interfacial bond. The effects of reinforcement corrosion on the behavior of reinforced concrete elements are schematically shown in Fig.1.1.

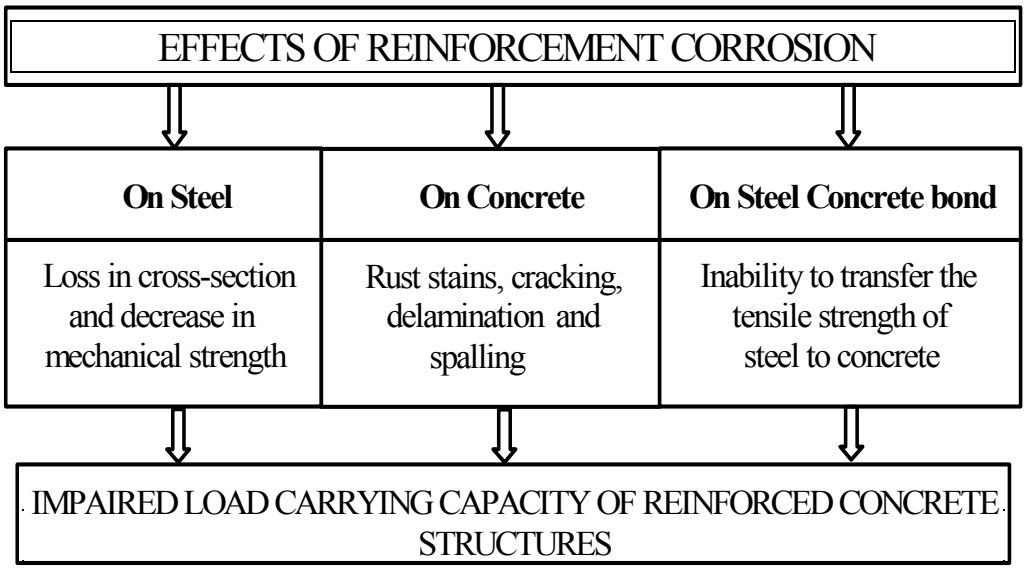

Figure 1.1:Effects of Reinforcement Corrosion on Reinforced Concrete Structures.

1.3 EFFECT OF REINFORCEMENT CORROSION ON THE FLEXURAL STRENGTH

The moment carrying capacity of an under-reinforced concrete beam depends mostly on the strength of reinforcing steels. Therefore, loss of reinforcing steel may be critical and requires special consideration. Corrosion is one of the important causes of steel area loss. General corrosion, which appears uniformly along the length of the reinforcement, will have two effects: firstly, it will reduce the cross-sectional area of the steel and secondly, it will create local discontinuities in the steel surface. These effects reduce the tensile capacity of the steel in proportion to the loss of its cross-sectional area. Thus, as the corrosion products increase, the cross-sectional area of steel decreases and hence, in addition to the bond deterioration, the ultimate moment capacity of structure also decreases, till the area of the steel becomes so small that it can no longer withstand the load and hence results in the collapse of the structure.

Reinforcement corrosion does not affect the mechanical strength of the bars to a large extent, but the corrosion products exert stresses within the concrete, which cannot be supported by the limited tensile strength of concrete resulting in the formation of cracks along the reinforcing bars. These cracks weaken the bond and anchorage between steel and concrete, because of which stresses in concrete cannot be transferred to the reinforcing steel properly thus affecting the serviceability and ultimate strength of concrete elements.

1.4 NEED FOR THIS RESEARCH

Considerable research has been devoted to corrosion of reinforcement in reinforced concrete dealing with various issues related to corrosion process, its initiation and damaging effects. The prediction of time-to-corrosion cracking has been of great interest that resulted in the proposition of several predictive models for which several references [7-10] can be cited as representative samples of work.

In view of the fact that corrosion damage reduces the strength of a reinforced concrete element, it is of great interest to develop models that can be used to predict the residual strength of a corroding concrete element. The need for the prediction of the residual strength often arises to determine the underlying safety of the corroding members and to decide when the repair or strengthening must be undertaken without any further delay. Of the limited research that has been carried out in this area, mention can be made of the works of Mangat and Elgarf [11], Rodriguez et al. [12] and Tachibana et al. [13].

This study aims to make a contribution in the area of the prediction of the residual strength of corroded reinforced concrete beam type members by suggesting a predictive model that has been developed through an extended experimental work on beams that were subjected to different degrees of corrosion damage.

1.5 SCOPE AND OBJECTIVES

The scope of this work was limited to the development of an approach for the prediction of residual strength of concrete beams using test data generated on 56 beams that were subjected to different degrees of corrosion damage.

The general objective of this work is to study the effect of reinforcement corrosion on the residual strength of reinforced concrete beams. The specific objectives are as follows:

i. To study the effect of corrosion on the residual strength of reinforced concrete beams,

ii. To assess the cumulative effect of cover to reinforcement and rebar diameter, on reinforcement corrosion, and

iii. To develop an approach for predicting the residual flexural strength of concrete beams subjected to reinforcement corrosion, based on a damage model that includes the corrosion rate and other applicable parameters, such as rebar diameter and cover thickness.

CHAPTER 2

LITERATURE REVIEW

2.1 NATURE OF REINFORCEMENT CORROSION IN CONCRETE

A few metals, notably gold, silver, and platinum, occur naturally; whereas engineering metals, including steel, must be derived from their ores by smelting. Ores are natural oxides, sulfides, and other reaction products of metals with the environment. During smelting, a metal absorbs the energy required to free it from the ore; and, this energy is retained within the metal after it is recovered. However, this metallic state is unstable, because the metal tends to rid itself of this extra energy by recombining with the environment to revert to its more stable and natural state as an ore. This reversion process is known as oxidation or, more specifically, corrosion.

A refined metal such as iron or steel has a natural tendency to corrode and thereby return to the stable state that it exists in nature, as iron ore (typically iron oxide, Fe_2O_3). The rate of steel corrosion depends on its composition, grain structure, and the presence of entrained stress from fabrication. It also depends on the nature of the surrounding environment, such as the availability of water, oxygen, and ionic species, pH, and temperature.

The pore solution in a hydrated cement is highly alkaline (pH between 13 and 13.8). Thus, on ordinary reinforcing steel embedded in alkaline concrete a thin protective oxide film (the passive film) is formed spontaneously. This passive film is only a few nanometers thick and is composed of more or less hydrated iron oxides with varying quantities of Fe^{2+} and Fe^{3+}. The protective action of the passive film is immune to mechanical damage of the steel surface. As long as this film is not disturbed, it will keep the steel passive and protected from corrosion. When a concrete structure is exposed to deicing salts, salt splashes, salt spray, or seawater, chloride ions from these sources diffuse slowly into the concrete, mostly through the pores in the hydrated cement paste. The chloride ions eventually reach the steel and then accumulate to beyond a certain concentration level, at which the protective film is destroyed and the steel begins to corrode, when oxygen and moisture are present at the steel-concrete interface [14-15].

2.2 MECHANISM OF REINFORCEMENT CORROSION

Corrosion of steel embedded in concrete is an electrochemical process in which the energy gained in the conversion of iron ore to steel is released in the form of a direct current. The surface of the corroding steel functions as a mixed electrode that is a composite of anodes and cathodes electrically connected through the body of steel itself, upon which coupled anodic and cathodic reactions take place. At anodic sites, metal atoms pass into solution as positively charged steel ions (anodic oxidation) and the excess of electrons flow through the metal to cathodic sites where an electron acceptor like dissolved oxygen is available to consume them (cathodic reduction) to generate hydroxyl ions. The electrons created in the anodic reaction must be consumed elsewhere on the steel surface establishing the corrosion reaction. The process is completed by the transport of ions through the aqueous phase, leading to the formation of corrosion products at the anodic sites either soluble (e.g. ferrous chloride) or insoluble (e.g. rust, hydrated ferric oxide). The different behavior of the same metal at two different locations is usually found due to variations arising either during the manufacturing, storage or transportation stages. Anodic and cathodic sites are electronically connected as they exist on the same rod and they are ionically connected by concrete pore water functioning as an aqueous medium, i.e., a complex electrolyte. Therefore, a reinforcement micro-corrosion cell is formed as shown in Figure 2.1.

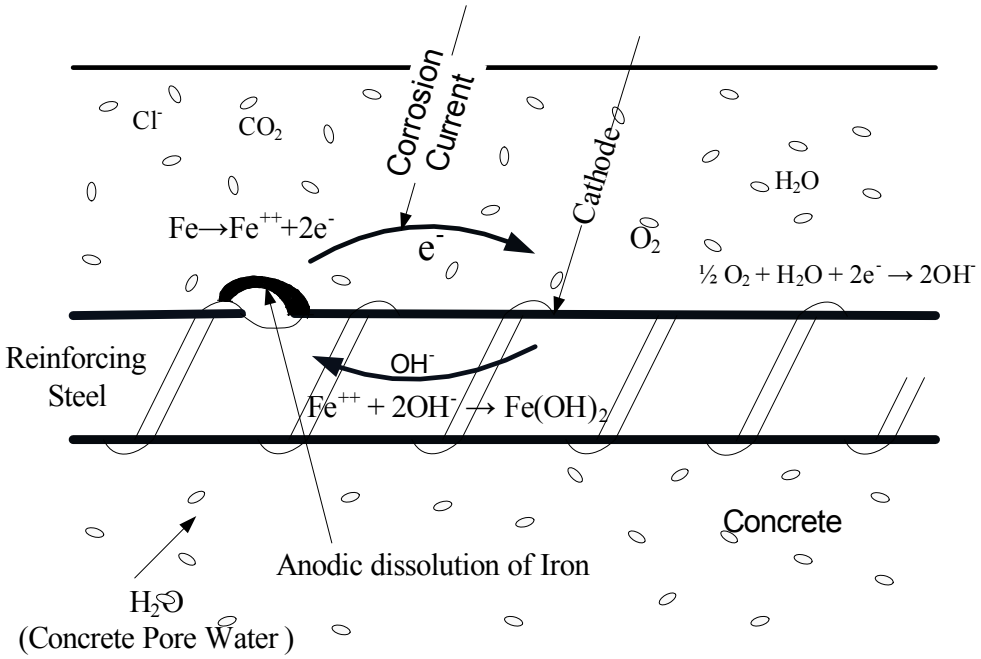

Figure 2.1: Micro-corrosion cell formation in reinforced concrete.

The voltage difference created between the anodic and cathodic sites causes the electrons to flow from the anodic areas, via the body of the reinforcing steel, to the cathodic locations.

The electrochemical mechanism of corrosion of steel can be summarized with the following three partial processes

i. the oxidation of iron (anodic process) that liberates electrons in the metallic phase and gives rise to the formation of iron ions ($Fe \rightarrow Fe^{++} + 2e^{-}$);

ii. the reduction of oxygen (cathodic process) that consumes the electrons produced at the anodic site and produces hydroxyl ions ($O_2 + 2H_2O + 4e^- \rightarrow 4OH^-$) i.e. electrons (coming from anodic sites) + water + oxygen → hydroxyl ions; and

iii. finally, the OH^- ions flow back to the anode through the concrete to complete the circuit. The rate of this transfer depends on the temperature, moisture content, ionic concentration and electrical resistivity of concrete. The OH^- ions at the anode then combine with the Fe^{++} cation to form a fairly soluble ferrous hydroxide, $Fe(OH)_2$:

$Fe^{++} + 2OH^- \rightarrow Fe(OH)_2$

If sufficient oxygen is available, this product can be further oxidized to form insoluble hydrated red rust. This rust can have a volume 2 to 14 times that of the parent iron from which it is formed. The rust product can exert tensile stresses of the order of 4000 psi, which is 10 times the tensile strength of concrete. This excessive pressure causes the concrete cover to crack leading to its eventual spalling at an advanced stage of the corrosion process leading to a reduction in the cross-sectional area of the structural member. In addition to loss of cover concrete, a reinforced concrete member may suffer structural damage due to the loss of bond between steel and concrete and loss of rebar cross section [16].

Hence, it can be noted that oxygen and moisture are the most important ingredients for reinforcement corrosion to occur and the ingress of these elements through the concrete must be controlled to avoid corrosion.

Reactions at anodes and cathodes are broadly referred to as “half-cell reactions”. The ‘anodic reaction’ is the oxidation process, which results in dissolution or loss of metal (loss of electrons) while the ‘cathodic reaction’ is the reduction process which results in the reduction of dissolved oxygen forming hydroxyl ions. According to the different spatial location of anode and cathode, corrosion of steel in concrete can occur in different forms:

i. as mircocells, where anodic and cathodic reactions are immediately adjacent to each other, leading to uniform iron dissolution over the whole surface. The distance between the two sites may be a micron. Uniform corrosion is generally caused by carbonation of concrete or by very high chloride content at the steel surface, and

ii. as macrocells, where, corroding areas of the rebar (anode) and non-corroding, passive surfaces (cathode) are separated by a finite distance, which may be centimeters or meters. The anode and cathode may occur on the same bar or on different bars with electrical continuity.

Macrocell corrosion is of great concern because the local dissolution rate (reduction in cross-section of the rebar) may greatly be accelerated due to the

large cathode/anode area ratio. This rapid corrosion attack may lead to structural safety problems.

Generally, the surface of active reinforcing steel in concrete will corrode under the effect of a combination of many microcell and macrocell interactions.

2.3 EFFECT OF REINFORCEMENT CORROSION ON BEHAVIOR OF CONCRETE MEMBERS

In order to review the works of earlier researchers on the topics related to the behavior of concrete member with reinforcement corrosion, an extensive literature survey was carried out. It has been observed that the work related to this study has been carried out on three fronts, namely: (i) time to cover cracking of concrete after initiation of corrosion, (ii) loss of bond between steel and concrete due to corrosion, and (iii) flexural strength of a corroding reinforced concrete member. The literature review is therefore presented in the following three sections addressing the aforesaid parameters.

2.3.1 Time to Cover Cracking of Concrete Due to Corrosion

As the mechanisms producing reinforcement corrosion are time-dependent, effective design and specifications for whole-life performance should be based, where possible, on models of the effects of those mechanisms on service

life. There are several ways of predicting service life due to the corrosion damage of reinforcement in concrete using different deterioration models. Several researchers have documented the processes of diffusion of chloride, oxygen and moisture through concrete, and their effects on corrosion initiation and subsequent rate of concrete deterioration.

Fick's second law has been used extensively to predict the initiation of chloride-induced reinforcement corrosion in concrete. This is in spite of the fact that the assumptions that validate this application hardly exist in the world of reinforced concrete structures in service [17]. Results produced from a comprehensive test program [18] have provided quantitative evidence that Fick's second law is not applicable to concrete structural members with crack widths of greater than 0.1 mm and many concrete design codes and standards prescribe the limit of crack width to greater than 0.1 mm.

Tuutti [19] suggested a model for predicting the service life of reinforced concrete structures. The maximum acceptable corrosion level was related to the appearance of cracks. This depicted corrosion as a two-stage process. First there is an initiation period during which carbonation or chloride ingress occurs, starting at the surface and progressing on a time-dependent basis to the reinforcement. This is followed by a propagation period from the onset of corrosion to the point at which some unacceptable level of deterioration in concrete is reached. This might be the onset of cracking or some predetermined loss of reinforcement cross-

sectional area or perhaps some degree of reduction in serviceability or load-carrying capacity.

Bazant [9] developed a simplified mathematical model to determine the time to cracking of concrete due to chloride-induced reinforcement corrosion based on steady-state corrosion. Bazant's model for the prediction of corrosion damage considers the volume expansion due to the formation of hydrated red rust, [$Fe(OH)_3$], over the residual rebar core. This red rust is expansive in nature and occupies two to ten times the volume of parent steel. Thus, a uniform radial pressure is exerted onto the surrounding concrete resulting in outward radial deformation of concrete. This deformation increases with an increase in the volume of rust till the cover concrete cracks and it is rendered functionally unsatisfactory. When corrosion is in a steady-state with a constant rate, the unacceptable deformation of concrete at cracking can be related to the duration of steady-state corrosion.

In the Bazant's model, the time to cracking is a function of corrosion rate, cover depth, spacing, and certain mechanical properties of concrete, such as tensile strength, modulus of elasticity, Poisson's ratio and creep coefficient. A sensitivity analysis of Bazant's model demonstrates that for these parameters, corrosion rate is the most significant parameter in determining the time to cracking of the cover concrete. Unfortunately, Bazant's model has never been validated experimentally.

Based on field and laboratory data, Morinaga [7], suggested empirical equations that can be used for predicting the time to cracking. It is assumed that cracking of concrete will first occur when a certain quantity of the corrosion product is formed. The model can be used to compute the amount of corrosion products, when concrete cover cracks due to expansion by means of rust formation on rebar surface. The calculated value of the amount of rust may be divided by the steady-state corrosion rate to obtain the time of cover cracking. According to Morinaga's equations, the time to cracking is a function of the corrosion rate, concrete cover thickness and bar diameter.

Bazant's mathematical models and Morinaga's empirical equations are based on the steady state corrosion process to calculate the time to cracking. But since, the corrosion is a dynamic process, use of a simple linear function to describe the relationship between the growth of rust products and time may underestimate the time to cracking of corrosion of steel in concrete.

Wang and Zhao [10] have suggested a step method of using finite element analysis to determine the thickness of the corrosion product corresponding to the time duration when the surface concrete cracks. Further, by analyzing a large number of rebar corrosion data collected from laboratory studies and then by comparing them with the results of finite element analysis, the authors have established an empirical expression to determine the ratio of thickness of the corrosion product to the depth of rebar penetration corresponding to the cracks in

cover concrete. This ratio is termed as expansion coefficient and has been expressed as a function of cube strength of concrete.

Using the value of the thickness of corrosion product, obtained through the finite element model, the depth of rebar penetration corresponding to cracks in cover concrete can be obtained. Further, the depth of rebar penetration can be used to determine the time necessary for longitudinal cracking of concrete cover.

However, the model suggested by Wang and Zhao [10] can be used only in conjunction with the finite element model requiring the determination of the thickness of the corrosion product.

Dagher and Kulendran [8] have also carried out finite element modeling of corrosion damage in concrete structures. Their numerical model is rather versatile in terms of estimating the radial bar expansion, Δ, and includes: (a) a number of options for modeling crack formation and propagation, (b) the capacity to accept any shape of corrosion around the rebars, (c) the ability to incorporate dead and live load stress and initial shrinkage and temperature cracks in the analysis, and (d) pre- and post-processing modules that offer automatic mesh generation and visual representation of crack propagation.

In the context of service life prediction of RC structures subjected to rebar corrosion, the model of Dagher and Kulendran [8], can be used more reliably to determine the radial bar expansion, at which the cracks in cover concrete would

occur. However, their work will require extension to make it capable to predict service life.

Above studies indicate that it is possible to determine the time of corrosion cracking, if the data pertaining to corrosion rate, cover thickness, rebar diameter, etc could be collected. However, the cover cracking due to reinforcement corrosion may not be considered as an indication of the end of the service life. The member with cracked cover may continue to be in service provided that the residual strength of the structure is still large enough to resist the loads.

2.3.2 Effect of Reinforcement Corrosion on Bond between Steel and Concrete

In the field of reinforced concrete, the bond between concrete and reinforcing bar can be thought of as the property which causes hardened concrete to grip an embedded steel bar and thus prevent the longitudinal sliding of the reinforcing bar through the concrete. This property ensures an effective interaction between steel and concrete. Bond stress can be defined as the force per unit of normal surface area of the reinforcing bar acting parallel to the bar on the interface between the bar and the surrounding concrete.

Bond stress may also be thought as the rate of transfer of load between concrete and steel. In other words, if there is bond stress there will be a change in steel stress and vice versa. Whenever the tensile or compressive forces in a bar

change, to maintain the equilibrium, this change in bar force must be resisted at the contact surface between the steel and concrete by an equal and opposite force produced by bond between the reinforcing bar and concrete.

Since the external load is not directly applied to the reinforcement, steel receives its share of the load only from the surrounding concrete. The composite action of concrete and steel as one member is assured only if there exists, a perfect bond between steel and concrete in order to transfer the stresses from concrete to steel. Efficient bond ensures an efficient structural behavior of a reinforced concrete member.

Amleh and Mirza [20] studied the influence of corrosion on bond between the reinforcing steel and concrete using a preliminary series of tests on 14 tension specimens, each 100 mm in diameter and 1-m long and reinforced with one No. 20 bar (19 mm in diameter). 12 of the 14 specimens were placed in a tank filled with a 5% NaCl solution. The study was carried out for seven different levels of corrosion, ranging from no corrosion (with no cracks), to extensive corrosion, with a 9-mm longitudinal crack caused by the bursting pressure resulting from the volume expansion of the corrosion products. They have reported a 9% loss of bond strength due to 4% loss of weight from corrosion accompanied by transverse cracks, while a 17.5% weight loss with no transverse cracks before yielding of the bar resulted in 92% loss of bond between the steel and the surrounding concrete.

The width of these transverse cracks increased as the corrosion level increased, and it signified a reduction of bond between the reinforcing steel bar and concrete.

Fu and Chung [21] have reported that the corrosion of steel rebar in concrete immersed in saturated $Ca(OH)_2$ solution caused the bond strength to increase while the contact resistivity increased. This behavior persisted until 5 weeks of corrosion. Further corrosion, beyond 5 weeks, caused the bond strength to decrease while the contact resistivity continued to increase. This means that slight corrosion (<5 weeks) increased the bond strength, whereas severe corrosion (>5 weeks) decreased the bond strength.

Auyeung et al. [22] in their study on bond behavior of corroded reinforcement bars have found that when the mass loss of the reinforcement due to corrosion reaches approximately 2%, concrete cracks along the bar. A small amount of corrosion increases both the bond strength and bond stiffness, but the slip at failure decreases considerably. However, they stated that when the mass loss exceeds 2%, bond stiffness decreases considerably. Therefore, failure of specimens with corroded bars can be expected to be much more brittle compared to control specimens with uncorroded bars. Even when there is extensive corrosion with considerable cracking of concrete, bond is not completely destroyed. Measurable bond strength exists even when the mass loss approaches 6%. This partially explains the fact that structures with extensively corroded reinforcement sometimes sustain considerable loads.

Al-Sulaimani et al. [23] carried out research to relate corrosion of reinforcement to bond deterioration by testing beams that were designed to fail in bending. These beams were of 150 × 150 × 1000 mm, reinforced with two 10 mm dia top bars, two 12 mm dia bottom bars and links 6 mm dia at 50 mm spacing. The reinforcement was corroded by applying a constant current density of 2 mA/cm^2 to the bottom bar. The shear span at loading test was 300 mm. They found that the bond strength increased with corrosion upto a certain level of corrosion, but progressively decreased when corrosion was very high. They attributed the initial increase in bond to the increased roughness of the reinforcing bar surface with the growth of a firm layer of corrosion, whereas the loss in bond with further corrosion, especially in the case of severe localised corrosion, was due to severe degrading of bar ribs, the lubricating effect of the flaky corroded metal on the bar surface, and the reduced concrete confinement of the bar due to the widening of the longitudinal corrosion crack. They attributed the reduction of the load carrying capacity to the reduction in the bar cross section. They also concluded that corrosion up to about 1.5% does not affect the ultimate load in flexure, but with 4.5% corrosion, the ultimate load is reduced by approximately 12% because of loss in the diameter of the bars.

Cabrera and Ghoddoussi [24], investigated the effect of reinforcement corrosion on bond strength. They studied two types of specimens, i.e., pullout test specimens and beam test specimens. The pullout tests were carried out on 150 mm concrete cubes with 12 mm diameter reinforcing bars centrally embedded in the

cube. The beam specimens were 125 × 160 × 1000 mm, reinforced with two 10 mm plain top bars, two 12 mm bottom bars and plain links of 8 mm at 40 mm spacing, as a web reinforcement along the shear span of 384 mm. In order to obtain corrosion in a reasonable time, a voltage of 3 V was impressed through the specimen bottom bars up to 40 days. Maximum reduction of the cross section (9%) at bottom bar caused a reduction of 20% of the ultimate bending moment, and an increase of 40% of the deflection at mid-span corresponding to the service load.

Almusallam et al. [25] investigated the effect of reinforcement corrosion on the bond strength between steel and concrete. They noticed that in the precracking stage (0-4% corrosion) the ultimate bond strength increases. When reinforcement corrosion is in the range of 4 to 6%, the bond failure occurs suddenly at a very low free-end slip. Beyond 6% rebar corrosion, the bond failure resulted from a continuous slippage of rebars. The ultimate bond strength initially increased with an increase in the degree of corrosion, until it attained a maximum value of 4% rebar corrosion after which there was a sharp decrease in the ultimate bond strength up to 6% rebar corrosion. Beyond the 6% rebar corrosion level the ultimate bond strength did not vary very much even up to 80% corrosion.

The above researchers have correlated reinforcement corrosion with the loss of bond between steel and concrete. Corrosion of steel embedded in concrete is not visually evident until the damage reaches to the external signs of

deterioration as rust spots, cracks or spalling. In order to predict the corrosion service life of reinforced concrete structures, it is therefore more useful to determine the residual load carrying capacity of a corroding reinforced concrete member than the loss of bond.

2.3.3 Flexural Strength of a Corroding Reinforced Concrete Member

From the available literature it has been observed that research related to the determination of flexural strength of corroding reinforced concrete members has been carried out mostly on two fronts: (i) corrosion of steel in concrete in relation to bar diameter and cover thickness, and (ii) residual flexural strength of corroding reinforced concrete structures. These aspects are discussed in the following subsections.

2.3.3.1 Corrosion of steel in concrete in relation to bar diameter and cover thickness

The concrete cover over reinforcing steel is one among the factors that significantly controls the durability performance of reinforced concrete structures. It influences the time for the ingress of the aggressive species to the steel surface. Non-uniform cover leads to the formation of concentration cells that may lead to corrosion initiation. Cover also plays a significant role in determining the extent of cracking in fresh concrete occuring over top reinforcement due to restraint

provided by the top bars to the settlement of concrete. Results of some long-term exposure tests in seawater or in sprayed salt solution also indicated significant eduction of corrosion, as the cover was progressively increased from ½ in. to 1.5 in., and almost no corrosion at a cover of 2 in.

Ravindrarajah and Ong [26] investigated the effect of the diameter of the steel bar, and the thickness of the cover on the degree of corrosion of mild steel bars embedded in mortar. The main parameters of the study were the quality of cover mortar, the diameter of the steel bar, and the thickness of the cover. The specimens were cylindrical in shape and each specimen consisted of a single mild teel bar placed centrally. All the corrosion specimens were partially submerged in a 5% sodium chloride solution. The current was impressed on the steel bars from a DC rectifier of a constant voltage. A 5V supply was selected to cause a significant intensity of corrosion in steel bars within a reasonable period. They found that there is a significant effect of rebar diameter, cover thickness, and specimen size on the corrosion intensity. The intensity of corrosion of reinforcing steel in concrete was found to increase with an increase in the bar diameter. With the increase in the bar diameter the cover thickness reduces and the corrosion resistance decreases. This is expected since larger bar size have lower electrical resistance and smaller cover thickness shortens the diffusion path for the chloride ions. The relationship between the iron loss and cover/bar diameter was found to be linear. For the same diameter of bar, the corrosion intensity of steel increased when the cover thickness was decreased. The surface area of the corrosion

specimen through which the chloride ions diffuse was also found to be an important parameter in determining the rate and extent of corrosion of embedded steel in concrete.

From condition surveys and laboratory and exposure site studies, Rasheeduzzafar et al. [27-28] indicated that the cover over reinforcement has the most significant effect on the extent of rebar corrosion. In condition surveys on 42 reinforced concrete framed structures, 15 to 20 years old and located in Eastern Saudi Arabia, 76 spalls of varying dimensions and severity were observed during 168 observations covering approximately 12,000 square feet of concrete area. In 68% of the observed spalls, the thickness of concrete cover was less than ½ in.; while in 53%, it was less than 3/8 in.; and in 18% of observations, it was less than ¼ in. There were seven cases (9.2%) where there was almost no cover over reinforcing steel. Cover measurements on several partially spalled floor slabs showed that spalls were invariably located in regions of insufficient cover.

Rasheeduzzafar et al. [29], based on their field and laboratory results, recommended the following cover for structures serving in various environments of the Arabian Gulf:

i. Building components which are permanently exposed to the salt-laden corrosive atmosphere: 2.0 inch

ii. Building components which are protected against weather and the aggressive conditions of exposure: 1.0 to 1.5 inch

iii. Concrete components exposed to seawater and footings as well as other main structural members cast against the ground: 3.0 inch.

Tarek Uddin et al. [30], studied the influence of crack width and type of bars (plain and deformed) on corrosion of steel bars in cracked concrete. Microcell and macrocell corrosions of plain and deformed steel bars were investigated on 100 × 100 × 400 mm, single cracked specimens with crack widths of 0.1 mm, 0.3 mm and 0.7 mm. Electrochemical investigations were also conducted on 150 × 150 × 1250 mm multicracked specimens with plain and deformed bars. For these specimens, crack widths were varied from 0.1 to 0.4 mm. After electrochemical investigations, the chloride ions in concrete, the corroded areas, the weight loss of the rebar and pit diameters of the steel bars were investigated. It was observed that deformed bars showed more current densities than plain bars. The results indicate that the corrosion rate of plain bars is less than the corrosion rate of deformed bars. Also, for the same crack width, the specimens with deformed bars showed higher oxygen permeability than the specimens with plain bars.

2.3.3.2 Residual flexural strength of corroding reinforced concrete structures

The moment carrying capacity of a reinforced concrete beam depends mainly on the strength of reinforcing steel. Therefore, loss of reinforcing steel area may be critical and requires special consideration. Corrosion is one of the important causes of steel area loss. The strength reduction due to the reinforcing steel area loss is a linear function of the loss of material [31].

Ting and Nowak [31] developed a method for calculation of the effect of reinforcing steel area loss (due to corrosion or other causes like mechanical damage) on the moment carrying capacity of corroded reinforced concrete beams. They developed a numerical procedure using finite difference method by considering various types of concrete members including a solid slab, void slab, rectangular beam, T-beam and box beam. The procedure was demonstrated on evaluation of the reinforcing steel area loss effect for a typical reinforced concrete bridge girder. According to their approach, the reinforcing steel area loss is a linear function of the loss of material. This is in contrast to the results of Uomoto and Misra [32], who found that the deterioration of structures caused by the reinforcement corrosion is not always directly related to the loss of strength of the bars due to a reduction in cross-sectional area, but some other factors, such as crack formation in concrete and loss of bond could lead to greater reduction in strength of the structure.

Huang and Yang [33] carried out experiments on 32 corroded reinforced concrete beams, of dimensions 15 × 15 × 50 cm, of which 16 had predetermined cracks, so as to study the effect of reinforcing steel area loss on flexural behaviour of reinforced concrete beams. Two # 4 bars were used as flexural reinforcement and no shear reinforcement was provided. An impressed current was applied to the beams in order to accelerate steel corrosion. The load carrying capacity of RC beams decreased as the corrosion product increased. The percentage reduction in the loading capacity of the RC beam subjected to corrosion was approximated by the calculated loss of rebar diameter. Based on the results, it was found that for a 10% reduction in the loading capacity of an RC beam, the calculated loss of thickness of steel ranged from about 0.2 μm to 1.44 μm. By comparing the loss of steel thickness with the reduction of the stiffness or loading capacity of the RC beams, they concluded that a small loss of thickness may cause a significant reduction in the load carrying capacity for high strength concrete beams or defective beams.

Yoon et al. [34] investigated concrete beam specimens having dimensions 100 mm × 150 mm × 1170 mm, reinforced with a single standard No. 6 (19 mm diameter) Grade 60 reinforcing steel bar. The cover of the reinforcing steel was 30 mm. To avoid excessive corrosion at the ends of the reinforcing bar, the ends of 60 mm length of the bar was coated with epoxy. A normal strength concrete (water-cement ratio of 0.5) was used in the investigation. The effect of the extent

of steel corrosion on remaining loading capacity of the concrete beams was studied relating the remaining flexural loading to the percentage weight loss of reinforcing steel. A four-point loading configuration was used with the distance between two end supports of concrete beam specimens as 1050 mm, and a pure bending moment was generated within a region of 230 mm in the middle part of the beams. It was found that, for the beams having a degree of corrosion ≥ 3% weight loss of steel, the remaining loading capacity of the beams decreased as the percentage weight loss of the reinforcing steel increased indicating that the loss of the loading capacity might be primarily due to the loss of steel-concrete bond. They also stated that as the degree of steel corrosion increased, the failure mode of the reinforced concrete beams shifted from a shear failure to bond splitting failure. In fact, the lower the remaining load carrying capacity of a beam, the clearer the steel-concrete bond failure was seen from the flexure testing.

Cabrera [5] carried out loading tests with six corroded beams having a cross section of 125×160 mm, reinforced with two 10 mm plain top bars, two 12 mm bottom bars and plain links of 8 mm at 40 mm spacing, as a web reinforcement along the shear span of 384 mm. Around 2% chloride was added to the concrete to accelerate the corrosion process. The specimens were kept partially immersed in a chloride solution during the corrosion acceleration process which was achieved by applying a voltage of 3 V versus saturated calomel electrode (SCE) between external counter electrodes and the bars. The amount of steel loss

was estimated by the gravimetric mass-loss method. The beam specimens were tested as simply supported beams with two concentrated loads using an Instron testing machine. When the percent mass loss was smaller than 2%, the moment capacity increased almost 20%. Otherwise, an approximately linear decrease occurred in the moment capacity when the percent of mass loss increased. Maximum reduction of the cross section (9%) at bottom bar caused a reduction of 20% of the ultimate bending moment and an increase of 50% of the deflection at mid-span corresponding to the service load.

Rodriguez et al. [12] carried out experiments on six different types of reinforced concrete beams of 150 × 200 × 2300 mm. A constant anodic current of 0.1 mA/cm^2 was applied for a period of time ranging between 100 and 200 days. After the corrosion-acceleration stage, the beams were tested under bending by a four-point loading test using 400 mm spacing between the loads. The bending moment capacity of the control beams was about 37 KN-m. After 100 days of accelerated corrosion, the capacity was reduced to 26 KN-m (30% decrease). After 200 days, the capacity was reduced to 20 KN-m (46% decrease). They found that the experimental value of the bending moment at maximum load, in beam with only bottom bars corroded, was close to the calculated value, using the reduced section of the bottom bars. No damage occurred at the top concrete cover because neither the top bars nor the links were corroded in the beam. They concluded that, it is possible to predict a conservative value of either the ultimate bending moment or the ultimate shear force, for high levels of corrosion, by

means of using RC conventional models and considering the reduced section of both steel and concrete.

Uomoto and Misra [32] carried out a large experimental work with corroded beams and columns so as to study the load carrying capacity of concrete structures with corroded reinforcement. Accelerated corrosion was induced by adding sodium chloride to the mixing water and applying a constant current density to the reinforcement ranging from 280 to 380 $\mu A/cm^2$ for a period ranging from 7 to 14 days. Beam specimens $100 \times 100 \times 700$ mm, reinforced with two 10 mm dia bottom bars, were tested and it was observed that most beams failed in shear. Also, beams measuring $200 \times 100 \times 2100$ mm, reinforced with two 6mm dia top bars, 2-16mm dia bottom bars and links 6mm dia at 170 mm spacing, were tested, resulting in compression failure of concrete, with buckling of the top bars (no links existed at the constant moment span). They concluded that the reduction in the load-carrying capacity of the beams was not caused simply by the reduction in the effective area or the reduction in strength of reinforcing bars, but by the cracks formed by the corrosion process. Weight loss of 1% to 2.4 % in the main reinforcing bars (16 mm dia) corresponded to 4% to 17 % of reduction in the load carrying capacity.

Tachibana et al. [13] carried out tests with corroded beams of $200 \times 150 \times 2000$ mm. The beams had no shear reinforcement but were reinforced longitudinally with two 16 mm diameter bottom bars. All specimens, except the

control were corroded by applying an anodic current density of 0.5 mA/cm^2 for 0-day (non-corroded), 3, 6, 10 and 15 days. The specimens were fully immersed in a 3.5 % sodium chloride solution. The results of the loading tests showed that, non-corroded and mildly corroded specimens for the current period of 3 days had a normal behavior and failed in flexure with yielding of steel bars. On the other hand, the specimens for the current period of 10 days and 15 days showed deteriorated behaviour and failed in a brittle manner, and the reduction in stiffness and the load carrying capacity occurred, and specimens for the current period of 6 days showed intermediate behaviour. A 16% loss of capacity in the beams was reported after 15 days of current application. The maximum percentage weight loss of reinforcement was about 5%. With regard to the load carrying capacity of the RC beams with stirrups, they concluded that the reduction in load-carrying capacity of RC beams with stirrups will not be remarkable, as the transmission of shear stress between concrete and reinforcement will be secured through the stirrups even when bond of reinforcement has deteriorated.

Nokhasteh et al. [35], conducted preliminary flexural tests on three simply supported RC beams. The specimens were of dimensions 130 × 200 × 2350 mm with 16 mm smooth mild black steel bars. All beams carried two 6 mm mild steel bars as top steel. The ultimate load capacity of the control specimens was calculated theoretically using the stress-block factors derived from the empirically determined relationships of Hognestad et al. [36] suitably modified for use with concrete cube strengths. All three beams failed in a ductile manner, they all

suffered from fewer but wider cracks, larger central deflections and finally from a reduction in the ultimate load capacity. The authors developed a two-dimensional finite element model for the damaged beam. The load-central deflection curves derived from the FE analysis showed a decrease in stiffness of the damaged beams as compared with their undamaged counterparts. They concluded that corrosion of link reinforcement is likely to be more significant than the main bars because: (i) there is less cover to link reinforcement, (ii) stressing due to bending of the bars increases corrosion, and (iii) the links are smaller in diameter.

Aziz [37] investigated the effect of reinforcement corrosion on the flexural strength of a uniformly loaded and simply supported one-way slab. The slab dimensions were 305 × 711 × 63.5 mm, with a center-to-center span of 610 mm. Five # 2 (6 mm diameter) bars were used as the main reinforcement and were placed in the slab with a 57 mm center-to-center spacing and with a 9.5 mm clear cover. The specimens were partially immersed in a 5% sodium chloride solution and a constant current of 2 A was applied to all the specimens. They have reported a sharp reduction in the ultimate flexural strength of slabs with up to 20% reinforcement corrosion; thereafter, the strength decreased at a somewhat reduced rate with further increase in reinforcement corrosion. The reduction in the ultimate flexural strength of slabs with 5% reinforcement corrosion was 25%, while it was 60% in the slabs with 25% reinforcement corrosion.

Mangat and Elgarf [11] have carried out research work on developing a relationship between the degree of reinforcement corrosion and the residual strength of flexural members through an experimental scheme. The beam dimensions were 100 × 150 × 910 mm. Four different current densities from 1 mA/cm^2 to 4 mA/cm^2 were applied to induce different degree of accelerated reinforcement corrosion, without representing countervailing interactions with shear reinforcement since the shear reinforcement was provided externally. Exposure time was between 15 and 18 days. After the corrosion-acceleration period, the specimens were tested in flexure under four-point loading with the distance between the loading points being 300 mm. Up to a degree of corrosion (percentage reduction in reinforcement bar diameter) of 3.75%, there was very little effect of corrosion rate on flexural load capacity. However, at a corrosion degree of 5 % and beyond, the flexural load capacity decreased significantly with increasing corrosion rate. The study obtained a 75% decrease in load capacity for a 10% diameter reduction. They found that reinforcement corrosion in concrete has a marked effect on both the flexural load capacity and deflection of beams. Also, the reduction in reinforcing bar cross-section due to corrosion has an insignificant effect on the residual flexural strength of the beams. The reduction in residual strength was primarily attributed to the loss or breakdown of the steel/concrete interfacial bond. A trigonometric function, in terms of the rate of corrosion, corrosion time and bar diameter, was proposed to predict the residual strength of corroded beams.

Jin and Zhao [38] carried out beam tests to study the effect of reinforcement corrosion on the bending strength of reinforced concrete beams. Bending tests were carried out on beam specimens, which were 150 mm × 150 mm in cross section and 1140 mm in length. Each beam was reinforced with two 12 mm bottom bars, two 6 mm top bars and 6 mm closed stirrups spaced at 100 mm. Insulating rubberized fabrics and epoxy resin were used to isolate the 12 mm bottom bars from the rest of the reinforcement cage, so that 12 mm bottom bars underwent independent corrosion induced through the electrochemical corrosion technique. Direct Current was impressed to obtain the desired levels of reinforcement corrosion by controlling the current intensity and the electrifying time. The beam specimens were then tested as simply supported beams under a two-point load with a total span of 900 mm and shear span of 300 mm, using the hydraulic system. They observed that with the increase of the bar corrosion, the failure mode of corroded RC beams changed from ductile mode to brittle mode similar to that of under reinforced beams, and the distribution of cracks of corroded RC beams became concentrated instead of scattered. They developed an empirical model for determining the percentage residual flexural strength of the corroded beams in terms of the percentage reinforcement corrosion. They also developed expressions for calculating the reduced steel cross-sectional area, reduced yield strength and reduced bond strength.

It may be noted that researchers have attempted to empirically correlate the residual load-carrying capacity of a corroded reinforced concrete structure

with the degree of reinforcement corrosion and other parameters, such as rebar diameter and cover thickness.

In the present study, an attempt has been made to predict the residual flexural strength of a corroded beam through the use of conventional flexural formula by taking into account the loss of metal due to corrosion and applying an applicable correction factor, which is a function of corrosion current density and the corrosion time, and the rebar diameter.

CHAPTER 3

METHODOLOGY OF RESEARCH

3.1 EXPERIMENTAL PROGRAM

The present study involves casting, corroding and flexure testing of a series of reinforced concrete beam specimens. Beams with different bar diameters and cover thicknesses were subjected to reinforcement corrosion under impressed current of varying intensity and time periods to induce loss of metal. Results from the flexure test of corroded beams are used in relating the residual flexural strength to corrosion rate, time of corrosion, and rebar diameter.

3.2 EXPERIMENTAL VARIABLES

The following variables were used in this experimental program:

i. Two different tension bar diameters: 10 mm and 12 mm
ii. Two different clear covers to the tension reinforcement: 25 mm and 40 mm

iii. Two different levels of impressed corrosion current intensities : 2 mA/cm^2 and 3 mA/cm^2

iv. Three different corrosion durations: 4 days , 6 days and 8 days

3.3 TEST SPECIMENS

A total of 56 reinforced concrete beam specimens were cast to include all variables mentioned in Section 3.2. All tests were repeated twice, including the tests on control specimens. Table 3.1 shows the test variables and the corresponding number of beams cast and tested.

Table 3.1: Test variables and specimens.

Variables	**Levels**	**Number of test specimens for**			
		T_0	T_1	T_2	T_3
I T D C_v	2 3 2 2	$(D_1 + D_2) \times (C_{v1} + C_{v2}) \times 2$ Repetition = 8 Control Specimens	$(I_1 + I_2) \times (D_1 + D_2) \times (C_{v1} + C_{v2}) \times$ 2 Repetition = 16	$(I_1 + I_2) \times (D_1 + D_2) \times (C_{v1} + C_{v2}) \times$ 2 Repetition = 16	$(I_1 + I_2) \times (D_1 + D_2) \times (C_{v1} + C_{v2}) \times$ 2 Repetition = 16
Total number of specimens		**8 + 16 + 16 + 16 = 56**			

The following nomenclature applies to the parameters shown in Table 3.1.

I = impressed corrosion current intensity, mA/cm^2

T = impressed corrosion duration, days

D = diameter of tension bars, mm

C_v = clear cover to the tension bars, mm

3.4 DETAILS OF TEST SPECIMENS

Rectangular reinforced concrete beam specimens of size 150 × 150 × 1100 mm were used for this study. All beams were designed to fail in flexure by providing ample vertical shear reinforcement to exclude premature shear failure. The reinforcement details of the test specimens are shown in Fig. 3.1.

The chosen clear covers were 25 mm and 40 mm. The tension reinforcement consisted of a pair of 10 mm or a pair of 12 mm diameter steel bars. The vertical stirrups were of double-legged 6mm diameter steel bars spaced uniformly at 90 mm centers throughout the length of each beam. Deformed bars were used as reinforcement. While the top two 8 mm diameter bars used to serve as stirrup-holders were epoxy-coated to avoid corrosion, the stirrups were left uncoated so that they would be affected by corrosion along with the main tension bars. By allowing the stirrups to corrode, the corrosion damage of the test beams reflects the practical case in which all bars are subjected to corrosion.

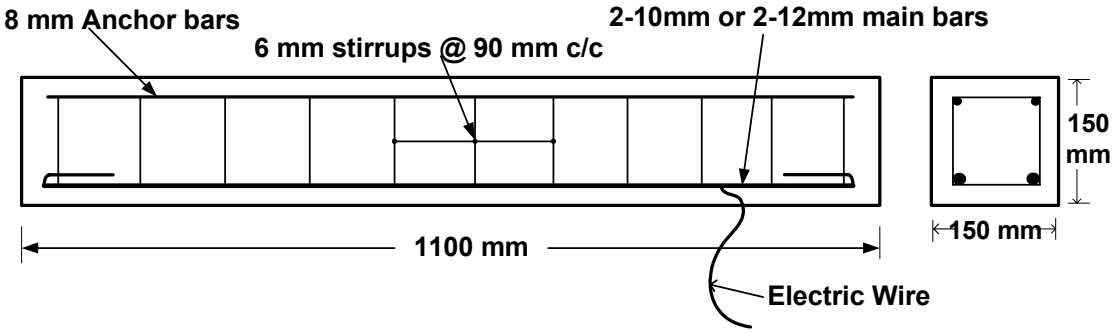

Figure 3.1: Reinforcement Details of Test Specimens.

3.5 CONCRETE CONSTITUENTS

ASTM C 150 Type I Portland cement, which is extensively used in Saudi Arabia, was used in the preparation of concrete specimens. The coarse aggregate for this study was crushed limestone processed from the quarries on Riyadh Road. The average values of specific gravity and absorption of the coarse aggregates, determined in accordance with ASTM C 127, were 2.5, and 1.3 %, respectively.

Medium coarse sand was used as fine aggregate. The specific gravity and absorption of the fine aggregates were 2.6 and 0.40 %, respectively. Potable water was used for mixing and curing of concrete.

3.6 PREPARATION OF BEAM SPECIMENS

3.6.1 Concrete Mix Proportions

Mix design parameters of concrete such as water-cement ratio, cement content, grading of coarse aggregate, and coarse to fine aggregate ratio were same for all the concrete mixtures. The following mix proportions were used:

Water-cement ratio = 0.45

Cement content = 350 kg/m^3

Coarse to fine aggregate ratio = 1.65

The grading of coarse aggregate is shown in Table 3.2.

Two percent sodium chloride (NaCl) by weight of cement was mixed in the concrete to facilitate the flow of current in the specimens.

Calculations for the weight of each ingredient were made using the above specification. Calculated weights of the constituents are presented in Table 3.3.

Table 3.2: Grading of Coarse Aggregates.

Sieve opening	% Weight Retained
1/2"	35
3/8"	35
3/16"	20
3/32"	10

Table 3.3: Weight of constituents in one cubic meter of concrete.

Constituent		Weight (kg)
Cement		350.00
Water		157.50
Fine aggregate		751.82
Coarse aggregate	1/2 in.	434.10
	3/8 in.	434.10
	3/16 in.	248.20
	3/32 in.	124.00

3.6.2 Casting and Curing of Beam Specimens

Casting of 56 beam specimens was carried out in 10 batches. Three cylindrical concrete specimens were also cast from each batch of concrete mix to determine the corresponding compressive strength. The concrete ingredients were mixed in a revolving drum type mixer till it was uniform. The moulds were oiled and the steel reinforcement cages prepared beforehand were placed securely in their proper position in the moulds. The moulds were filled with concrete in three layers. After placement of each layer, the concrete was vibrated to ensure proper consolidation. After casting, the specimens were covered with plastic sheet to avoid loss of water due to evaporation. The specimens were demolded after 24 hours of casting and then covered with wet towels to cure at laboratory

temperature of 18 to 20°C. The towels were wetted from time to time. Moist curing was carried out for a period of seven days followed by air curing at room temperature.

3.7 DESIGNATION FOR BEAM SPECIMENS

Fifty six beam specimens were divided into four basic groups, BT1 to BT4, based on the clear cover to the tension reinforcement and the rebar diameter. Table 3.4 shows the designation of the control beam specimens that were not subjected to accelerated corrosion.

Table 3.4: Designation for control specimens.

Bar diameter, mm	Cover, mm	Designation
10	25	**BT 1-C**
12	25	**BT 2-C**
10	40	**BT 3-C**
12	40	**BT 4-C**

The designation for the corroded beams is shown in Table 3.5. For clarity, a designation indicates the intensity and the duration of the applied current for inducing corrosion. As an explanation of the designation used for a corroded beam, BT1-2-4 implies a beam of group BT1 that was subjected to an applied current intensity of 2mA/cm^2 for a period of 4 days.

Table 3.5: Designation for corroded specimens.

Diameter, mm	Cover, mm	Applied current, mA/cm^2	Time, days	Designation
10	25	2	4	BT1-2-4
10	25	2	6	BT1-2-6
10	25	2	8	BT1-2-8
10	25	3	4	BT1-3-4
10	25	3	6	BT1-3-6
10	25	3	8	BT1-3-8
12	25	2	4	BT2-2-4
12	25	2	6	BT2-2-6
12	25	2	8	BT2-2-8
12	25	3	4	BT2-3-4
12	25	3	6	BT2-3-6
12	25	3	8	BT2-3-8
10	40	2	4	BT3-2-4
10	40	2	6	BT3-2-6
10	40	2	8	BT3-2-8
10	40	3	4	BT3-3-4
10	40	3	6	BT3-3-6
10	40	3	8	BT3-3-8
12	40	2	4	BT4-2-4
12	40	2	6	BT4-2-6
12	40	2	8	BT4-2-8
12	40	3	4	BT4-3-4
12	40	3	6	BT4-3-6
12	40	3	8	BT4-3-8

3.8 EXPERIMENTAL TECHNIQUES

3.8.1 Compressive Strength of Concrete

The 28 day compressive strength of concrete, f_c' was determined by testing 75 × 150 mm cylindrical specimens in accordance with ASTM C39. The average of the three cylinders cast from each batch was taken as the applicable value of f_c' for that concrete.

3.8.2 Tensile Strength of Reinforcing Bars

For determination of yield and tensile strength of tension bars, bar specimens of 10 mm and 12 mm diameter were tested in tension in an Universal Testing Machine and the complete load-elongation, hence stress-strain plots, were obtained. From the stress-strain plots, yield strength and tensile strength of the bars were determined. An extensometer, of 50 mm gauge length, was used to measure the extension of the bars during the test and a data logger connected to a computer recorded the load and the corresponding extension of the bar as the test progressed. The test arrangement is shown in Figure 3.2.

Figure 3.2: Arrangement for evaluating the tensile strength of steel bars.

3.8.3 Corrosion Rate Measurements

The RC beam specimens were tested for determining the corrosion current density, I_{corr}, using the linear polarization resistance measurement (LPRM) technique [39-40].

The LPRM procedure is based on the Stern-Geary characterization of the typical polarization curve for the corroding metal. In this method, a linear relationship is described mathematically for a region on the polarization curve in which slight change in the current applied to the corroding metal in an ionic solution causes corresponding change in the potential of the metal. In other words, if a large current is required to change the potentials by a given amount, the corrosion rate is high and on the other hand, if only a small current is required, the corrosion rate is low.

The corrosion cell consisted of a reference electrode, a working electrode which was the reinforcing steel embedded in the concrete specimen, and a counter electrode which was placed in the salt solution around the concrete specimen. The reinforcing steel bar was polarized by applying a small potential shift to it (ΔE = 10 mV) and the resultant current (ΔI) between the working electrode and the counter electrode was measured.

The linear polarization resistance, R_p, was determined from the slope of the plot of applied potential versus the measured current. The corrosion current density was then calculated by using the Stern-Geary formula [41].

$$I_{corr} = \frac{\Delta E}{\Delta I} = \frac{B}{R_p}, \tag{3.1}$$

Where:

I_{corr} is the corrosion current density ($\mu A/cm^2$),

R_p is the polarization resistance ($k\Omega\ cm^2$),

$$B = \frac{2.3(\beta_a.\beta_c)}{(\beta_a + \beta_c)} \tag{3.2}$$

β_a is the anodic Tafel constant,

β_c is the cathodic Tafel constant

The values of β_a and β_c are determined from the Tafel plot. However, in the absence of sufficient data on β_a and β_c for steel in concrete, a value of B equal to 52 mV for steel in passive condition and a value equal to 26 mV for steel in active condition are normally used. For steel in aqueous media, values of β_a and β_c equal to 120 mV are normally used.

A major uncertainty in obtaining the polarization resistance is the area of the steel bar that is affected by the current flowing from the counter electrode. $\Delta E/\Delta I$ measurements using a small counter electrode provides an apparent

polarization resistance that differs from the true R_p value depending on the experimental conditions. Thus, if the metal is actively corroding, the current applied from a small counter electrode located on the concrete surface is 'drained' very efficiently by the rebars and it tends to confine itself on a small surface area as shown in Fig. 3.3. Conversely, if the metal is passive and R_p is high, the current applied tends to spread far away from the application point (right part on the rebar in Fig 3.3.) [42].

Therefore, in an effort to better control the current path from the counter electrode to the bar, counter electrode was prepared such that it covered both the sides of the specimen throughout the length and it is assumed while evaluating I_{corr} that corrosion is occurring uniformly over the entire steel area. Figure 3.4 shows the schematic representation of the test set-up used to measure the corrosion current density.

One of the most important problems in evaluating I_{corr} in the field lies in evaluating the area of reinforcing bar that is being polarized by the test. It is impractical to polarize the entire reinforcement system in a concrete structure. The area that is actually polarized by a small auxiliary electrode will be influenced by the resistance of the concrete and by the polarization resistance of the steel reinforcement. This area cannot be easily quantified [43].

The test beam was half immersed in the electrolyte during the corrosion rate measurements. The surface area of the steel polarized, considered for

calculating I_{corr} was therefore, taken as the area of the main tension bars plus half of the area of the stirrups, i.e. only the submerged area of all steel reinforcement.

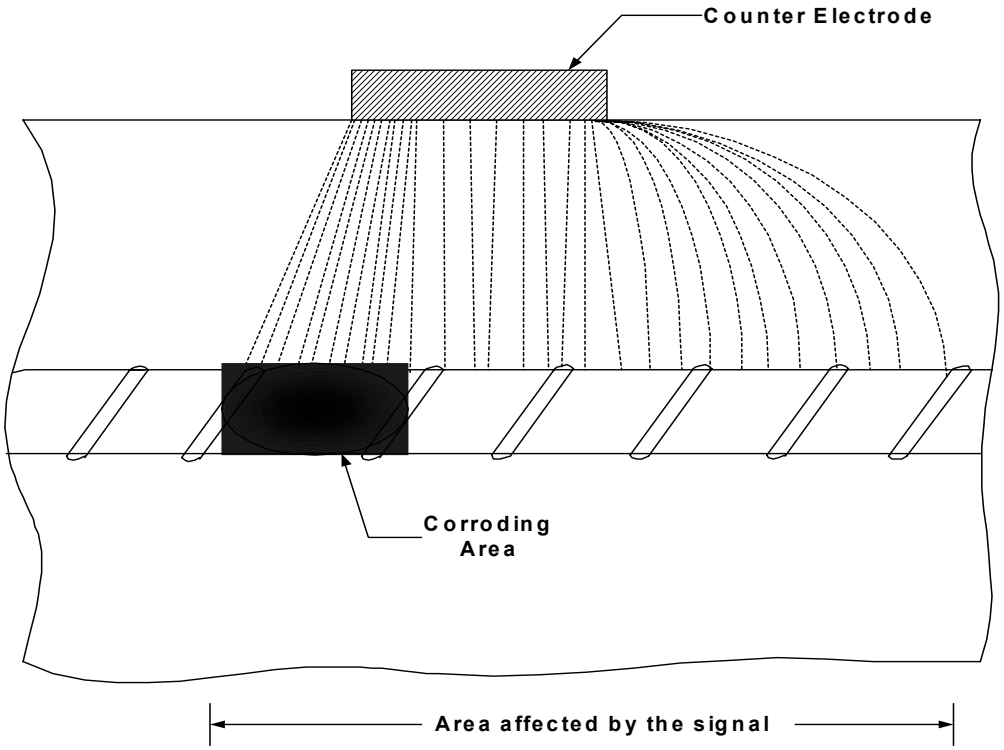

Figure 3.3: Spread of an electrical signal applied from a counter electrode [42].

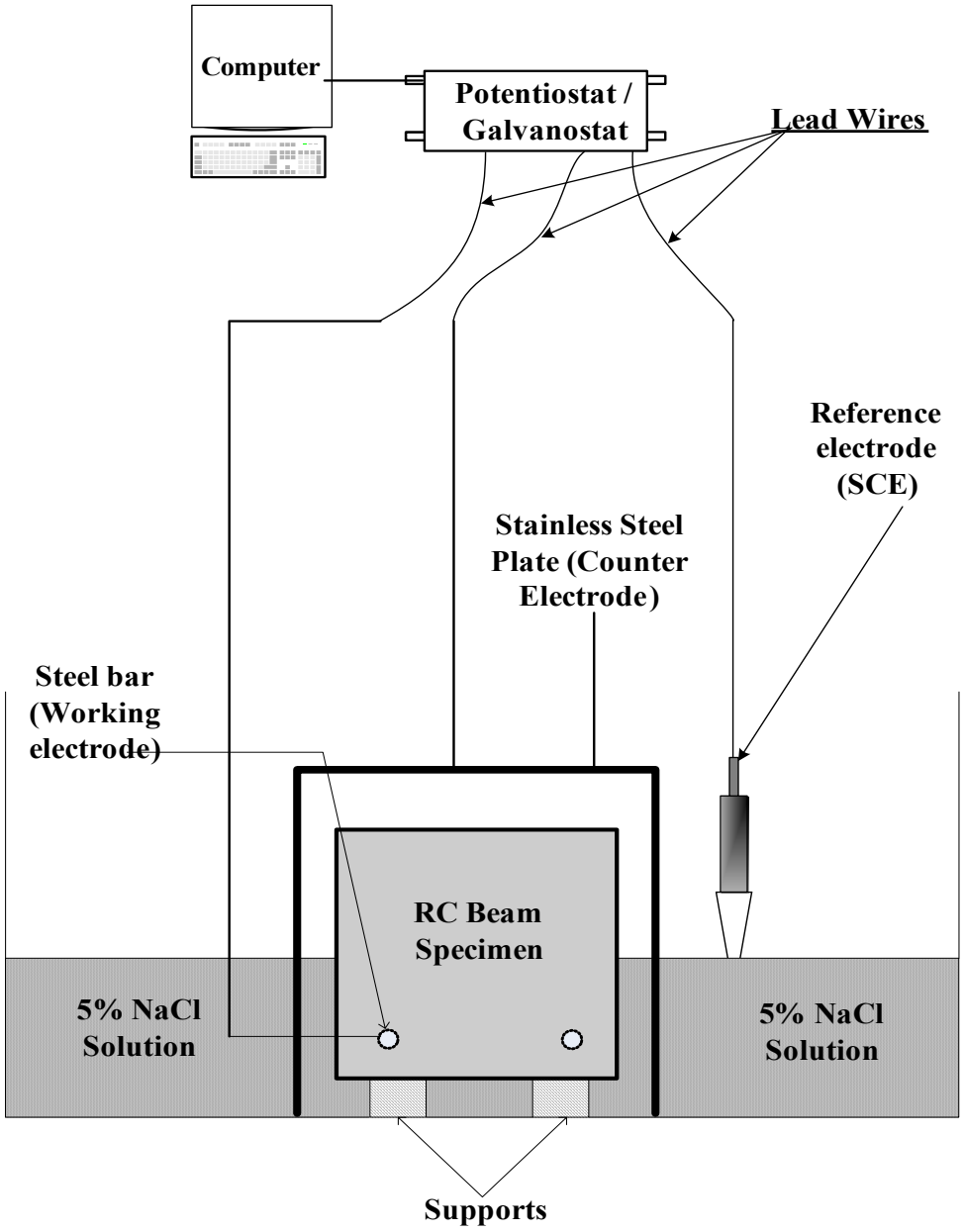

Figure 3.4: Schematic representation of the set-up utilized to measure the corrosion current density.

3.8.4 Test Setup for Inducing Reinforcement Corrosion

After completion of curing and measurement of the initial corrosion current density, the specimens were subjected to accelerated corrosion by applying anodic current of specified intensities and for specified time periods. This was achieved through a small DC power supply with a built-in ammeter to monitor the current and a potentiometer to control the current intensity. The concrete specimens were partially immersed in 5% sodium chloride solution in a tank such that the base of the specimen was just in contact with water. The direction of the current was adjusted so that the reinforcing steel became an anode and a stainless steel plate placed on the concrete specimen served as a cathode. The stainless steel plate was placed in the tank in such a manner that it covered both the sides of the specimen throughout the length. This arrangement ensured a uniform distribution of the corrosion current along the whole length of the bar. A schematic representation of the test set-up is shown in Fig. 3.5.

Though accelerated corrosion does corrode the bars and leads to crack formation, it differs considerably from the actual corrosion in structures, in rate and characteristics. The corrosion in existing structures is extremely slow and hence; even when the bars corrode and expand; cracks may not always form in surrounding concrete because of concrete creep [32].

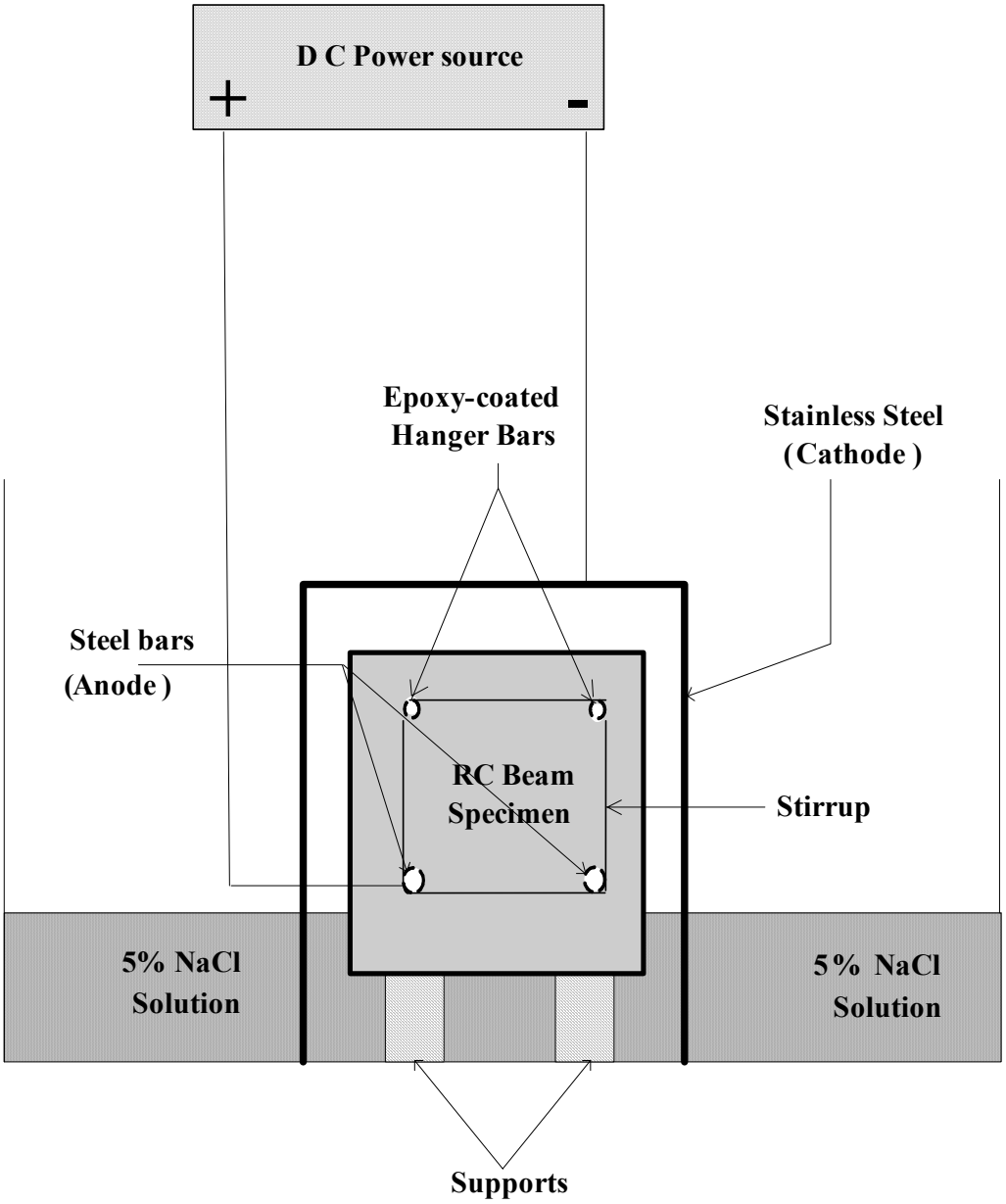

Figure 3.5: Schematic representation of the accelerated corrosion test setup.

Another difference lies in the fact that in Galvanostatic corrosion, the reinforcement is forced to corrode by impressing direct current and this results in all the reinforcing bars becoming anodic to external cathode (in this series of experiments a stainless steel plate). This entails overall corrosion, at an almost uniform rate. This may not be the case in existing structures, where we see a difference in the degree of corrosion of rebars depending upon various factors, such as, their distance from the concrete surface.

However, it has been found by some investigators [32], that the cracks formed by accelerated corrosion are quite similar to those formed during exposure tests. This justifies the choice of the accelerated corrosion induction method to cause a significant amount of corrosion in a short span of time in laboratory tests.

It is observed from the previous accelerated corrosion tests on reinforced concrete members that the applied impressed current densities have typically ranged from, as low as 0.1 mA/cm^2 [12] to as high as 4 mA/cm^2 [11]. So as to complete the experiments within a reasonable amount of time, impressed current intensities chosen were 2 mA/cm^2 and 3 mA/cm^2.

The total current required for each type of beam specimen was calculated based on their respective steel surface area, as shown in Table 3.6.

Table 3.6: Total current applied to beam specimens.

Beam Type	**D (mm)**	**C_v (mm)**	**Total surface area of tension steel and stirrups (cm^2)**	**Total current I (Amps) @ 2mA/cm^2**	**Total current I (Amps) @ 3mA/cm^2**
BT 1	10	25	1762.43	3.53	5.29
BT 2	12	25	1928.30	3.86	5.80
BT 3	10	40	1472.15	2.94	4.42
BT 4	12	40	1638.02	3.28	4.92

The current supplied to each concrete specimen was checked on a regular basis and any drift was corrected. Typical beam specimens subjected to accelerated corrosion are shown in Fig. 3.6. A close-up view of the corrosion acceleration is shown in Fig. 3.7.

Figure 3.6: Beam specimens being subjected to accelerated reinforcement corrosion.

Figure 3.7: A close-up view of the set-up utilized to accelerate reinforcement corrosion in the beam specimens.

3.8.5 Flexure testing of Beam Specimens

After curing, a set of 8 beam specimens was kept in control condition to prevent reinforcement corrosion. These eight control beam specimens were tested for determining the reference flexural strength.

The other 48 beam specimens that were subjected to accelerated reinforcement corrosion were tested to determine their residual flexural strength.

The beam specimens were tested as simply supported beams under a four-point loading system with a total span of 900 mm and a shear span of 350 mm. A schematic representation of the test set-up is shown in Fig. 3.8.

The flexure test was conducted using an Instron Universal Testing Machine of 250KN capacity at a slow loading rate of 1 mm/min. Fig. 3.9 shows test set-up. The load and midspan deflection data for each specimen was recorded using a computerized data acquisition system at pre-determined load intervals till failure. The data so generated was utilized to plot load-deflection curves for each of the tested specimens.

The control specimens and those corroded for different specified time periods (4, 6, and 8 days) are shown in Figs. 3.10 through 3.13.

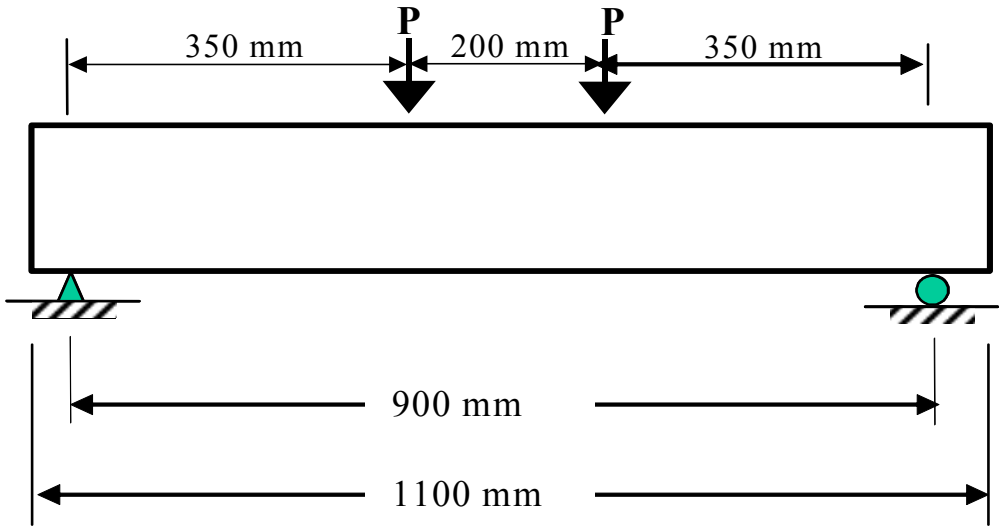

Figure 3.8: Set-up for four-point bend test of beam specimens.

Figure 3.9: Flexural strength test using Instron Universal Testing Machine.

Figure 3.10: Control beam specimen being tested in flexure.

Figure 3.11: A typical beam specimen being tested after
4 days of corrosion acceleration.

Figure 3.12: A typical beam specimen being tested after
6 days of corrosion acceleration.

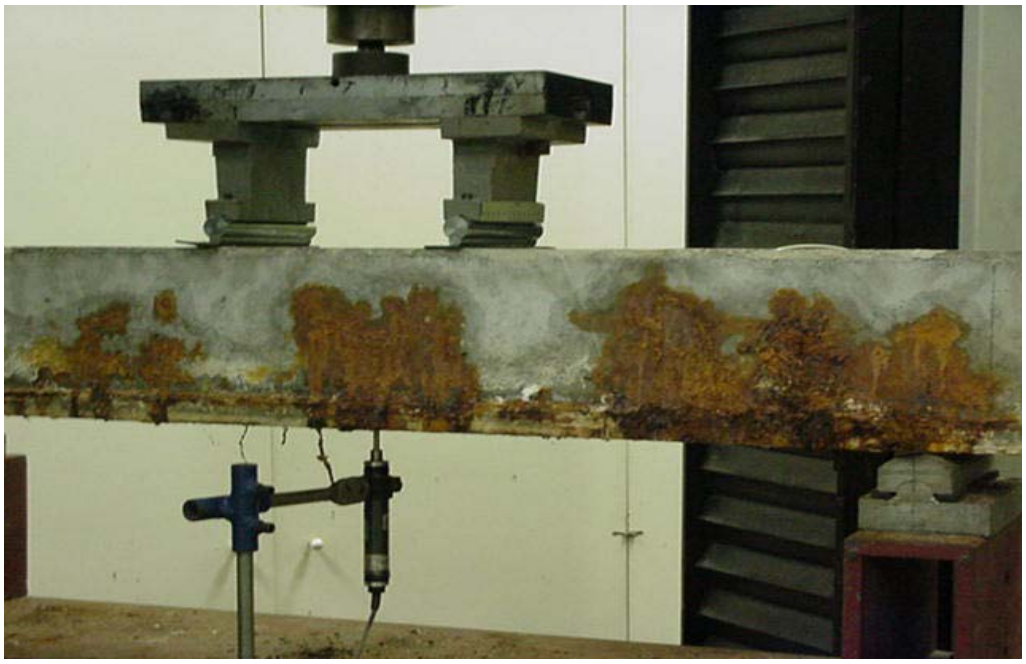

Figure 3.13: A typical beam specimen being tested after
8 days of corrosion acceleration.

3.8.6 Gravimetric Weight loss

Following the flexure test on a corroded beam, it was broken to remove the two corroded tension bars to measure the gravimetric weight loss due to induced corrosion. The bars were cleaned to remove the entire rust product using Clarke's solution and then they were weighed to determine the net weight of steel. Preparation, cleaning and evaluation of weight loss were carried out in accordance with ASTM G1 [44].

The percentage weight loss was calculated as:

$$\text{Percentage weight loss} = \frac{W_i - W_f}{W_i} \times 100 \tag{3.3}$$

Where:

W_i = initial weight of the bar before corrosion

W_f = weight after corrosion.

Since the current was applied through the stainless steel plates covering the entire length of the corroding bar, ensuring the efficient distribution of the current, it can be expected that the corrosion will be uniform along the entire embedded length. However, the presence of deformations and variation in permeability of the concrete results in some non-uniformity. Samples of corroded rebars after evaluating the gravimetric weight loss are shown in Figs. 3.14 and 3.15. These

figures reaffirm the general perception that corrosion, in general, is not expected to be uniform throughout the length of the bar, as the loss of rebar at some section is considerably higher than that at other sections.

Figure 3.14: 10 mm diameter corroded bars.

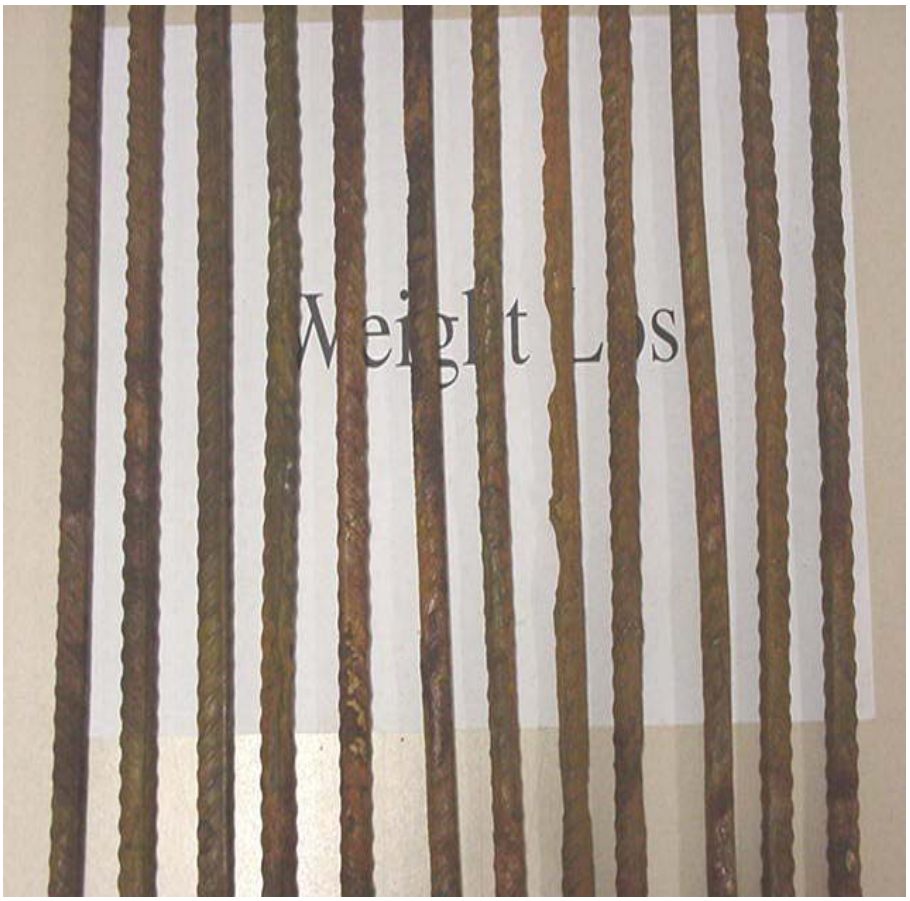

Figure 3.15: 12 mm diameter corroded bars.

CHAPTER 4

RESULTS AND DISCUSSION

4.1 COMPRESSIVE STRENGTH OF CONCRETE

The average values of 28-day compressive strength of concrete, f'_c, for each batch are shown in Table 4.1. It is observed that f'_c values varied from batch to batch, despite the use of same mix proportions, same materials, and similar casting procedure. The recorded values, average of three cylinders, varied from 33.4 MPa to 46.5 MPa with a standard deviation of 4.95.

4.2 TENSILE STRENGTH OF REINFORCING STEEL BARS

The stress-strain curves for the 10 mm and 12 mm reinforcing steel bars were obtained by plotting the tension test data. Typical stress-strain curves are shown in Figures 4.1 and 4.2. The values of yield and ultimate strengths (f_y and f_u) and the corresponding strains (ε_y and ε_u) for both bars, obtained from Figures 4.1 and 4.2, are presented in Table 4.2.

Table 4.1: Average 28-day compressive strength of concrete, for 10 batches.

Batch Number	Compressive Strength, f'_c (MPa)
1	37.7
2	44.7
3	44.2
4	35.7
5	36.9
6	33.4
7	40.9
8	46.5
9	46.5
10	45.8

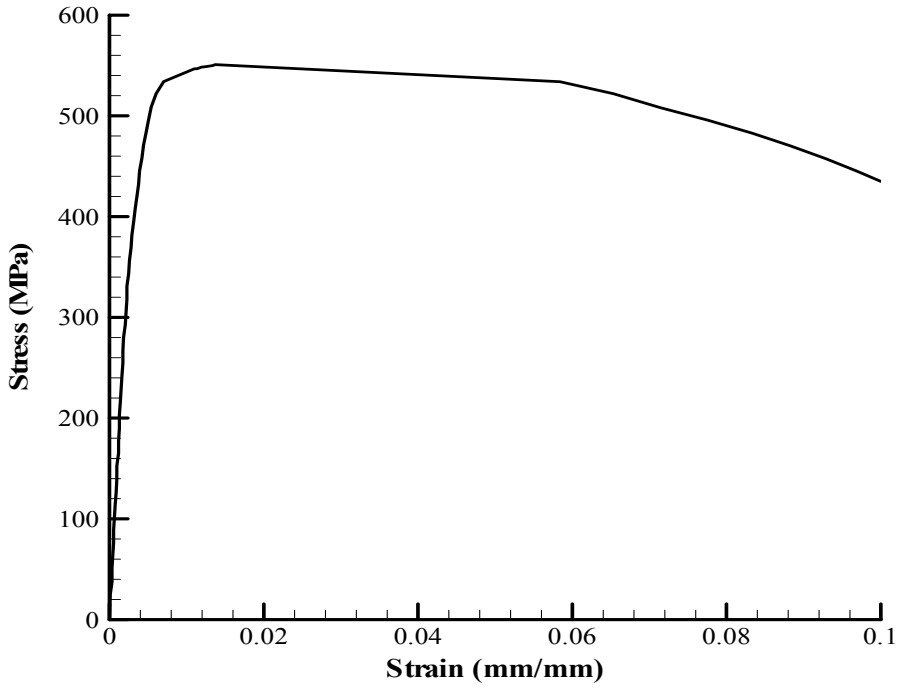

Figure 4.1: Stress-strain plot for 10 mm diameter reinforcing steel bar.

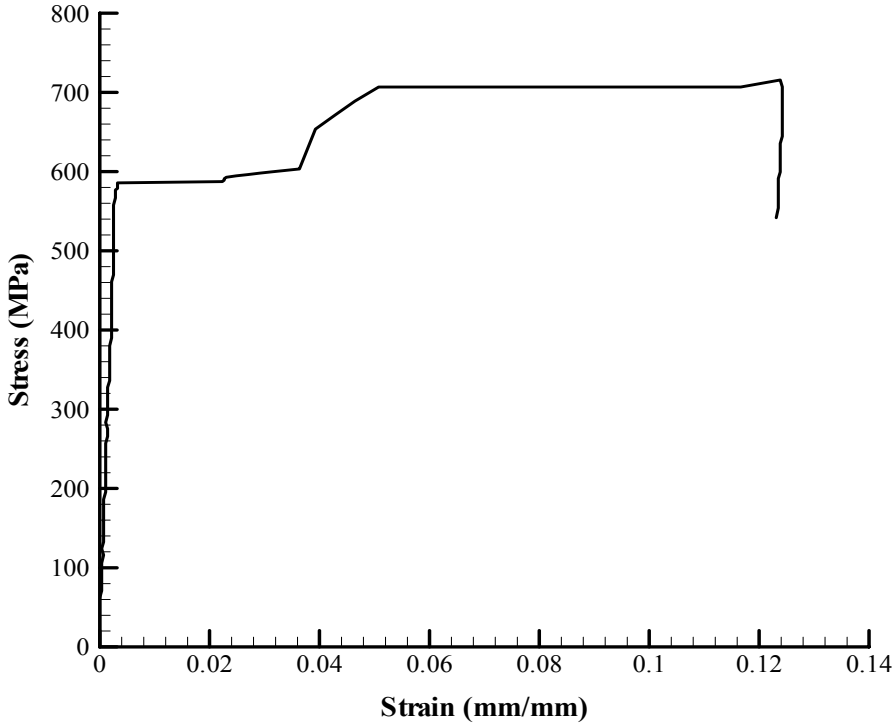

Figure 4.2: Stress-strain plot for 12 mm diameter reinforcing steel bar.

Table 4.2: Yield and Tensile strength and strain of steel bars.

Diameter, D (mm)	**Yield Strength, f_y (MPa)**	**Yield Strain, ε_y (mm/mm)**	**Tensile Strength, f_u (MPa)**	**Tensile Strain, ε_u (mm/mm)**
10	520	0.0054	551	0.0130
12	590	0.0030	700	0.0508

The stress-strain plots in Figures 4.1 and 4.2 indicate that the 12 mm diameter steel bar has a sharp yield point with distinct elastic, plastic and strain-hardening zones. The 10 mm diameter steel bar, however, shows no sharp yield. The yield stress for 10 mm diameter bars is calculated as 520 MPa, using offset method with a strain of 0.002.

4.3 FLEXURAL STRENGTH OF BEAM SPECIMENS

The average failure load, 2P, and the corresponding midspan deflection for the beam specimens were obtained by averaging the results of two beams tested in each case and are presented in Tables 4.3 and 4.4 for control and the corroded beams, respectively.

Table 4.3: Flexure Test Results of Control Beams.

Beam	f_c' (MPa)	Failure Load, 2P (KN)	Midspan Deflection (mm)
BT1-C	45.8	66.52	9.49
BT2-C	36.3	84.55	7.52
BT3-C	46.5	67.20	6.29
BT4-C	46.2	75.00	5.94

As expected, the load carrying capacity of the RC beam increased with an increase in the bar diameter. The highest load was noted in specimen BT2 (12 mm diameter rebar with a cover of 25 mm), while it was the least in the specimen BT1 (10 mm diameter rebar with a cover of 25 mm).

Table 4.4: Flexure Test Results of Corroded Beams.

Beam	f_c' (MPa)	Failure Load 2P (KN)	Midspan Deflection (mm)
BT1-2-4	38.9	61.00	7.69
BT1-3-4	36.9	58.00	9.40
BT1-2-6	45.8	59.79	6.31
BT1-3-6	46.5	52.30	8.22
BT1-2-8	33.4	44.70	6.29
BT1-3-8	46.5	37.02	4.24
BT2-2-4	39.9	72.93	5.86
BT2-3-4	35.7	68.39	6.35
BT2-2-6	44.5	59.57	4.36
BT2-3-6	44.2	60.28	6.29
BT2-2-8	44.7	50.76	5.71
BT2-3-8	37.7	48.51	4.74
BT3-2-4	40.2	62.42	9.70
BT3-3-4	35.7	58.24	7.43
BT3-2-6	33.4	56.44	4.33
BT3-3-6	44.2	53.05	6.28
BT3-2-8	33.4	52.10	5.61
BT3-3-8	33.4	37.70	5.51
BT4-2-4	36.9	68.74	5.98
BT4-3-4	46.5	62.47	6.83
BT4-2-6	46.5	57.26	6.64
BT4-3-6	40.9	51.30	5.65
BT4-2-8	40.9	51.41	4.28
BT4-3-8	37.7	43.24	4.96

Table 4.4 shows that both the failure loads and the mid-span deflections are affected by the duration and intensity of the applied current.

4.4 EFFECT OF CORROSION ON LOAD-DEFLECTION BEHAVIOR OF BEAMS

Typical load-deflection curves for both control and the corroded beam specimens are shown in Figures 4.3 through 4.6. The load-deflection curves for all control and corroded beams arranged with respect to the applied current and the duration are shown in Appendix I. The load-deflection curves representing the average of two specimens tested in each case for both the control specimens and the corroded reinforcement are compared in Figures 4.7 through 4.10. These data indicate that reinforcement corrosion has a marked influence on the flexural behavior of the concrete specimen. As expected the corroded beams had higher deflection than the corresponding control beams due to degrading stiffness of the beams. For example, at a load of 37 KN, beam BT1-3-8 recorded a midspan deflection of 4.20 mm, compared to 3.01 mm for the control beam BT1-C. The ultimate deflection of the beams, however, decreased with increasing reinforcement corrosion, leading to a reduction in the ductility of the beams.

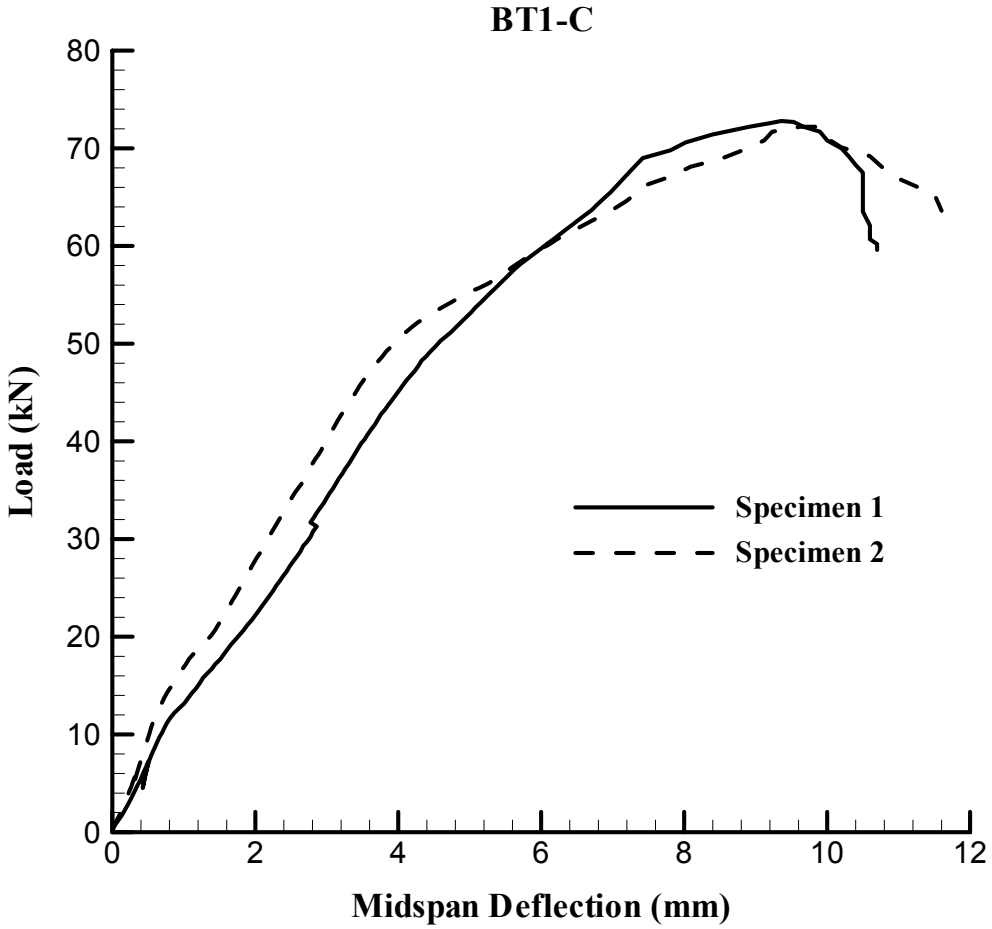

Figure 4.3: Typical Load-deflection plots for two control (BT1-C) specimens.

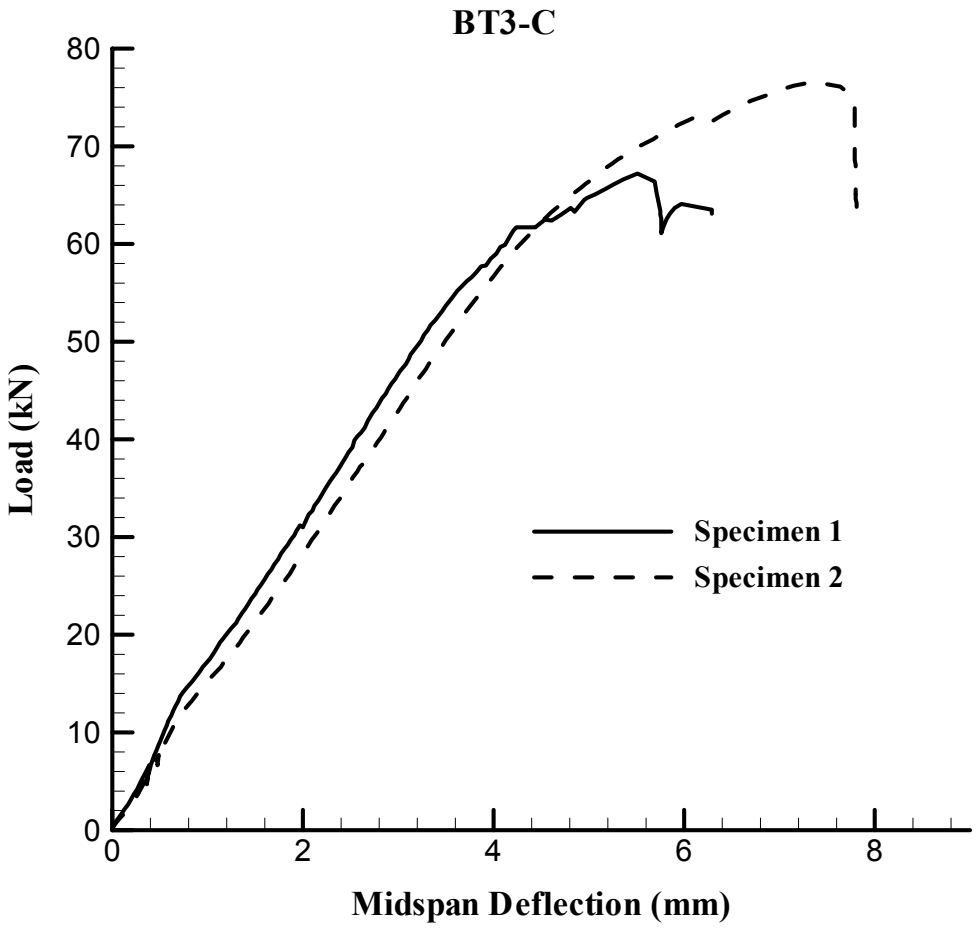

Figure 4. 4: Typical Load-deflection plots for two control (BT3-C) specimens.

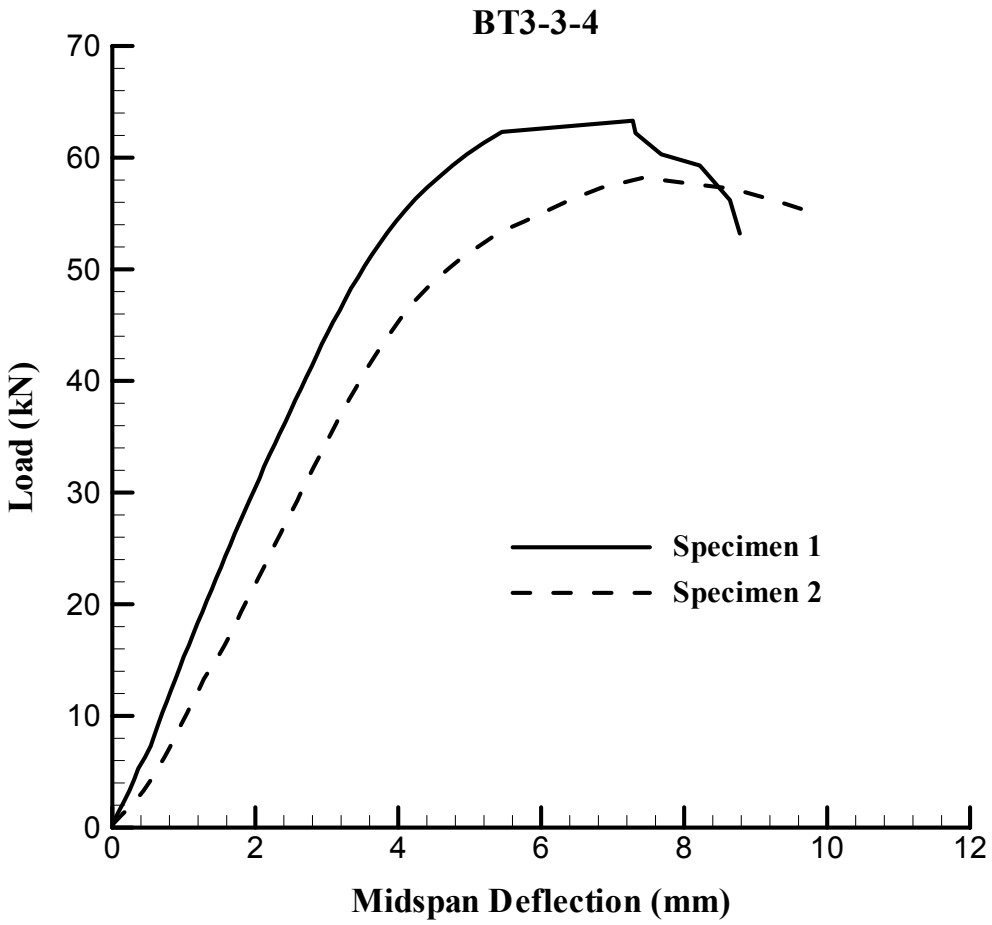

Figure 4. 5: Typical Load-deflection plots for two corroded (BT3-3-4) specimens.

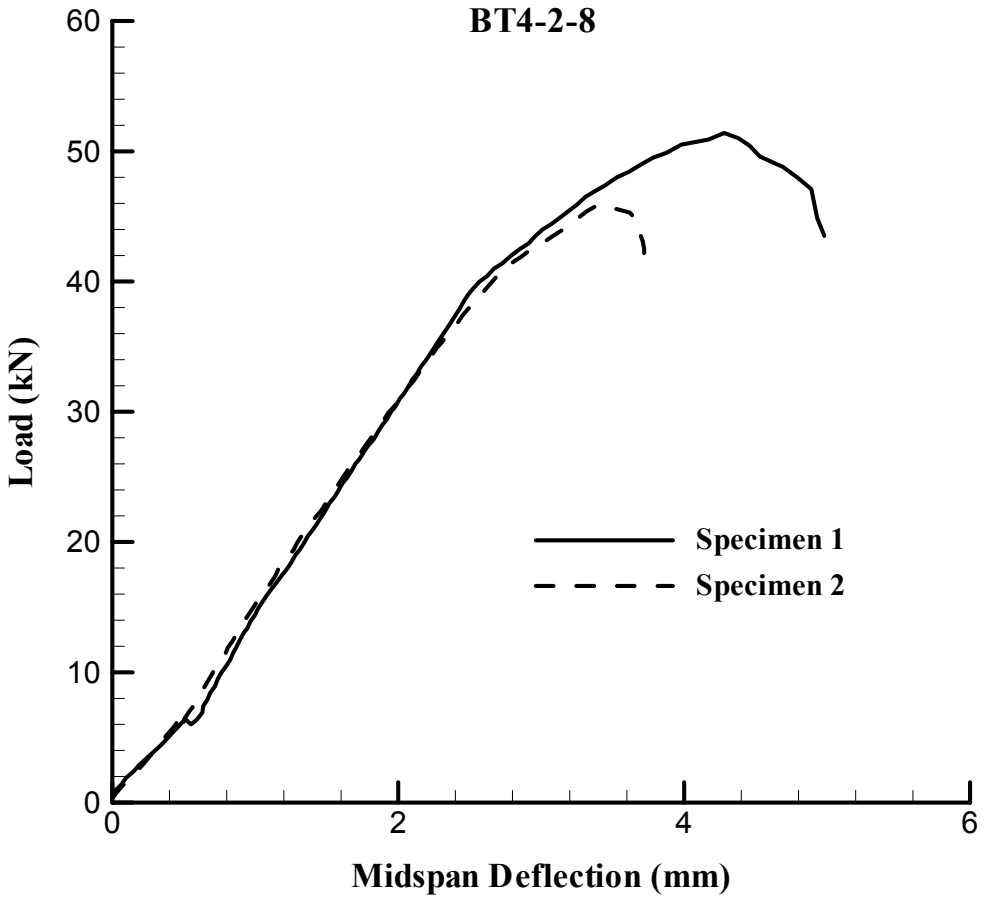

Figure 4. 6: Typical Load-deflection plots for two corroded (BT4-2-8) specimens.

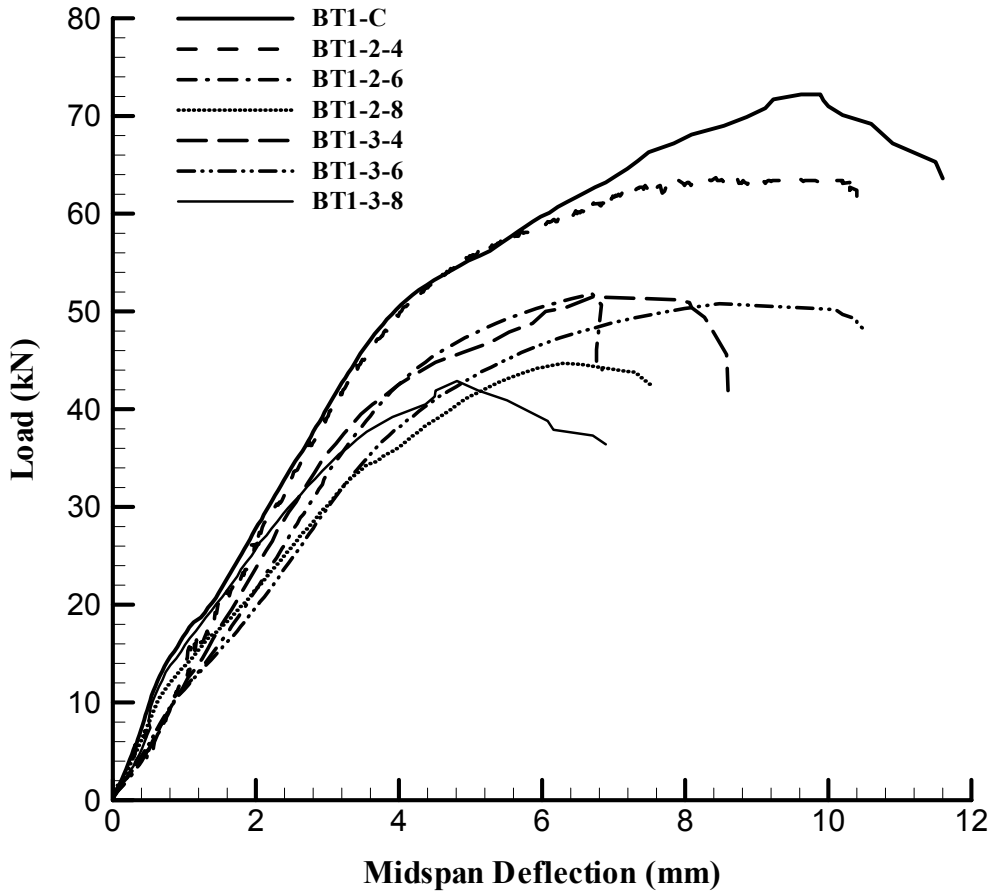

Figure 4. 7: Load-midspan deflection plot for BT1 subjected to different corrosion intensities.

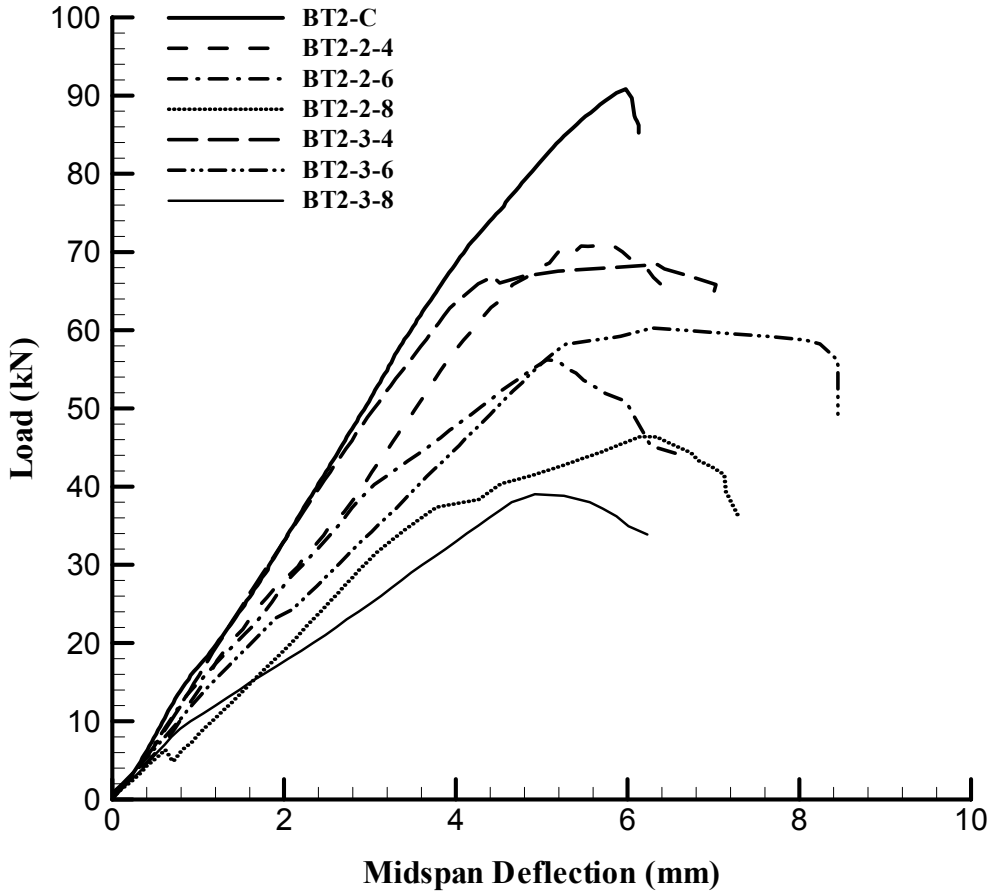

Figure 4. 8: Load-midspan deflection plot for BT2 subjected to different corrosion intensities.

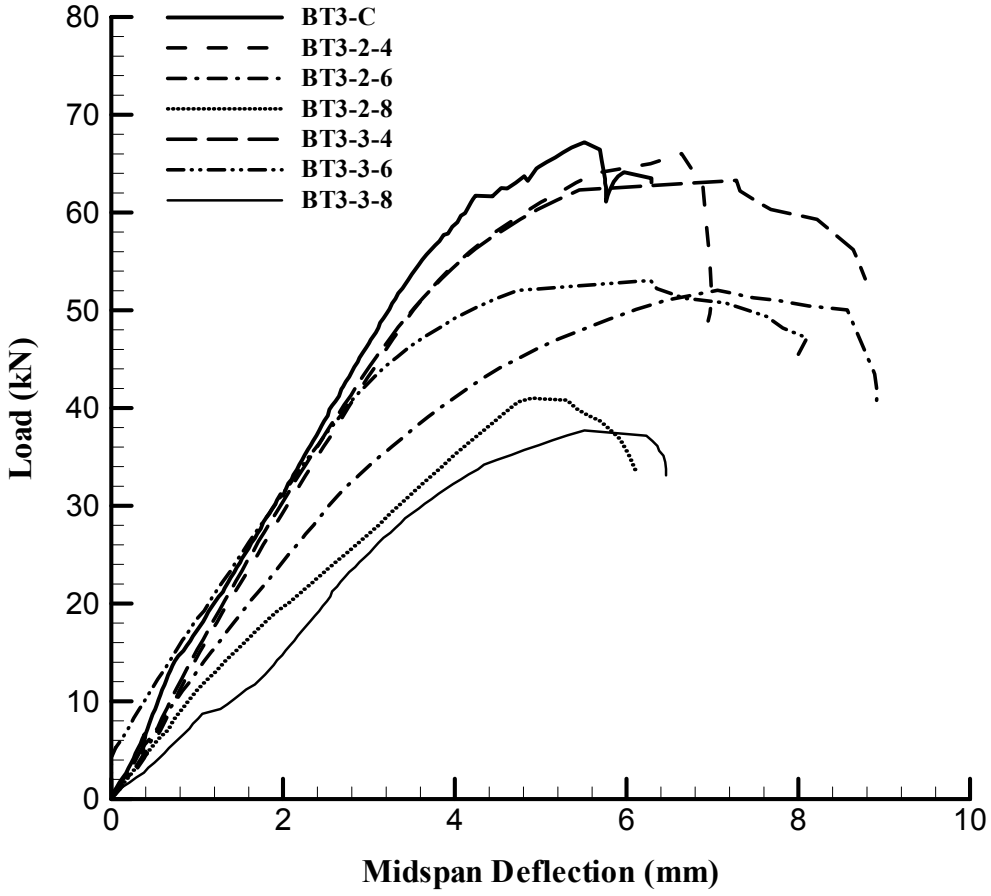

Figure 4. 9: Load-midspan deflection plot for BT3 subjected to different corrosion intensities.

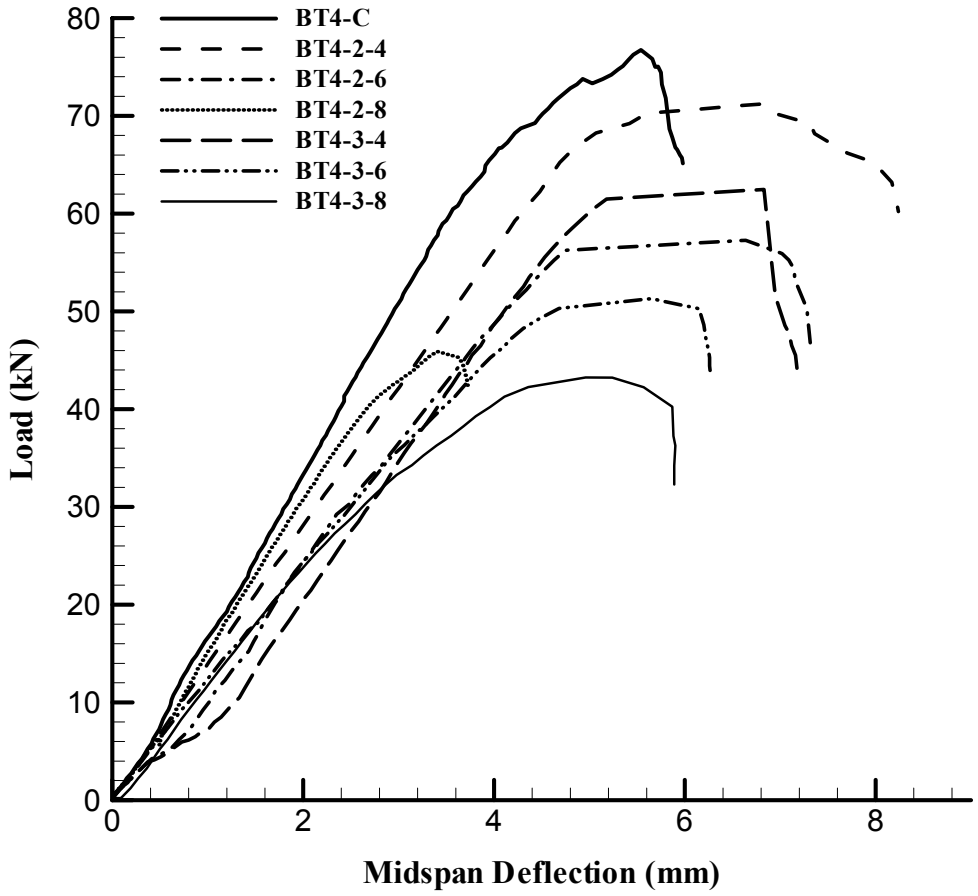

Figure 4. 10: Load-midspan deflection plot for BT4 subjected to different corrosion intensities.

Figures 4.7 through 4.10 show that load-deflection plots are virtually linear up to about 70 percent of the ultimate load and that the degradation or loss of stiffness of beams increases with increasing corrosion activity.

Apart from the loss of flexural capacity, reinforcement corrosion also produces higher deflection that my lead to serviceability problems. Both strength and serviceability, major concern for a corroding beam, get progressively impaired with increasing corrosion intensity.

4.5 EFFECT OF CORROSION ON THE DUCTILITY OF BEAMS

From the data in Figures 4.7 through 4.10, it is clear that as the corrosion intensity increases, there is a corresponding decrease in the ultimate deflection of the beams. This implies that the area under the load-deflection curves decreases with an increase in the corrosion intensity. Since the area under the load-deflection curve is an indication of the absorbed energy and ductility, the increase in the corrosion intensity decreases the absorbed energy and hence the ductility of the beams. This indicates that the corrosion not only affects the strength of the beams but also induces brittleness in their behavior. Hence, the large deformations, which occur in under-reinforced flexural members prior to failure, will not occur in the case of severely corroded reinforcement, thereby eliminating the most desirable warning before failure of the structure. Reduction in the ductility of beams made

with bars corroded to different intensities has also been reported by Uomoto et al. [45] and Uomoto and Misra [32].

4.6 WEIGHT LOSS OF BARS AND EQUIVALENT CORROSION CURRENT DENSITY

Corroded tensile steel bars from each of the four types of beams are compared with the original (uncorroded) bars in Figs. 4.11 through 4.14. The highest weight loss (34.8%) was in corroded rebars from BT3, while it was the lowest (20.7%) in BT4.

The measured weight loss was used to calculate the instantaneous corrosion rate (J_r) as follows:

$$J_r = \frac{\text{weight loss}}{\text{surface area of bar} \times \text{corrosion period}} \tag{4.1}$$

Calculated values of J_r were used to determine the equivalent corrosion current density (I_{corr}), using the following expression [46]:

$$J_r = \left(\frac{W}{F}\right) I_{corr} \tag{4.2}$$

where

W = equivalent weight of steel

F = Faraday's constant

Substituting W = 55.85/2 = 27.925 g and F = 96487 Coulombs (A-sec) in Eq. (4.2), the following simplified equation for calculating I_{corr} from the value of J_r is obtained:

$$I_{corr} = 0.1096\, J_r \tag{4.3}$$

where: I_{corr} is in mA/cm^2 and J_r is in gm/cm^2/year.

From Eqs. (4.1) and (4.2), the weight loss of a bar can be expressed as

$$\text{Weight loss/surface area of a bar} = \left(\frac{W}{F}\right) I_{corr} T = 0.289\, I_{cor} T \tag{4.4}$$

where: I_{corr} is in mA/cm^2 and T is in seconds.

The weight loss of a given bar is directly proportional to $I_{corr}T$, as W/F for steel is a constant.

The calculated values of equivalent I_{corr} from Eq. (4.3) are shown collectively for all corroded beams in Table 4.5. It is observed that the equivalent I_{corr} values established from gravimetric analysis are lower than the applied corrosion current density, I_{app}. Similar observations have been reported by other researchers [47-48]. The difference between I_{corr} and I_{app} can be attributed to several factors among which mention can be made of the concrete cover around the bars, quality of concrete, non-uniform corrosion rate along the length of the bars and the diameter of bars.

Figure 4.11: Corroded steel bars compared with original (uncorroded) bars from BT1 group. (Maximum Weight loss - 31 %).

Figure 4.12: Corroded steel bars compared with original (uncorroded) bars from BT2 group. (Maximum Weight loss - 25.5 %).

Figure 4.13: Corroded steel bars compared with original (uncorroded) bars from BT3 group. (Maximum Weight loss - 34.8 %).

Figure 4.14: Corroded steel bars compared with original (uncorroded) bars from BT4 group. (Maximum Weight loss - 20.7 %).

Table 4.5: Gravimetric weight loss and their conversion to $I_{corr.}$

Beam	Conversion of weight loss into I_{corr}								
	Gravimetric test results							J_r (Eq. 4.1) g/cm²/yr	I_{corr} (Eq.4.3) mA/cm²
	D, mm	I_{app}, mA/cm²	T d	Ave. length of sample, cm	Ave. original wt. of sample, g	Ave wt. Loss , g	ρ, % wt. loss		
BT1-2-4	10	2	4	41.77	249.95	13.5	5.40	9.37	1.03
BT1-3-4	10	3	4	38.90	232.78	33.0	14.20	24.83	2.72
BT1-2-6	10	2	6	46.10	275.86	42.0	15.20	17.96	1.97
BT1-3-6	10	3	6	42.20	252.52	54.0	21.40	25.00	2.74
BT1-2-8	10	2	8	39.65	237.26	51.0	21.50	19.94	2.18
BT1-3-8	10	3	8	46.40	277.66	86.0	31.00	27.33	2.99
BT2-2-4	12	2	4	41.07	350.74	19.5	5.50	11.40	1.25
BT2-3-4	12	3	4	42.10	359.53	31.5	8.80	17.92	1.96
BT2-2-6	12	2	6	47.12	402.40	80.9	20.10	27.35	2.99
BT2-3-6	12	3	6	45.00	384.30	53.9	14.00	19.07	2.09
BT2-2-8	12	2	8	43.70	373.20	85.3	22.90	23.53	2.58
BT2-3-8	12	3	8	50.90	434.70	111	25.50	23.88	2.62
BT3-2-4	10	2	4	41.47	248.16	19.8	8.00	13.88	1.52
BT3-3-4	10	3	4	43.75	261.80	23.7	9.10	15.75	1.73
BT3-2-6	10	2	6	44.85	268.40	27.2	10.10	11.72	1.28
BT3-3-6	10	3	6	44.20	264.50	46.5	17.60	20.18	2.21
BT3-2-8	10	2	8	47.40	283.64	60.7	21.40	18.41	2.02
BT3-3-8	10	3	8	45.35	271.37	94.4	34.80	28.54	3.13
BT4-2-4	12	2	4	38.62	329.80	26.1	7.90	15.81	1.74
BT4-3-4	12	3	4	41.05	350.60	38.3	10.90	22.69	2.49
BT4-2-6	12	2	6	45.05	384.73	51.4	13.40	18.52	2.03
BT4-3-6	12	3	6	40.85	348.86	64.8	18.60	25.60	2.80
BT4-2-8	12	2	8	42.95	366.80	66.0	18.00	19.01	2.08
BT4-3-8	12	3	8	39.30	335.62	69.6	20.70	21.60	2.37

4.7 RELATIONSHIP BETWEEN I_{corr} AND I_{app}

In theoretical prediction, it is assumed that corrosion starts as soon as the electrical energy is applied. This is true for bars suspended in liquid. But when the bars are embedded in concrete, because of the resistance provided by the concrete, certain amount of energy is needed to initiate the corrosion [47]. Hence, for laboratory tests using impressed current technique, I_{corr} calculated using gravimetric method will be less than the applied current density, I_{app}, as is evident from Table 4.5.

By comparing the values of I_{corr}, determined from the gravimetric weight loss method and the applied current density, I_{app}, an attempt has been made to relate I_{corr} and the I_{app} with the current efficiency, η, as

$$\eta = Efficiency\ of\ the\ applied\ current = \frac{I_{corr}}{I_{app}} \times 100 \tag{4.5}$$

The average current efficiency, η is calculated for both 10 mm and 12 mm diameter bars and is presented in Table 4.6.

From Table 4.6, the average value of η for 10 mm and 12 mm diameter bars is found to be 0.848 and 0.926, respectively. Yubun et al., [47] have reported a current efficiency of 0.293 for 19 mm diameter. Using this data, Table 4.7 is prepared to list the variation in current efficiency with rebar diameter.

Table 4.6: Relationship between I_{corr} and $I_{app.}$

Beam	%Weight Loss (Gravimetric)	I_{corr} (mA/cm^2)	I_{app} (mA/cm^2)	Current Efficiency η(%)	Average Efficiency η(%)
BT1-2-4	5.40	1.03	2	51.50	90.11
BT1-3-4	14.20	2.72	3	90.67	
BT1-2-6	15.20	1.97	2	98.50	
BT1-3-6	21.40	2.74	3	91.34	
BT1-2-8	21.50	2.18	2	109.00	
BT1-3-8	31.00	2.99	3	99.67	
BT2-2-4	5.50	1.25	2	62.50	93.89
BT2-3-4	8.80	1.96	3	65.34	
BT2-2-6	20.10	2.99	2	149.50	
BT2-3-6	14.00	2.09	3	69.67	
BT2-2-8	22.90	2.58	2	129.00	
BT2-3-8	25.50	2.62	3	87.34	
BT3-2-4	8.00	1.52	2	76.00	79.44
BT3-3-4	9.10	1.73	3	57.67	
BT3-2-6	10.10	1.28	2	64.00	
BT3-3-6	17.60	2.21	3	73.67	
BT3-2-8	21.40	2.02	2	101.00	
BT3-3-8	34.80	3.13	3	104.33	
BT4-2-4	7.90	1.74	2	87.00	91.30
BT4-3-4	10.90	2.49	3	83.00	
BT4-2-6	13.40	2.03	2	101.50	
BT4-3-6	18.60	2.80	3	93.33	
BT4-2-8	18.00	2.08	2	104.00	
BT4-3-8	20.74	2.37	3	79.00	

Table 4.7: Variation in Current efficiency with the rebar diameter.

D (mm)	Current Efficiency (η)	Source
10	0.848	Present Study
12	0.926	Present Study
19	0.293	Yabun et al. [47]

Using the data from Table 4.7, the value of η in terms of D, is obtained as

$$\eta = 66.81\ D^{-1.82}$$

$$\text{Hence, } I_{corr} = 66.81\ D^{-1.82}\ I_{app} \qquad (4.6)$$

As gravimetric weight loss for all the corroded bars was determined, the I_{corr} obtained using the measured weight loss, was used in this study.

4.8 EFFECT OF CHOSEN VARIABLES ON REINFORCEMENT CORROSION

The variables chosen in this study include: the applied current intensity, $I_{app;}$ duration of current application, T; reinforcement diameter, D; and the concrete cover, C_v. As discussed in Section 4.6, a difference exists between the applied current intensity, I_{app}, and the measured corrosion intensity, I_{corr}, in accelerated corrosion tests. In laboratory or field tests on corroded beams, I_{corr} is determined through Galvanostatic or Potentiostatic measurement and it is regarded as the key parameter of corrosion activity. In view of this, I_{corr} as determined through

gravimetric analysis is taken as the applicable value of corrosion current density for all computations.

From Eq. (4.4), it is noted that the weight loss of a bar is directly proportional to the product $I_{corr}T$, implying that a higher corrosion current density, I_{corr} for a lesser period of corrosion would be as damaging as a lesser value of I_{corr} for a longer corrosion period in terms of metal loss of a corroding bar. The product $I_{corr}T$ can be termed as *'corrosion activity index'*.

The values of $I_{corr}T$ and percentage weight loss, ρ of all beams, taken from Table 4.5, are presented in Table 4.8, in four groups with respect to diameter D and cover C_v.

The percentage weight loss of tension bars in each beam, ρ, is plotted with respect to $I_{corr}T$ in Fig. 4.15 for each group of data in Table 4.8.

Table 4.8: $I_{corr}T$ versus ρ Data for all Sets of C_v and D Values.

D=10mm;C_v=25mm		D=10mm;C_v=40mm		D=12mm;C_v=25mm		D=12mm;C_v=40mm	
$I_{corr}T$ (mA-days/cm^2)	**ρ** (% wt.loss)	**$I_{corr}T$** (mA-days/cm^2)	**ρ** (% wt.loss)	**$I_{corr}T$** (mA-days/cm^2)	**ρ** (% wt.loss)	**$I_{corr}T$** (mA-days/cm^2)	**ρ** (% wt.loss)
4.12	5.40	6.08	7.96	5.00	5.55	6.96	7.91
10.88	14.18	6.92	9.05	7.84	8.76	9.96	10.92
11.82	15.23	7.68	10.13	17.94	20.12	12.18	13.37
16.44	21.38	13.26	17.58	12.54	14.03	16.80	18.56
17.44	21.50	16.16	21.40	20.64	22.87	16.64	17.99
23.92	30.97	25.04	34.79	20.96	25.51	18.96	20.74

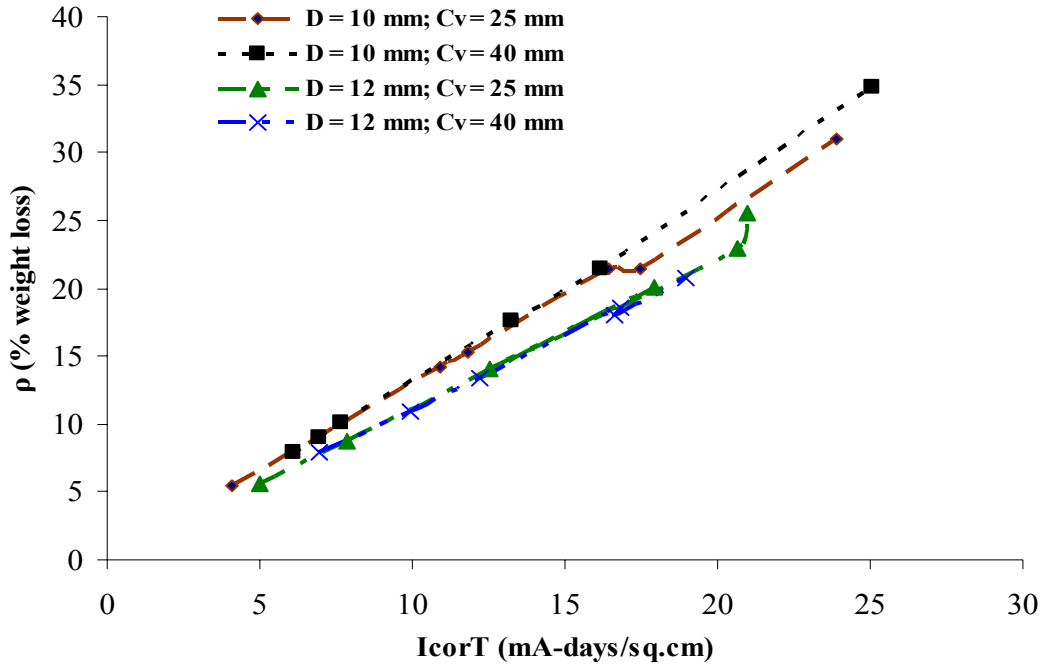

Figure 4. 15: Percentage weight loss versus $I_{corr}T$.

The following observations are made from Fig. 4.15:

(i) The plots of $I_{corr}T$ versus ρ (corrosion activity index versus percentage weight loss of bars) for the four groups of beams affirm a linear relationship between $I_{corr}T$ and ρ.

(ii) For a given $I_{corr}T$, ρ for a beam with 12mm diameter bars is less than that with 10mm diameter bars. This implies that percentage-wise metal loss will be smaller for higher diameter bars at a given value of $I_{corr}T$.

(iii) The effect of cover C_v on percentage weight loss appears to be insignificant.

Rasheeduzzafar et al. [28] have also reported that, although an increase in cover leads to a sharp reduction in corrosion in the range of ½ in. (12.7 mm) to 1 in. (25.4 mm) cover, no significant reduction in corrosion was indicated beyond the cover thickness of the order of 1.25 in. (32 mm).

4.9 EFFECT OF CORROSION ON LOAD CARRYING CAPACITY OF BEAMS

Using data from Table 4.4, and Table 4.5, Table 4.9 is prepared to list the strength of the corroded beams with respect to the control beams for varying degrees of corrosion (% weight loss). Table 4.9 shows that the degree of corrosion has a marked influence on the load carrying capacity of the beam specimens. Figure 4.16 shows the effect of the weight loss on the reduction in the load carrying capacity.

It can be observed from Fig. 4.16, that, there is a relatively sharp reduction in the load carrying capacity of a beam with increasing weight loss for both 10 mm and 12 mm diameter bars, the loss being comparatively more in 12 mm than in 10 mm diameter bars. Similar sharp reduction in strength with increasing weight loss has also been reported by Aziz [37] for slab specimens.

Table 4.9: Effect of percentage weight loss on Load carrying capacity of corroded beams.

Beam	% Weight Loss	Failure Load, 2P (KN)	Load (% of Control)	% Loss in load
BT1-2-4	5.40	61.00	91.70	8.30
BT1-3-4	14.20	58.00	87.19	12.81
BT1-2-6	15.20	59.79	89.88	10.12
BT1-3-6	21.40	52.30	78.62	21.38
BT1-2-8	21.50	44.70	67.20	32.80
BT1-3-8	31.00	37.02	55.65	44.35
BT2-2-4	5.50	72.93	86.26	13.74
BT2-3-4	8.80	68.39	80.89	19.11
BT2-2-6	20.10	59.57	70.46	29.54
BT2-3-6	14.00	60.28	71.30	28.70
BT2-2-8	22.90	50.76	60.04	39.96
BT2-3-8	25.50	48.51	57.37	42.63
BT3-2-4	8.00	62.42	92.89	7.11
BT3-3-4	9.10	58.24	86.67	13.33
BT3-2-6	10.10	56.44	83.99	16.01
BT3-3-6	17.60	53.05	78.94	21.06
BT3-2-8	21.40	52.10	77.53	22.47
BT3-3-8	34.80	37.70	56.10	43.90
BT4-2-4	7.90	68.74	91.65	8.35
BT4-3-4	10.90	62.47	83.30	16.70
BT4-2-6	13.40	57.26	76.35	23.65
BT4-3-6	18.60	51.30	68.40	31.60
BT4-2-8	18.00	51.41	68.55	31.45
BT4-3-8	20.70	43.24	57.65	42.35

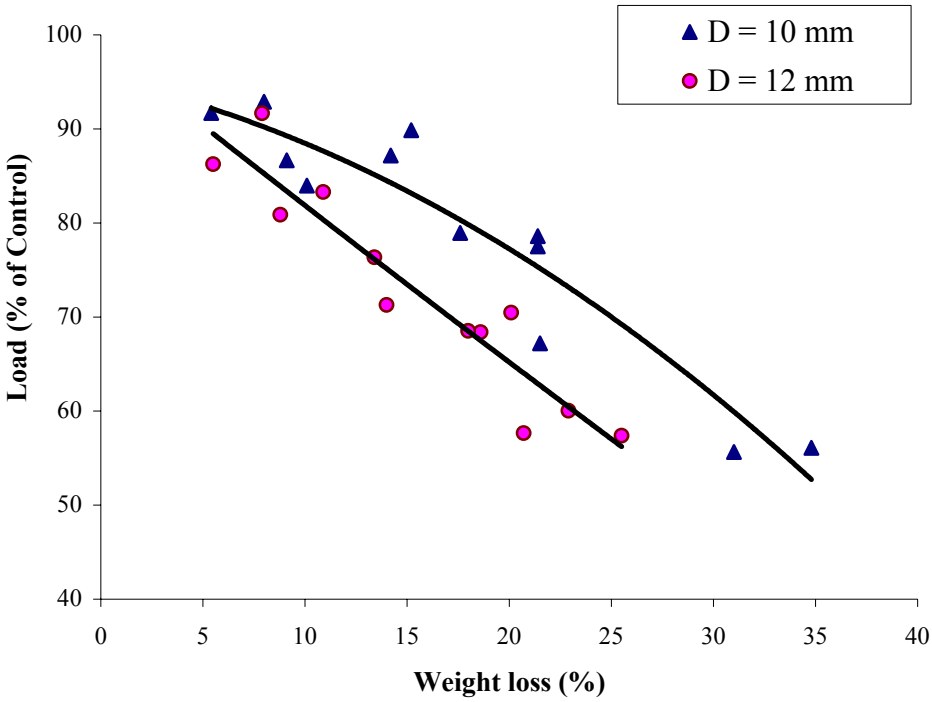

Figure 4. 16: Variation of load carrying capacity with percentage weight loss.

It can also be seen that in case of beams with 10 mm diameter bars, for about 30 % weight loss, the reduction in strength is around 40%, whereas a similar strength reduction is observed, in beams with 12 mm diameter bars at just around 20% weight loss. This implies that the strength of a corroded beam is significantly affected by the reinforcing bar diameter. The cover to the tension reinforcement, however, did not show any significant effect on the strength of a corroded beam for the range of cover investigated in this study.

4.10 EXPERIMENTAL FLEXURAL CAPACITY OF CONTROL BEAMS

Experimental values of ultimate moment capacity, $M_{ex,uc}$, for each control beam (BT1 to BT4) were calculated from simple statics as $M_{ex,uc}$ = 350P kN-mm, where P is the load applied to the beam (Fig. 3.7) at failure in kN and 350 mm is the shear span, i.e., the distance between the center of support and the load P. For each control beam, the average of two test beams was taken as the representative value of $M_{ex,uc}$.

The values of $M_{ex,uc}$, for the four control beams with varying C_V and D, are presented in Table 4.10.

Table 4.10: Average Experimental Moment Capacity of Control Beams.

Beam	f_c' **(MPa)**	P **(kN)**	$M_{ex,uc}$ **(kN-mm)**
BT1-C	45.8	36.25	11640
BT2-C	36.3	42.27	14795
BT3-C	46.5	33.60	11760
BT4-C	46.1	37.50	13125

4.11 EXPERIMENTAL FLEXURAL CAPACITY OF CORRODED BEAMS

The experimentally determined values of flexural strength of the corroded beams, $M_{ex,c}$, calculated in the same manner as for the control beams (i.e. $M_{ex,c}$ = 350P kN-mm), are shown collectively for all beams in Table 4.11. These values are the average of two test results.

The ratio of $M_{ex,c}/M_{ex,uc}$ multiplied by 100, designated as R, is indicative of the percentage residual strength, after loss due to reinforcement corrosion. The values of R for all corroded beams are shown in Table 4.11.

The values of f_c' as determined for all the batches (Table 4.1) show that corroded beams had values of f_c' somewhat different from the corresponding control beams. However, for calculation of R, the experimentally determined moment capacity for a control beam is assumed to be the same for all beams in the same group.

Table 4.11: Relationship between Experimental Moment Capacity Of Corroded and Uncorroded Beams.

Beam	$M_{ex,c}$ **(KN-mm)**	$M_{ex,uc}$ **(KN-mm) (from Table 4.10)**	$R = \frac{M_{ex,c}}{M_{ex,uc}} \times 100$
BT1-2-4	10675	11640	92
BT1-3-4	10150	11640	87
BT1-2-6	10463	11640	90
BT1-3-6	9152	11640	79
BT1-2-8	7823	11640	67
BT1-3-8	6478	11640	56
BT2-2-4	12762	14795	86
BT2-3-4	11968	14795	81
BT2-2-6	10433	14795	71
BT2-3-6	10549	14795	71
BT2-2-8	8883	14795	60
BT2-3-8	8489	14795	57
BT3-2-4	10923	11760	93
BT3-3-4	10192	11760	87
BT3-2-6	9875	11760	84
BT3-3-6	9284	11760	79
BT3-2-8	9118	11760	78
BT3-3-8	6598	11760	56
BT4-2-4	12030	13125	92
BT4-3-4	10932	13125	83
BT4-2-6	10021	13125	76
BT4-3-6	8978	13125	68
BT4-2-8	8997	13125	69
BT4-3-8	7567	13125	58

4.12 EFFECT OF CORROSION ACTIVITY INDEX ON RESIDUAL STRENGTH OF CORRODED BEAMS

Using data from Tables 4.5 and 4.10, Table 4.12 is prepared to list the values of $I_{corr}T$ and the percentage residual strength, R for all corroded beams, arranged into four groups with respect to D and C_V.

The values of R are plotted with respect to $I_{corr}T$ in Fig. 4.17 for each group of data in Table 4.12. As expected, R decreased with increasing $I_{corr}T$. With increasing $I_{corr}T$, the metal loss will be higher and this inevitably will reduce the residual flexural strength. As an example, for beams with D = 10 mm and C_V = 25 mm, the value of R decreased from 92% to 56% when $I_{corr}T$ increased from 4.12 to 23.92 mA-days/cm^2.

Table 4.12: $I_{corr}T$ versus R Data for all Sets of C_V and D Values.

D=10mm;C_V=25mm		D=10mm;C_V=40mm		D=12mm;C_V=25mm		D=12mm;C_V=40mm	
$I_{corr}T$ (mA-days/cm^2)	**R** (% residual strength)	**$I_{corr}T$** (mA-days/cm^2)	**R** (% residual strength)	**$I_{corr}T$** (mA-days/cm^2)	**R** (% residual strength)	**$I_{corr}T$** (mA-days/cm^2)	**R** (% residual strength)
4.12	92	6.08	93	5.00	86	6.96	92
10.88	87	6.92	87	7.84	81	9.96	83
11.82	90	7.68	84	17.94	71	12.18	76
16.44	79	13.26	79	12.54	71	16.80	68
17.44	67	16.16	78	20.64	60	16.64	69
23.92	56	25.04	56	20.96	57	18.96	58

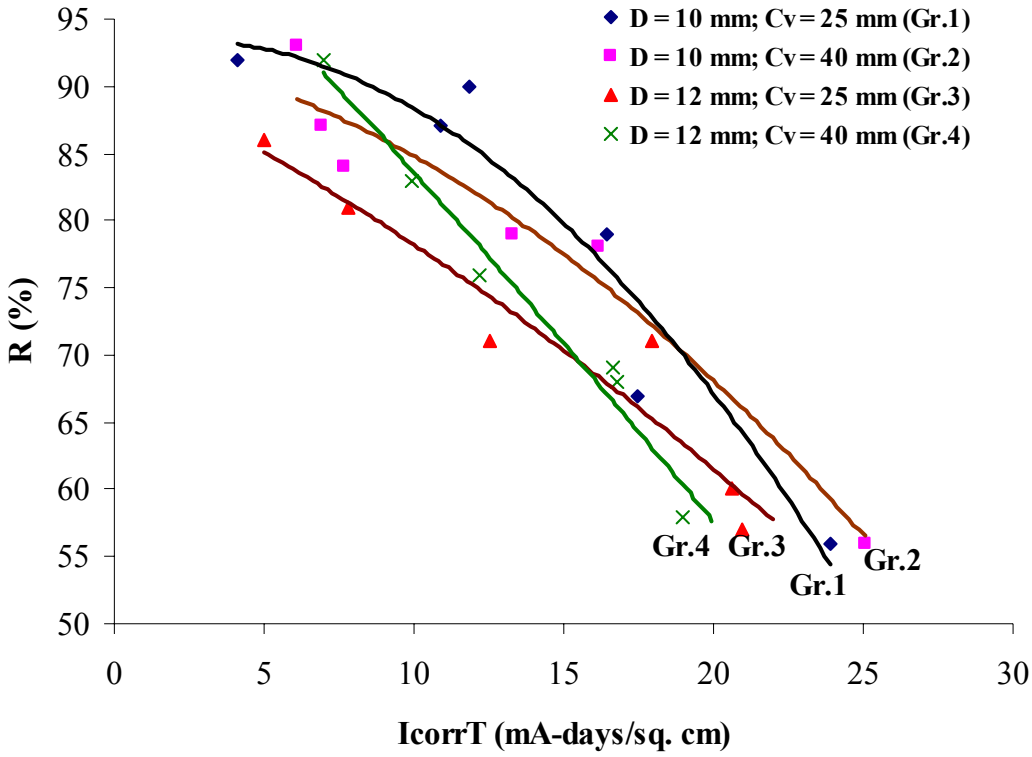

Figure 4.17: Variation of Residual Strength with $I_{corr}T$ and D.

A comparison of the plots for Gr.1 and Gr.2 (D = 10 mm, C_v = 25mm and D = 10mm, C_v = 40mm) and those for Gr.3 and Gr.4 shows that the value of R is not significantly affected by C_v, within the range of C_v considered, when $I_{corr}T$ exceeds say 12 mA-days/cm^2.

4.13 THEORETICAL FLEXURAL CAPACITY OF CONTROL BEAMS

The theoretical values of ultimate moment capacity of the control beams, $M_{th,uc}$, were calculated using conventional strength theory based on strain compatibility analysis, as the location of the top 8 mm bars was found to be within the tension zone and 10 mm bars showed nonlinear stress-strain relationship after the proportional limit. A typical calculation of $M_{th,uc}$ is presented in Appendix-II.

Table 4.13 lists the values of $M_{th,uc}$ as calculated together with the experimentally determined moment capacities, $M_{ex,uc}$ for the four control beams and the ratio of $M_{ex,uc}/M_{th,uc}$, designated as C_c.

Table 4.13: $M_{ex,uc}$, $M_{th,uc}$, and C_c for Four Control Beams.

Beam	f_c' **MPa**	$M_{th,uc}$ **kN-mm**	$M_{ex,uc}$ **N-mm**	$C_c = \frac{M_{ex,uc}}{M_{th,uc}}$
BT1-C	45.77	10476	11640	1.11
BT2-C	36.28	14015	14795	1.06
BT3-C	46.49	10146	11760	1.16
BT4-C	46.11	13404	13125	0.98

The results show that for beams with 12 mm diameter tension bars (BT2-C and BT4-C), C_c is close to 1.0, indicating high degree of accuracy for the theoretical predictions. However, for beams with 10 mm diameter bars (BT1-C and BT3-C), the values of C_c exceed 1.0 by over 10%, implying that the theoretical prediction was somewhat smaller than the actual strength.

4.14 FLEXURAL STRENGTH OF CORRODED BEAMS

The flexural strength of a corroded beam at a given value of $I_{corr}T$ is affected predominately by the following two phenomena:

(i) The loss of metal due to corrosion. The net cross-sectional area of a bar decreases with the loss of metal and this in turn would reduce the moment capacity of the beam.

(ii) Degradation of bond between reinforcement and concrete due to corrosion. Past research has emphatically shown that reinforcement corrosion leads to degradation of bond, following a small increase in strength at the early stage of corrosion. The loss of bond strength adversely affects the moment capacity of a corroded beam.

Additionally, Zhang et al. [49], Xi et al. [50], and Jin and Zhao [38] have reported that yield of a corroded bar is expected to increase. Uomoto et al. [45] evaluated the tensile strength of steel bars obtained from structures affected by reinforcement corrosion and reported that both the yield and ultimate strengths of corroded steel bars were within the range of 90-95% of the non-corroded bars. Also, Uomoto and Misra [32] conducted strength tests on the corroded bars from beams and columns exposed to marine environment for different periods and reported that the reduction in both the yield strength and the ultimate strength of steel bars ranged from 5 to 10 % of the original bars. Aziz [37] investigated the

effect of corrosion on the tensile strength of reinforcing bars and found that net tensile strength of bars is marginally affected due to corrosion. Almusallam [51] stated that the yield strength of the clean bars and those corroded to 75% weight loss as 796 MPa and 741 MPa, respectively. In view of the past contradicting findings, the original yield strength of bars has been used in all calculations.

The flexural capacity of a corroded beam is first calculated in the same manner as the control beams but using reduced diameter of tension bars D' due to corrosion in place of the original diameter, D. Any adverse implication of possible bond loss between reinforcement and concrete from corrosion on moment capacity has been ignored for this calculation.

The reduced diameter D' is calculated from the well-known formula for metal loss rate or penetration rate, P_r, given as [46]:

$$P_r = \frac{W}{F\gamma_{st}} I_{corr} = \frac{J_r}{\gamma_{st}} \tag{4.7}$$

Where:

γ_{st} = density of steel = 7.85 g/cm^3,

J_r = instantaneous corrosion rate, in g/cm^2/year,

W = equivalent weight of steel = 55.85/2 = 27.925 g, and

F = Faraday's constant = 96487 Coulombs (Amp-sec).

The reduction in bar diameter in active corrosion with steady-state corrosion current density I_{corr} for corrosion period T is $2P_rT$ and the percentage reduction in diameter of bar is $\frac{2P_rT}{D}\times 100$, where D is the original bar diameter. The reduced net diameter of a corroded bar, D', is then written as:

$$D' = D\left(1-\frac{2P_rT}{D}\right) \tag{4.8}$$

In terms of cross-sectional area, Eq. (4.8) can be recast for calculating the reduced cross-sectional area A_s' as:

$$A_s' = A_s(1-\alpha)^2 \tag{4.9}$$

where A_s is the original cross-sectional area of the bar and $\alpha = 2P_rT/D$, which can be better termed as 'metal loss factor'.

From Eqs. (4.4) and (4.7), the percentage weight loss ρ can be shown to be equal to (2α) times 100. In other words, the ratio of weight loss to the original weight of a bar equals 2α or twice the metal loss factor.

Using A_s' in place of A_s, $M_{th,c}$ values of all corroded beams were calculated using strain compatibility analysis for which a sample calculation is shown in

Appendix-II. The calculated values of $M_{th,c}$ are presented in Table 4.14 along with the values of C_f, which is the ratio of $\frac{M_{ex,c}}{M_{th,c}}$.

Two important observations can be made from the trend of the values of C_f for beams. Firstly, C_f value progressively declines with increasing $I_{corr}T$ for each type of beam BT1 to BT4. This implies that the prediction of flexural strength, based only on the use of reduced cross-sectional area of steel reinforcement A_s', calculated from Eq. (4.8), would not yield satisfactory results for higher values of $I_{corr}T$, i.e. with higher degree of corrosion or metal loss. Higher $I_{corr}T$ will cause more corrosion damage that would result in loss of bond between steel and concrete. The moment capacity of a corroded beam, therefore, cannot be calculated simply on the basis of A_s' alone at a higher $I_{corr}T$, for which bond effect must be taken into account.

Secondly, it is also observed that C_f values at lower $I_{corr}T$ (Table 4.14) are closer to 1.0, or greater than 1.0 for beams reinforced with 10 mm diameter bars (BT1 and BT3 groups). This observation lends support to the postulation that moment capacity of a corroded beam at a low value of $I_{corr}T$ can be calculated with an acceptable degree of accuracy using only A_s' from Eq. (4.9) and ignoring any implication of bond. This is consistent with the prevailing notion that at the early stage of corrosion, bond loss is minimal or there may be a small increase in bond strength.

Table 4.14: D′, $M_{ex,c}$, $M_{th,c}$ and C_f for the Corroded Beams.

Beam	C_v (mm)	D (mm)	$I_{corr}T$ (mA-d/cm^2)	f'_c (MPa)	D′ (Eq.4.8) (mm)	$M_{th,c}$ (KN-mm)	$M_{ex,c}$ (KN-mm)	$C_f = \frac{M_{ex,c}}{M_{th,c}}$
BT1-2-4	25	10	4.12	38.9	9.74	9685	10675	1.10
BT1-3-4	25	10	10.88	36.9	9.31	8952	10150	1.13
BT1-2-6	25	10	11.82	45.8	9.25	9380	10463	1.11
BT1-3-6	25	10	16.44	46.5	8.95	8998	9152	1.01
BT1-2-8	25	10	17.44	33.4	8.89	8167	7823	0.95
BT1-3-8	25	10	23.92	46.5	8.47	8353	6478	0.77
BT2-2-4	25	12	5.00	39.9	11.68	13654	12762	0.93
BT2-3-4	25	12	7.84	35.7	11.50	13039	11968	0.92
BT2-2-6	25	12	17.94	44.5	10.85	12398	10433	0.84
BT2-3-6	25	12	12.54	44.2	11.20	13018	10549	0.81
BT2-2-8	25	12	20.64	44.7	10.69	12128	8883	0.73
BT2-3-8	25	12	20.96	37.7	10.67	11687	8489	0.72
BT3-2-4	40	10	6.08	40.2	9.61	9324	10923	1.17
BT3-3-4	40	10	6.92	35.7	9.56	8828	10192	1.15
BT3-2-6	40	10	7.68	33.4	9.51	8540	9875	1.15
BT3-3-6	40	10	13.26	44.2	9.15	8959	9284	1.03
BT3-2-8	40	10	16.16	33.4	8.97	8038	9118	1.13
BT3-3-8	40	10	25.04	33.4	8.41	7547	6598	0.87
BT4-2-4	40	12	6.96	36.9	11.56	11923	12030	1.01
BT4-3-4	40	12	9.96	46.5	11.37	12540	10932	0.87
BT4-2-6	40	12	12.18	46.5	11.22	12333	10021	0.81
BT4-3-6	40	12	16.80	40.9	10.93	11462	8978	0.78
BT4-2-8	40	12	16.64	40.9	10.94	11475	8997	0.78
BT4-3-8	40	12	18.96	37.7	10.79	10979	7567	0.69

The values of C_f and $I_{corr}T$ from Table 4.14 are plotted in Fig. 4.18 for each group of beams to show the decline in C_f values with $I_{corr}T$.

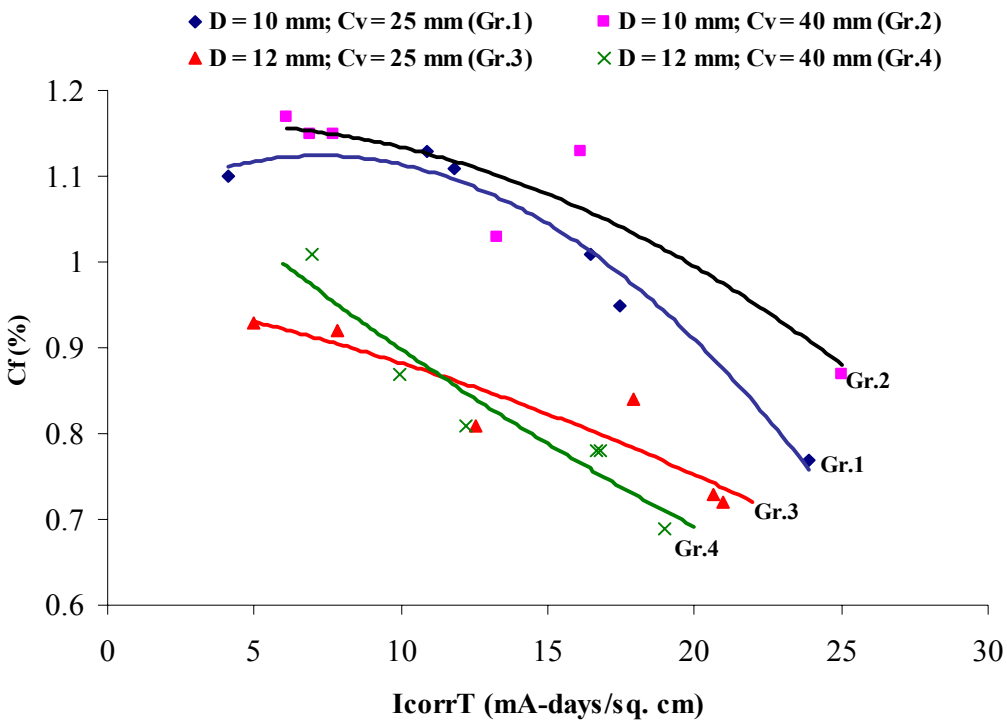

Figure 4.18: Variation of C_f with $I_{corr}T$ and D.

The comparison of two plots of beam groups BT1 and BT3 (beams with 10 mm diameter bars) and of the plots for beam groups BT2 and BT4 (beams with 12 mm diameter bars) shows that the effect of cover C_v does not have appreciable effect on C_f values within the range of $I_{corr}T$ between 8 and 20 mA-days/cm^2.

4.15 POST-CRACKING COMPLIANCE OF CORRODED BEAMS

An attempt has been made to compute the post-cracking compliance (inverse of the slope of the linear part of *P*-δ plots) of the beam at the linear part of the load-deflection plot to see how the compliance is affected through corrosion induced damage.

The measured values of compliance in mm/N are shown in Table 4.15 for all beams. Results show that compliance increases with increasing $I_{corr}T$, as the beam stiffness gradually degrades. For the beam type BT1, the compliance increased from 0.074 to 0.122 mm/N, when $I_{corr}T$ was increased from 4 to 24 mA-days/cm^2.

4.16 MODE OF FAILURE OF CONTROL AND CORRODED BEAMS

Figures 4.19 and 4.20 show the crack pattern in a control beam and a corroded beam prior to failure. Essentially a flexure or flexure-shear type failure was observed in all the beams, in which the cracks advanced towards the top with new cracks emerging. Failure was assumed to occur when the applied load on the beams began to drop, with increasing midspan deflection.

Table 4.15: Measured Values of Compliance for Corroded Beams.

Beam	$I_{corr}T$ (mA-days/cm^2)	Compliance (mm/N)
BT1-2-4	4.12	0.074
BT1-3-4	10.88	0.073
BT1-2-6	11.82	0.076
BT1-3-6	16.44	0.088
BT1-2-8	17.44	0.109
BT1-3-8	23.92	0.122
BT2-2-4	5.00	0.061
BT2-3-4	7.84	0.066
BT2-2-6	17.94	0.071
BT2-3-6	12.54	0.072
BT2-2-8	20.64	0.088
BT2-3-8	20.96	0.118
BT3-2-4	6.08	0.103
BT3-3-4	6.92	0.078
BT3-2-6	7.68	0.090
BT3-3-6	13.26	0.079
BT3-2-8	16.16	0.101
BT3-3-8	25.04	0.105
BT4-2-4	6.96	0.070
BT4-3-4	9.96	0.069
BT4-2-6	12.18	0.068
BT4-3-6	16.8	0.068
BT4-2-8	16.64	0.064
BT4-3-8	18.96	0.100

The vertical shear reinforcement provided throughout the length of the specimens served its purpose by safeguarding against any unwanted premature shear failure. As the tension bars were anchored well at ends, no premature slip of bars occurred in any of the beams tested.

Figure 4. 19: Failure of a Typical Control Beam (BT1-C).

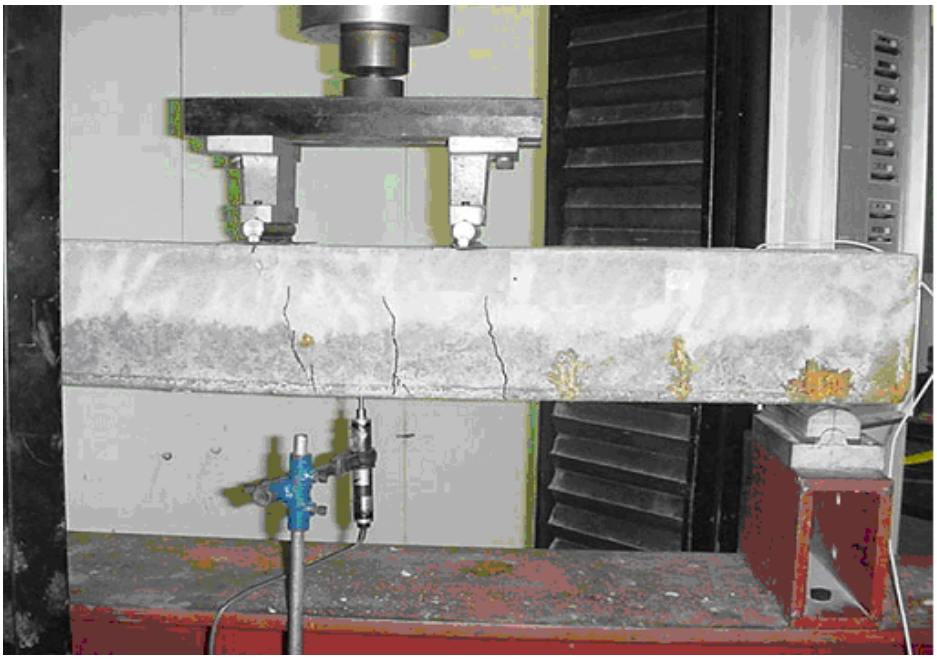

Figure 4. 20: Failure of a Typical Corroded Beam (BT1-3-4).

CHAPTER 5

PREDICTION OF RESIDUAL FLEXURAL STRENGTH OF CORRODED BEAMS

An attempt has been made to utilize the experimental data gathered in this study for proposing a predictive model for the estimation of the residual flexural strength of beams that are subjected to reinforcement corrosion.

5.1 BASIS FOR THE DEVELOPMENT OF THE MODEL

The prediction model for the residual flexural strength of corroded reinforced concrete beams was developed on the basis of the following observations, as discussed in Chapter 4:

(i) Degree of corrosion increases with increasing corrosion activity index, $I_{corr}T$, and consequently flexural strength of a corroded beam decreases with increasing $I_{corr}T$.

(ii) For a constant $I_{corr}T$, the percentage loss of metal and hence the cross-sectional area is smaller for a large diameter bars compared to the smaller diameter bars.

(iii) The effect of reinforcement cover, within the range considered in this study, has a small effect on metal loss at a constant $I_{corr}T$.

(iv) The values of C_f, determined on the basis of theoretical moment capacity, calculated using reduced cross-sectional area A_s' from Eq. (4.9), shows that such theoretical prediction would be inaccurate at higher $I_{corr}T$, if loss of bond is not addressed.

5.2 STRENGTH PREDICTION MODEL

The following **two-step** procedure is proposed to predict the residual strength of a corroded beam for which the cross-sectional details, materials strengths, corrosion activity index, $I_{corr}T$ and diameter of rebar, D are known:

(i) First, moment capacity, $M_{th,c}$ is calculated using reduced cross-sectional area of tensile reinforcement, A_s', calculated from Eq. (4.9).

(ii) The computed value of $M_{th,c}$ is then multiplied by a correction factor, C_f to obtain the predicted residual strength of the beam, M_{res}, as follows:

$$M_{res} = C_f M_{th,c} \tag{5.1}$$

The value of C_f reflects the effect of bond and the necessary correlation between M_{res} and $M_{th,c}$.

The proposed value of C_f is taken as a function of two important variables namely, $I_{corr}T$ and D. Based on the experimental observations and several trials, C_f is taken in the following empirical form

$$C_f = \frac{A}{(I_{corr}T)^m D^n} \tag{5.2}$$

A, m and n are constants that are determined through a multi-level regression of test data for C_f (Table 4.13).

Regression analysis with a best fit (regression coefficient = 0.906) yielded the values of constants as: A = 14.7, m = 0.15 and n = 1.0. Thus, the proposed equation for C_f is:

$$C_f = \frac{14.7}{D(I_{corr}T)^{0.15}} \tag{5.3}$$

where, D = diameter of rebar in mm; I_{corr} = corrosion current density in mA/cm^2 and T = duration of corrosion in days

The C_f values for all the 24 corroded beams are calculated by substituting $I_{corr}T$ and D values in Eq. (5.3). The residual flexural strength, M_{res}, for all the 24 corroded beams are calculated from Eq. (5.1) using the values of $M_{th,c}$ (Table 4.11). The values of C_f, $M_{ex,c}$ and predicted M_{res} for all the 24 corroded beams are presented in Table 5.1.

Table 5.1: Values of C_f, $M_{th,c}$, $M_{ex,c}$ and M_{res}.

Beam	C_f (Eq.5.3)	$M_{th,c}$ (KN-mm)	Measured $M_{res} = M_{ex,c}$ (KN-mm)	Predicted M_{res} (KN-mm)	% Error $\frac{(M_{ex,c} - M_{res})}{M_{ex,c}} \times 100$
BT1-2-4	1.19	9685	10675	11525	-7.96
BT1-3-4	1.03	8952	10150	9221	9.16
BT1-2-6	1.01	9380	10463	9474	9.45
BT1-3-6	0.97	8998	9152	8728	4.63
BT1-2-8	0.96	8167	7823	7840	-0.22
BT1-3-8	0.91	8353	6478	7601	-17.34
BT2-2-4	0.96	13654	12762	13108	-2.71
BT2-3-4	0.90	13039	11968	11735	1.95
BT2-2-6	0.79	12398	10433	9794	6.12
BT2-3-6	0.84	13018	10549	10935	-3.66
BT2-2-8	0.78	12128	8883	9460	-6.49
BT2-3-8	0.78	11687	8489	9116	-7.38
BT3-2-4	1.12	9324	10923	10443	4.40
BT3-3-4	1.10	8828	10192	9711	4.72
BT3-2-6	1.08	8540	9875	9223	6.60
BT3-3-6	1.00	8959	9284	8959	3.50
BT3-2-8	0.97	8038	9118	7797	14.49
BT3-3-8	0.91	7547	6598	6868	-4.09
BT4-2-4	0.92	11923	12030	10969	8.82
BT4-3-4	0.87	12540	10932	10910	0.20
BT4-2-6	0.84	12333	10021	10360	-3.38
BT4-3-6	0.80	11462	8978	9170	-2.13
BT4-2-8	0.80	11475	8997	9180	-2.03
BT4-3-8	0.79	10979	7567	8673	-14.62

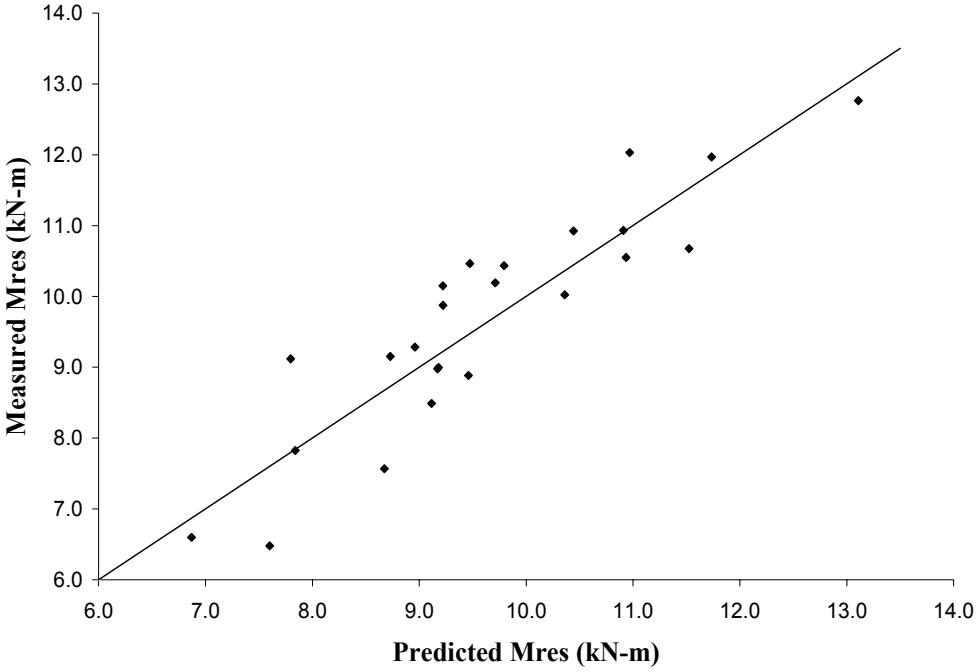

Figure 5.1: Comparison of Measured M_{res} and the Predicted M_{res}.

From Table 5.1, it is to be noted that out of total 24 predicted values of M_{res}, 21 values have less than 10% error. In more than 50% cases, the error is less than 5%. Also, the measured values of the residual strength M_{res} and the predicted values of M_{res} for all corroded beams that are plotted in Fig. 5.1, shows a reasonably good correlation between the predicted and measured values of M_{res}.

The proposed strength prediction model can be utilized either to find the residual flexural capacity of a beam that has suffered corrosion damage or to find the limit of I_{corr} for a given corrosion period that can be permitted for a beam at a

lowest level of compromised safety. The latter has practical significance, as I_{corr} is measured in-situ for a beam to determine the level of corrosion activity. The proposed model allows to predetermine the maximum level of $I_{corr}T$ or I_{corr} for a given T at which the residual moment capacity of a beam is expected to reach the minimum safe value.

The utility of the proposed strength prediction model can be explained through the following two examples:

Example # 1

A reinforced concrete beam (effective depth = 250mm, width = 200mm, A_s = 4 bars of 12 mm each, f_c' = 40 N/mm^2 and f_y = 500 N/mm^2) has been subjected to an active corrosion for a period of 25 years. The measured I_{corr} = 1 μA/cm^2. Determine the percentage residual flexural strength of the beam.

Solution:

T = 25 years = 9125 days

I_{corr} = 1 μA/cm^2 = 0.001 mA/cm^2

$I_{corr}T$ = $0.001 \times 9125 = 9.125$ mA-days/cm^2

D = 12 mm

A_s = $4 \times \frac{\pi}{4}(12)^2 = 452.4$ mm^2

$$M_{th,uc} = f_y A_s \left[d - \frac{a}{2} \right] = f_y A_s \left[d - \frac{0.5 f_y A_s}{0.85 b f'_c} \right]$$

$$= 500 \times 452.4 \left[250 - \frac{0.5 \times 500 \times 452.4}{0.85 \times 200 \times 40} \right]$$

$$= 52.78 \times 10^6 \text{ N-mm} = 52.78 \text{ kN-m}$$

From Eq. (4.7), $P_r = 3.1854 \times 10^{-5}$ mm/d

$$\alpha = 2 P_r T/D = 0.0484$$

From Eq. (4.9), $A_s' = 410$ mm^2

$$M_{th,c} = f_y A'_s \left[d - \frac{a'}{2} \right] = f_y A'_s \left[d - \frac{0.5 f_y A'_s}{0.85 b f'_c} \right]$$

$$= 500 \times 410 \left[250 - \frac{0.5 \times 500 \times 410}{0.85 \times 200 \times 40} \right]$$

$$= 48.16 \times 10^6 \text{ N-mm} = 48.16 \text{ kN-m}$$

From Eq. (5.3), correction factor C_f is calculated as: $C_f = 0.879$

From Eq. (5.1), the predicted residual strength of the beam,

$$M_{res} = 48.16 \times 0.879 = 42.34 \text{ kN-m.}$$

Percentage residual flexural strength of the beam is calculated as:

$$R = (M_{res}/M_{th,uc})100 = (42.34/52.78)\ 100 = 80.22\%$$

Example # 2

Specify the permissible limit of I_{corr} so that the flexural strength of a beam (effective depth = 250 mm, breadth = 200 mm, A_s = 4 bars of 12 mm each, f_c' = 40 N/mm^2 and f_y = 500 N/mm^2) would not fall below 85% due to reinforcement corrosion during a corrosion period of 50 years.

Solution:

T = 50 years = 18250 days

I_{corr} = ?

D = 12 mm

R = 85%

$$A_s = 4 \times \frac{\pi}{4}(12)^2 = 452.4 \text{ mm}^2$$

$$M_{th,uc} = f_y A_s \left[d - \frac{a}{2} \right] = f_y A_s \left[d - \frac{0.5 f_y A_s}{0.85 b f'_c} \right]$$

$$= 500 \times 452.4 \left[250 - \frac{0.5 \times 500 \times 452.4}{0.85 \times 200 \times 40} \right]$$

$$= 52.78 \times 10^6 \text{ N-mm} = 52.78 \text{ kN-m}$$

$R = (M_{res}/M_{th,uc})100 = 85$ (given)

$\Rightarrow M_{res} = 0.85 \times M_{th,uc} = 0.85 \times 52.78 = 44.86$ kN-m

From Eq. (4.7), $P_r = 0.03185\ I_{cor}$ (mm/d), where I_{corr} is in mA/cm^2

$\alpha = 2\ P_r T/D = 2 \times 0.03185$ Icor $\times$ 18250/12 $= 96.877\ I_{cor}$

$\Rightarrow I_{corr} = 0.0103\alpha$ (i)

From Eq. (5.3), correction factor C_f is calculated as:

$$C_f = \frac{14.7}{12(0.0103\alpha \times 18250)^{0.15}} = \frac{0.5585}{\alpha^{0.15}}$$

From Eq. (5.1)

$$M_{th,c} = \frac{M_{res}}{C_f} = \frac{44.86}{\frac{0.5585}{\alpha^{0.15}}} = 80.32\alpha^{0.15} \qquad \text{(ii)}$$

From Eq. (4.9)

$$A_s' = A_s\,(1-\alpha)^2 = 452.4\,(1-\alpha)^2 \text{ mm}^2$$

$$M_{th,c} = f_y A_s' \left[d - \frac{a'}{2} \right] = f_y A_s' \left[d - \frac{0.5 f_y A_s'}{0.85 b f_c'} \right]$$

$$= 500 \times 452.4(1-\alpha)^2 \left[250 - \frac{0.5 \times 500 \times 452.4(1-\alpha)^2}{0.85 \times 200 \times 40} \right] \qquad \text{(iii)}$$

$$= 56.55 \times 10^6 (1-\alpha)^2 - 3.76 \times 10^6 (1-\alpha)^4$$

Equating Eqs. (ii) and (iii):

$$80.32\alpha^{0.15} = 56.55 \times 10^6 (1-\alpha)^2 - 3.76 \times 10^6 (1-\alpha)^4$$

Solving the above equation by trial and error, the value of α is calculated as:

$$\alpha = 0.0382$$

Substituting the value of α in Eq. (i), the value of I_{cor} is calculated as:

$$I_{corr} = 0.0103 \times 0.0382 = 3.93 \times 10^{-4} \text{ mA/cm}^2 \ (0.393\ \mu\text{A/cm}^2)$$

5.3 A VERIFICATION OF THE ACCURACY OF PROPOSED METHOD WITH THE AVAILABLE DATA

To verify the accuracy of the proposed model, the results are compared with the data reported by other researchers. The test data reported by Rodriguez et al., [12], Tachibana et al., [13] and Mangat and Elgarf [11], are used for the comparison, as their data provide information on I_{corr}, T, D, the cross-section of the beam and material properties.

Rodriguez et al. [12], carried out experiments on beams of dimensions 2300 × 200 × 150 mm. Compressive strength varied from 34 MPa to 37 MPa, and the yield strength of the reinforcement varied from 575 MPa to 585 MPa, depending on the beam type. A constant current density of about, 100 $\mu A/cm^2$ was applied to the rebars for a period of time ranging between 100 and 200 days approximately. The details of the comparison are shown in Table 5.2.

A curve is plotted between the experimental moment as given by Rodriguez et al. [12], and the moment predicted by the proposed model in Fig 5.2.

From Fig. 5.2, it is clear that the proposed model predicts well the experimental results reported by Rodriguez et al. [12].

Table 5.2: Comparison of the Proposed Model results with those reported by Rodriguez et al. [12].

I_{corr} (mA/cm^2)	T (days)	Tension Steel	f_c' (MPa)	f_y (MPa)	$M_{ex-Rodriguez}$ (KN-mm)	$M_{pred.}$ using proposed model (KN-mm)	% Error
0.1	101	2-10ø	34	575	11600	13220	13.96
0.1	117	2-10ø	34	575	10500	12660	20.57
0.1	160	2-10ø	34	575	10100	11420	13.07
0.1	190	2-10ø	34	575	8600	10683	24.22
0.1	104	4-12ø	35	585	29000	29229	0.79
0.1	115	4-12ø	35	585	27200	28497	4.77
0.1	163	4-12ø	35	585	20400	21450	5.15
0.1	175	4-12ø	35	585	22900	21035	-8.14
0.1	108	4-12ø	35	585	28200	28952	2.67
0.1	127	4-12ø	35	585	26400	27773	5.20
0.1	154	4-12ø	35	585	19400	26306	-35.59
0.1	181	4-12ø	35	585	20900	25009	19.66
0.1	111	4-12ø	37	585	28200	29048	3.01
0.1	128	4-12ø	37	585	28500	27991	-1.78
0.1	164	4-12ø	37	585	27500	26035	-5.33
0.1	190	4-12ø	37	585	20200	25376	25.62

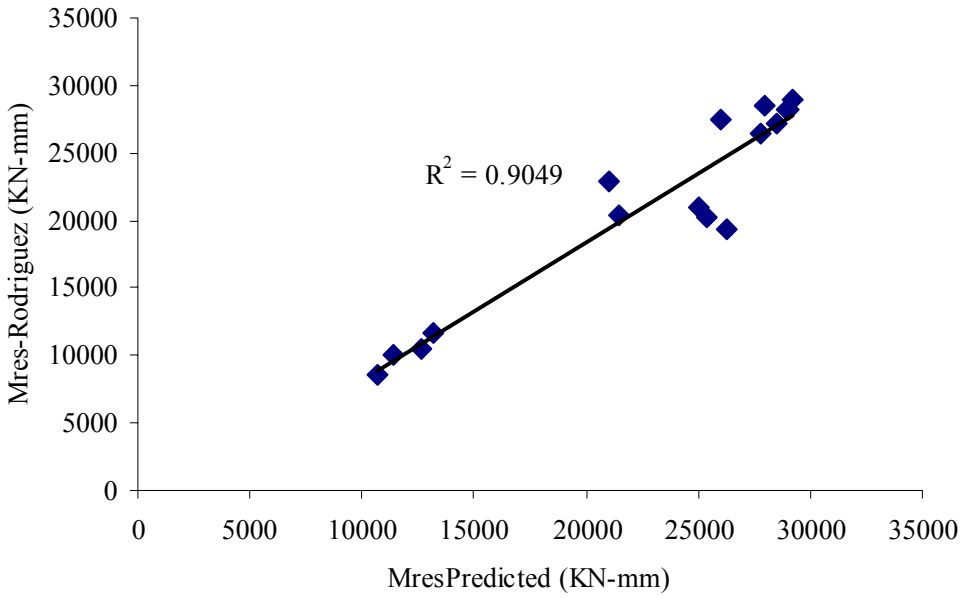

Figure 5.2: Relationship between M_{res}Actual-Rodriguez [12] and Predicted M_{res} using the proposed model.

Tachibana et al. [13] in their study on the mechanical behavior of RC beams damaged by corrosion of reinforcement, used beam specimens of cross-section 150 × 200 mm. The concrete strength was 35.6 MPa and the reinforcement was two 16 mm diameter bars of yield strength 353 MPa. A current density of, 0.5 mA/cm^2 was applied for 3, 6, 10, and 15 days. The results reported by Tachibana et al. [13] are compared with those calculated by the proposed model. The details of the comparison are shown in Table 5.3.

Table 5.3 : Comparison of Proposed Model results with those of Tachibana et al. [13].

I_{corr} (mA/cm^2)	T (days)	Tension Steel	f_c' (MPa)	f_y (MPa)	$M_{ex-Tachibana}$ (KN-mm)	$M_{pred.}$ using proposed model (KN-mm)	% Error
0.5	3	2-16ø	35.6	353	21128	18740	11.30
0.5	6	2-16ø	35.6	353	19035	16709	12.21
0.5	10	2-16ø	35.6	353	18055*	15251	15.53
0.5	15	2-16ø	35.6	353	18731*	14087	24.79

* Bond shear type failure.

Disregarding the results of the two sets of beams that failed in bond shear, as the proposed model is based on flexure dominated failure, it can be seen that the model predicted the experimental moment of Tachibana et al. [13], within an error of 12 %.

However, with regard to the test data reported by Mangat and Elgarf [11], the proposed model does not yield satisfactory results. This is presumably due to the fact that the researchers have reported a significant reduction in the flexural strength caused by a relatively small weight loss of metal, contrary to the findings of the present and other past studies [12-13].

In view of the fact that the proposed method is able to predict the residual strength of the corroded beams that have been reported by two researchers with reasonable accuracy, the method appears to have practical appeal.

CHAPTER 6

CONCLUSIONS AND RECOMMENDATIONS

In this experimental study, 48 reinforced concrete beam specimens were subjected to accelerated corrosion using impressed current and then they were tested in a four-point bend test to determine their residual flexural strength. The following variables were used: two levels of applied impressed current density, three levels of corrosion period and two different diameter of tension reinforcement with two different concrete cover thicknesses. Based on test data, a two-step procedure has been proposed to predict the flexure strength of corroded beams.

6.1 CONCLUSIONS

Based on the data developed in this study, the following conclusions are drawn:

1. Measured values of the corrosion current density, I_{corr} are less than the applied current density, I_{app} due to the resistance and the electrolytic properties of concrete surrounding the rebars.

2. The product of corrosion current density and the corrosion period, $I_{corr}T$, defined in this work as the 'Corrosion Activity Index', is the key measure of corrosion damage. The percentage metal loss and the loss of flexural strength increase with increasing $I_{corr}T$.

3. The effect of reinforcement cover on degree of corrosion at a constant value of $I_{corr}T$ is found to be small.

4. The percentage-wise loss of metal is smaller for a large diameter bar compared to that for smaller diameter bar at a constant $I_{corr}T$.

5. At a lower value of $I_{corr}T$, the residual flexural strength of a corroded beam can be predicted with a reasonable accuracy by considering only the reduced cross-sectional area of tension reinforcement A_s' from Eq. (4.9). However, at a higher value of $I_{corr}T$, the increasing adverse effect of bond cannot be ignored in determining the residual flexural capacity.

6. Based on the experimental data, an approach has been proposed to predict the residual flexural strength of a corroded beam for which $I_{corr}T$, rebar diameter D, cross-sectional details and material strengths are known. The proposed two-step approach consists of determination of a correction factor, C_f, that should be applied to correct the theoretical moment capacity of a corroded beam,

calculated on the basis of reduced cross-sectional area, A_s'. This approach appears to produce satisfactory results within the range of $I_{corr}T$ used in this study.

7. A comparison of the residual strengths of corroded beams predicted by the proposed model with those reported by other researchers shows a reasonably good agreement.

8. A corroded beam shows higher deflection than an un-corroded one, due to degradation in the flexural stiffness due to corrosion that increases with increasing $I_{corr}T$. The compliance of a corroded beam determined at the linear part of load-deflection response increases, albeit slowly, with increasing $I_{corr}T$.

6.2 SUGGESTIONS FOR FUTURE STUDY

The following studies are recommended to further strengthen the findings of this study:

1. The predictive model is developed on the basis of test data generated from beams of same size. Tests should be carried out on different beam sizes to verify the accuracy of the proposed method and to observe the size effect.

2. More tests are required to find out the maximum level of $I_{corr}T$ below which bond loss can be ignored and the strength prediction can be made simply by using A_s' from Eq. (4.9).

3. In the present study, corrosion of reinforcement was accelerated by the impressed current, for the specified duration and then tests were carried out on the corroded specimens to monitor its effects on flexural strength. In real structures, the corrosion of reinforcement takes with reinforcements being under stress. Hence, tests should be carried out to observe the simultaneous effect of stress-reinforcement corrosion on the flexural strength.

APPENDIX A

Load - Deflection Curves

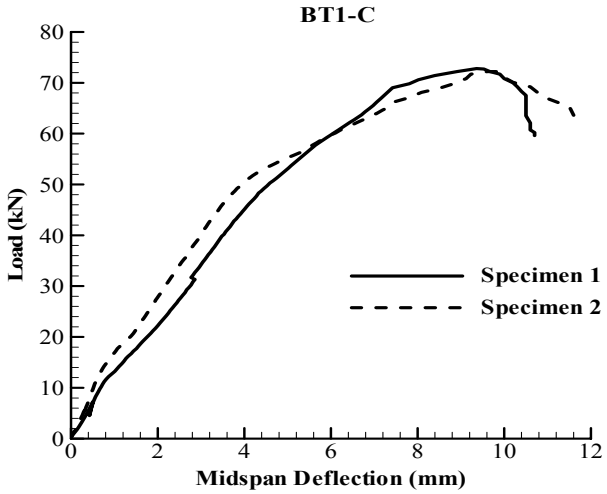

Figure A. 1: Load-midspan deflection plot for two BT1-C specimens

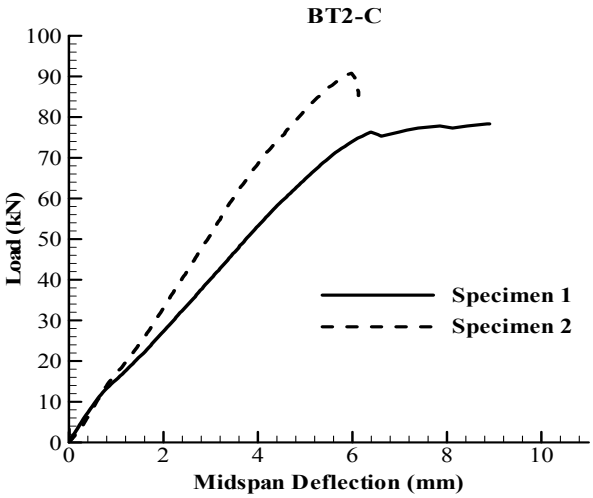

Figure A. 2: Load-midspan deflection plot for two BT2-C specimens

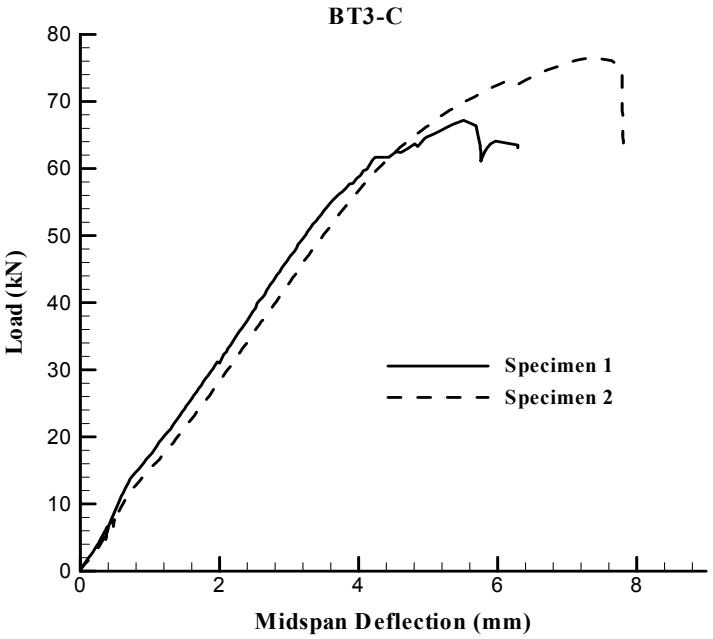

Figure A. 3: Load-midspan deflection plot for two BT3-C specimens

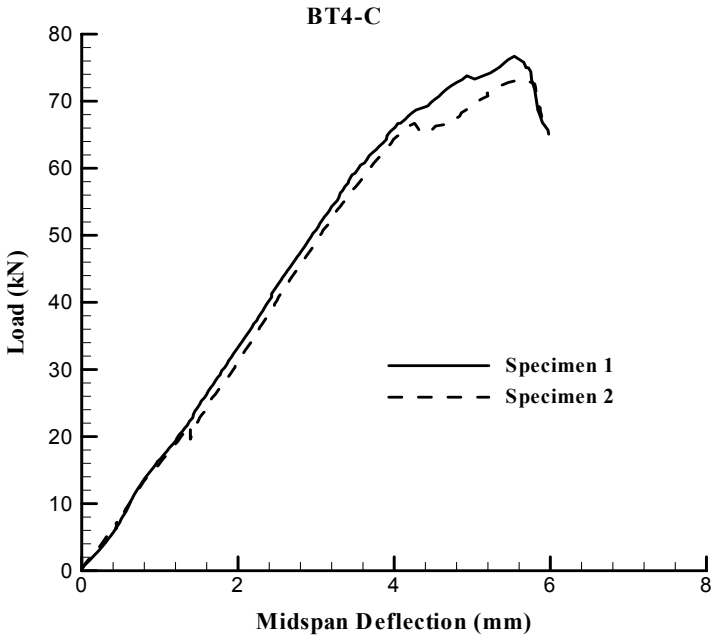

Figure A. 4: Load-midspan deflection plot for two BT4-C specimens

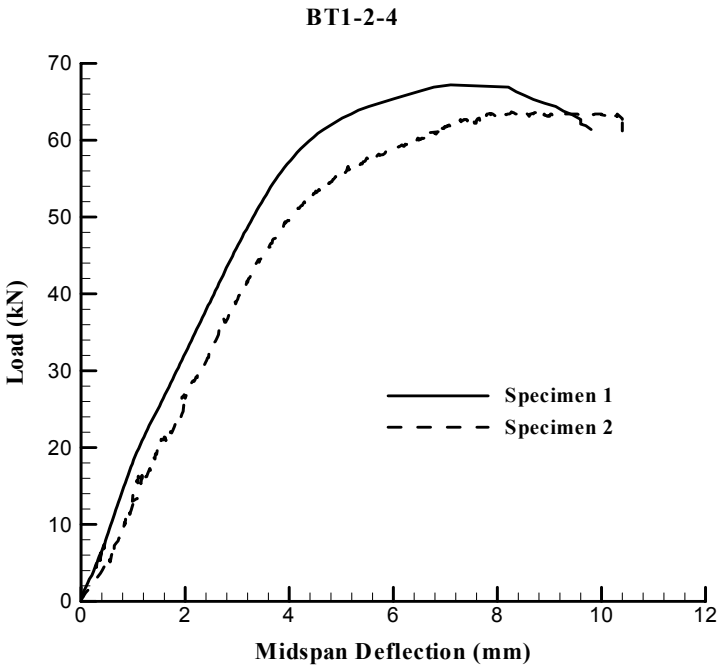

Figure A. 5: Load-midspan deflection plot for two BT1-2-4 specimens

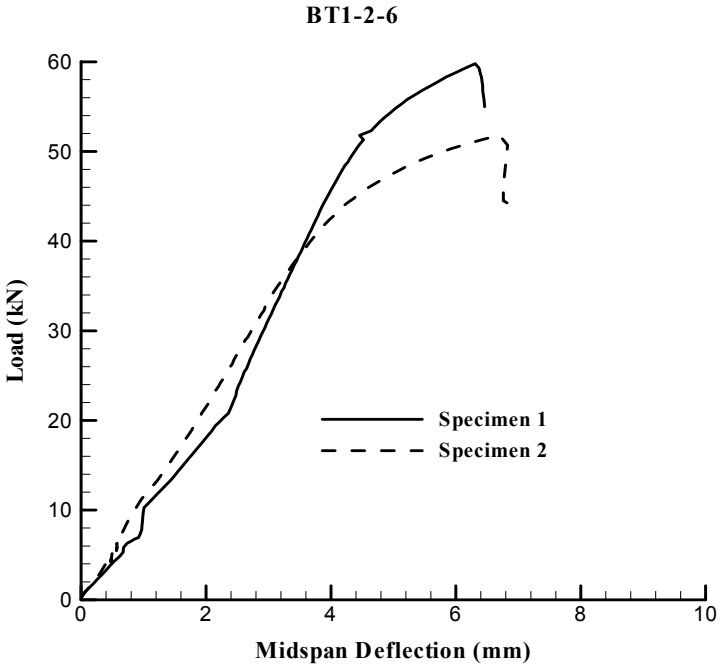

Figure A. 6: Load-midspan deflection plot for two BT1-2-6 specimens

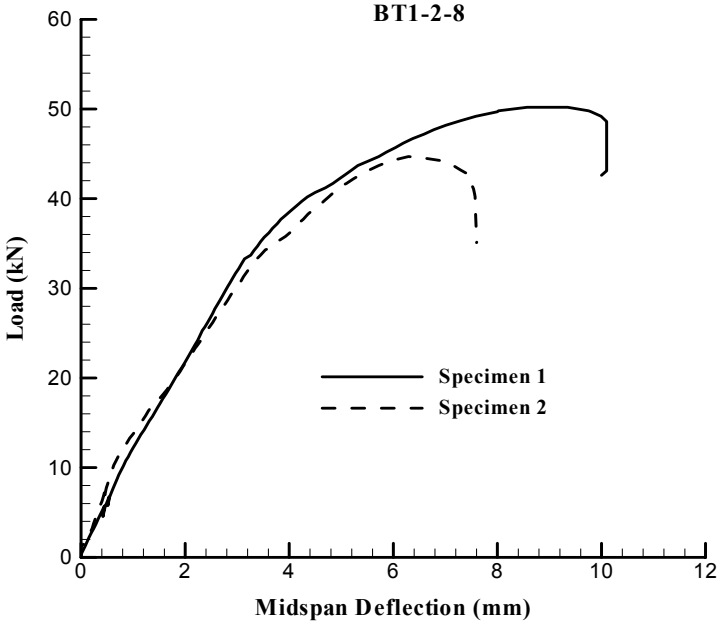

Figure A. 7: Load-midspan deflection plot for two BT1-2-8 specimens

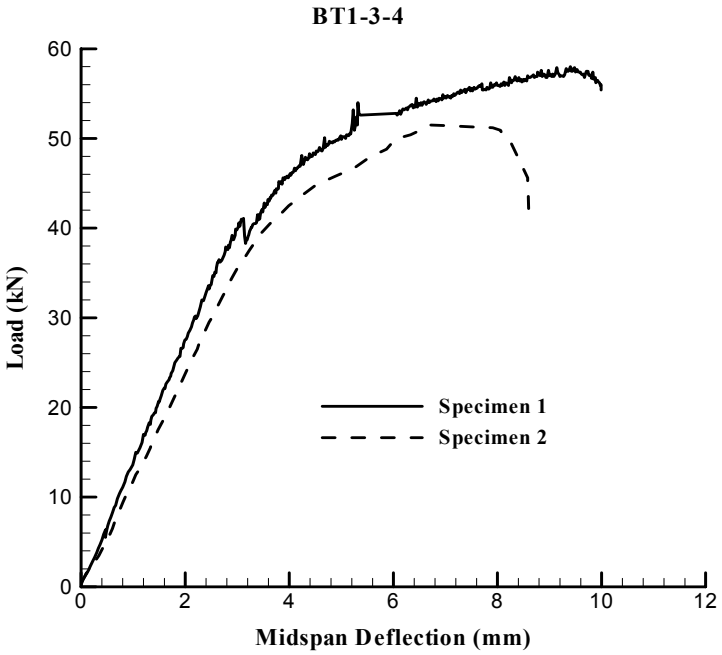

Figure A. 8: Load-midspan deflection plot for two BT1-3-4 specimens

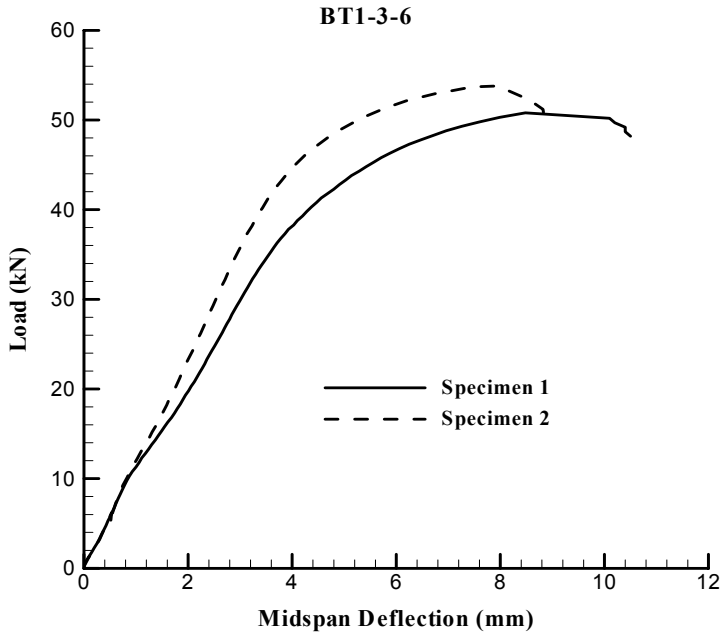

Figure A. 9: Load-midspan deflection plot for two BT1-3-6 specimens

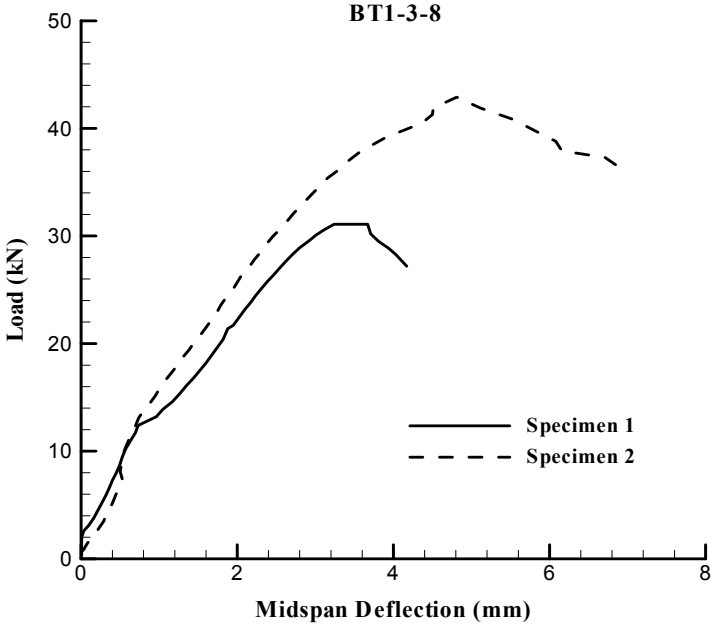

Figure A. 10: Load-midspan deflection plot for two BT1-3-8 specimens

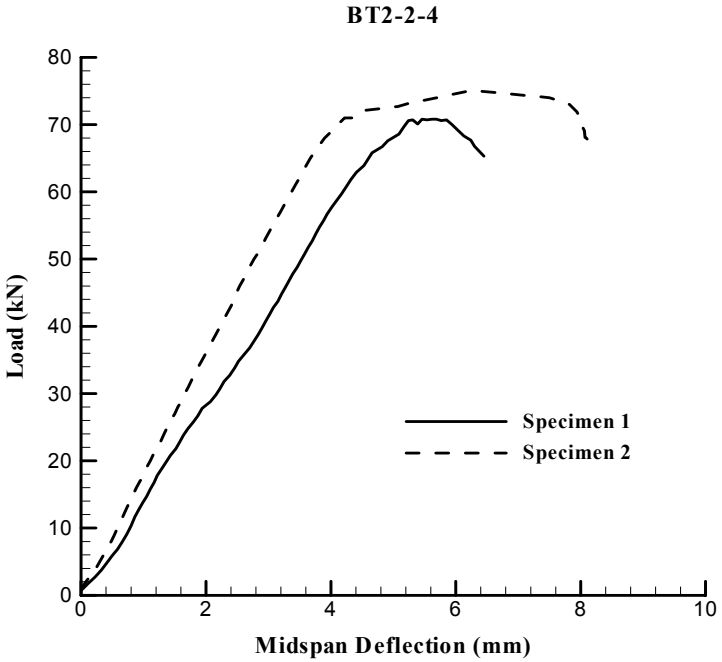

Figure A. 11: Load-midspan deflection plot for two BT2-2-4 specimens

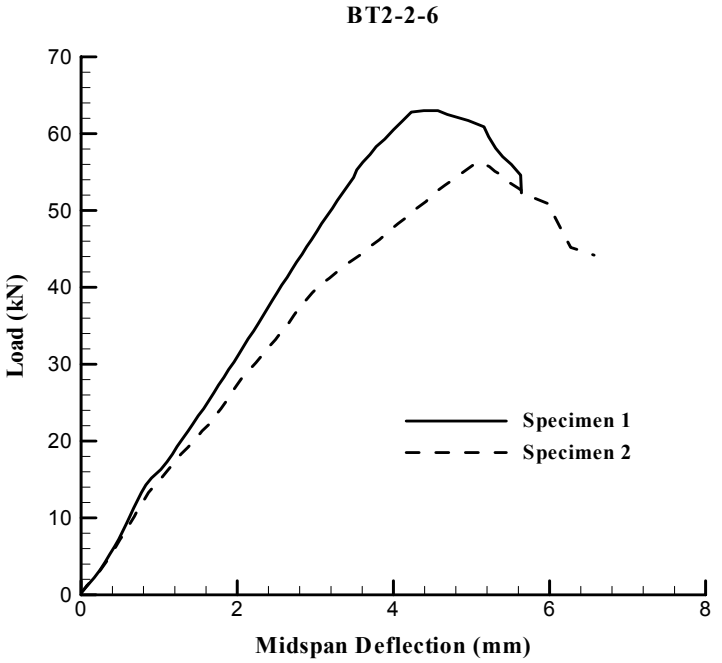

Figure A. 12 : Load-midspan deflection plot for two BT2-2-6 specimens

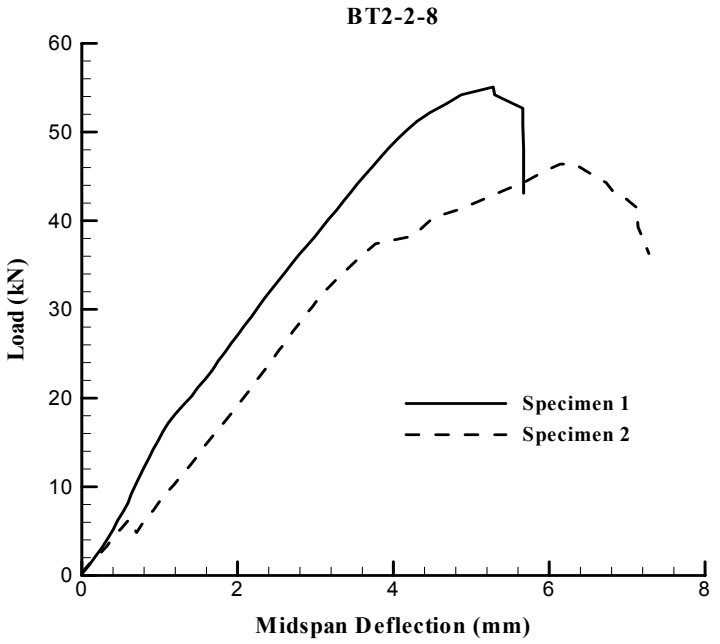

Figure A. 13: Load-midspan deflection plot for two BT2-2-8 specimens

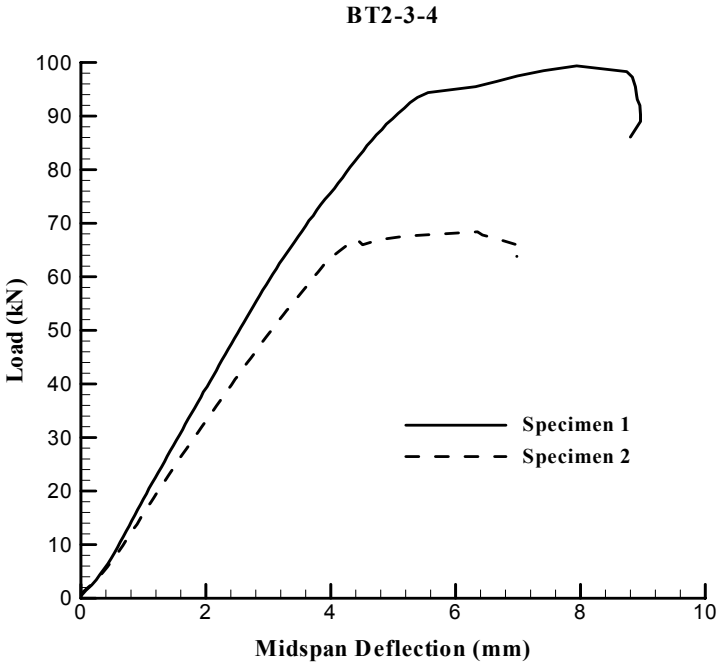

Figure A. 14: Load-midspan deflection plot for two BT2-3-4 specimens

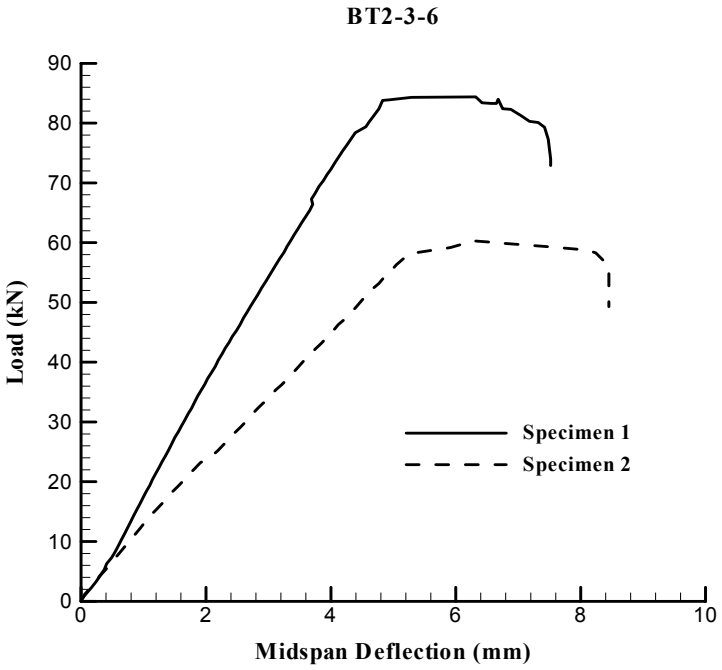

Figure A. 15: Load-midspan deflection plot for two BT2-3-6 specimens

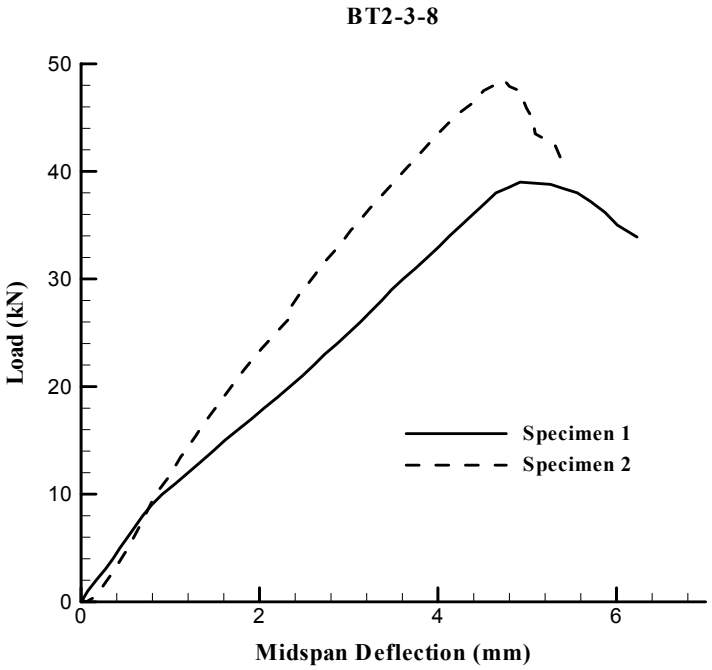

Figure A. 16: Load-midspan deflection plot for two BT2-3-8 specimens

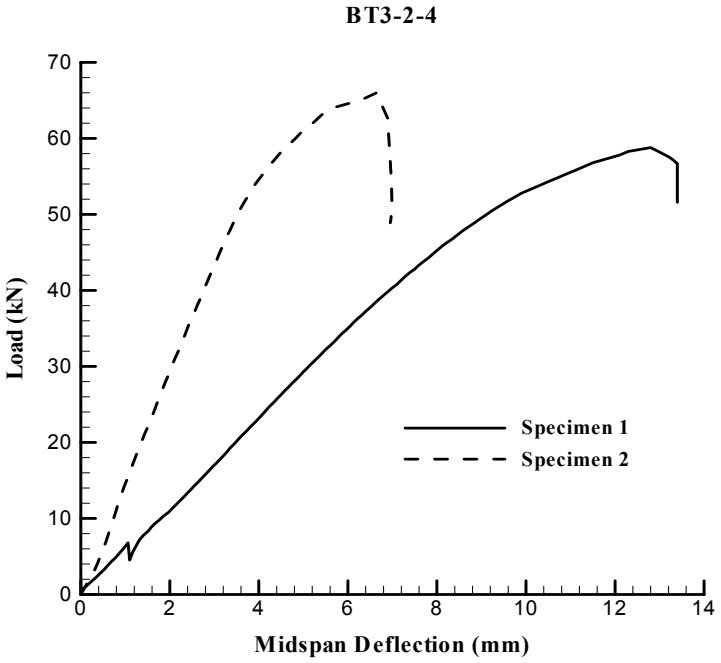

Figure A. 17: Load-midspan deflection plot for two BT3-2-4 specimens

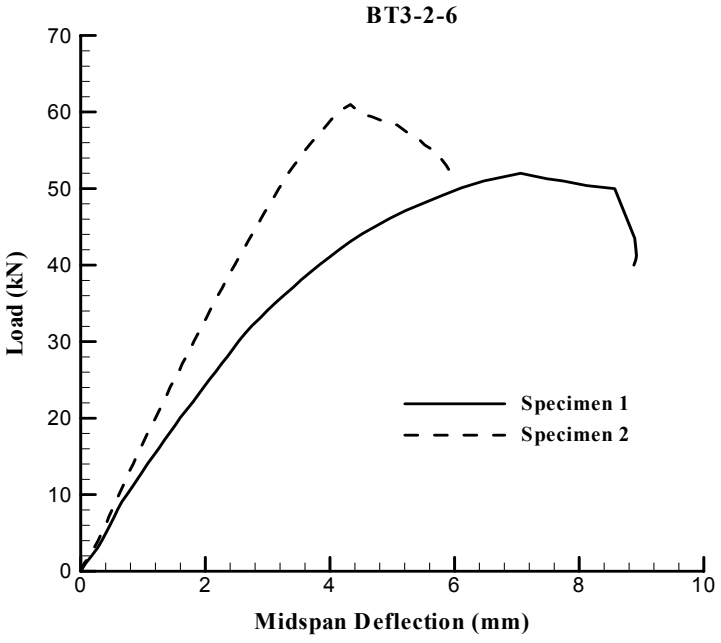

Figure A. 18: Load-midspan deflection plot for two BT3-2-6 specimens

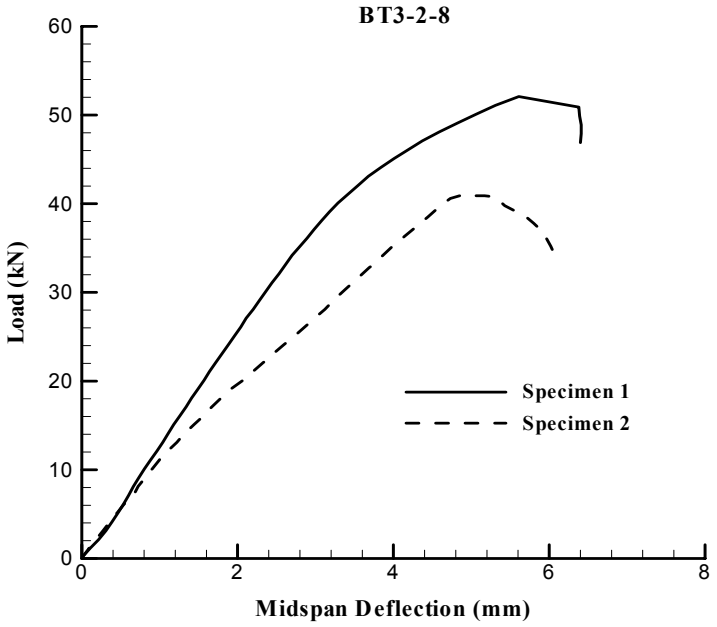

Figure A. 19: Load-midspan deflection plot for two BT3-2-8 specimens

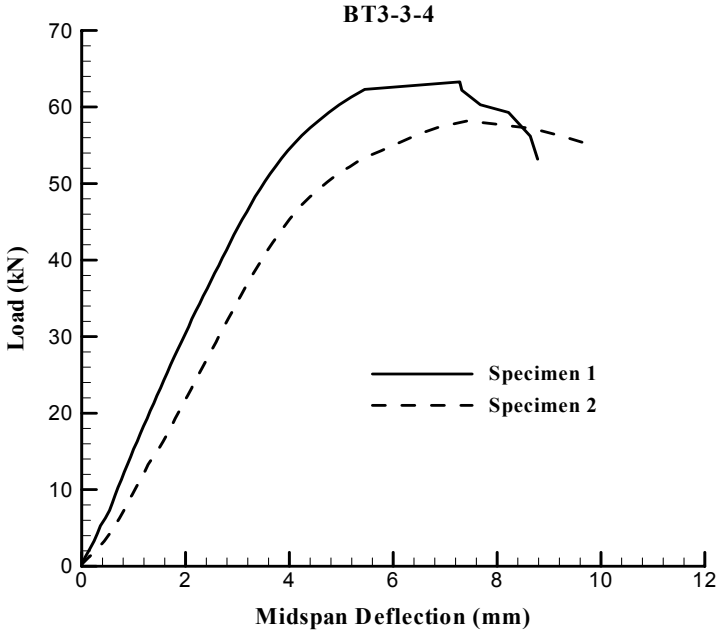

Figure A. 20: Load-midspan deflection plot for two BT3-3-4 specimens

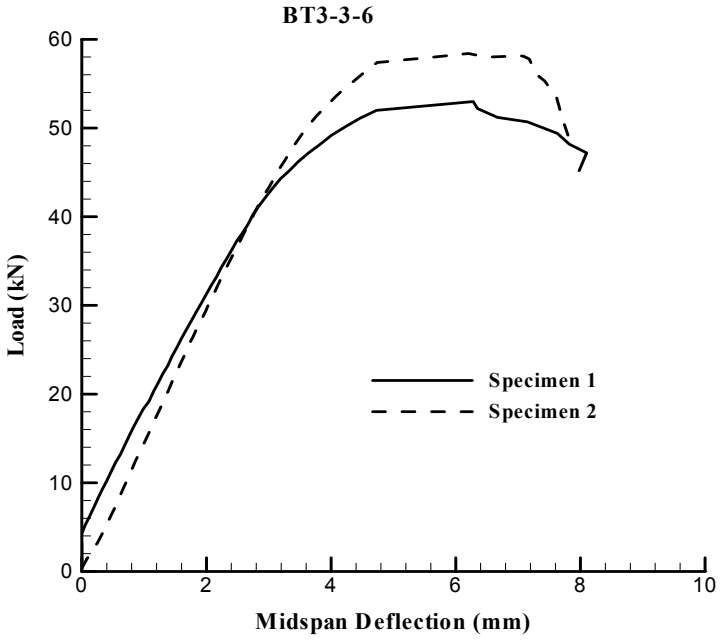

Figure A. 21: Load-midspan deflection plot for two BT3-3-6 specimens

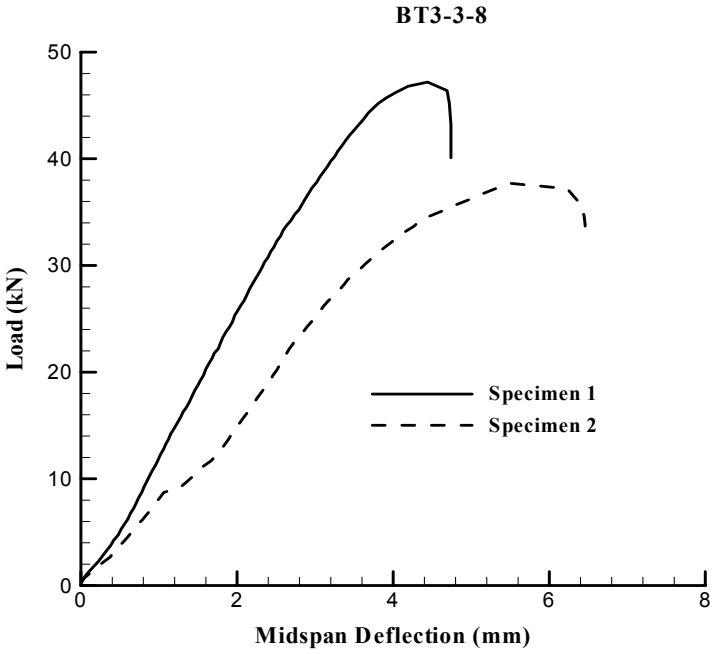

Figure A. 22: Load-midspan deflection plot for two BT3-3-8 specimens

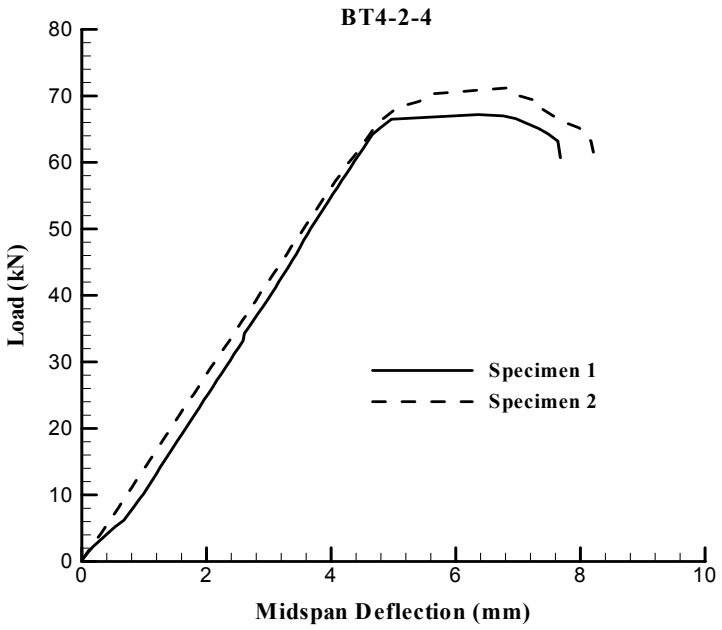

Figure A. 23: Load-midspan deflection plot for two BT4-2-4 specimens

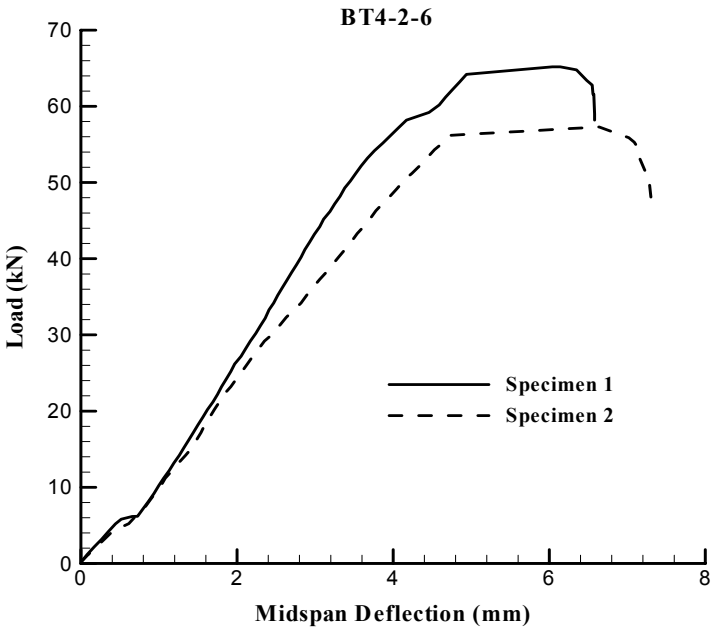

Figure A. 24: Load-midspan deflection plot for two BT4-2-6 specimens

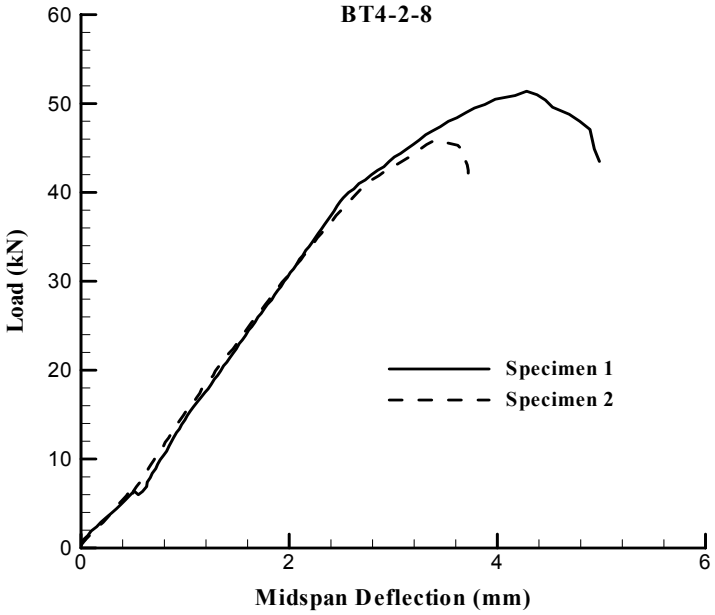

Figure A. 25: Load-midspan deflection plot for two BT4-2-8 specimens

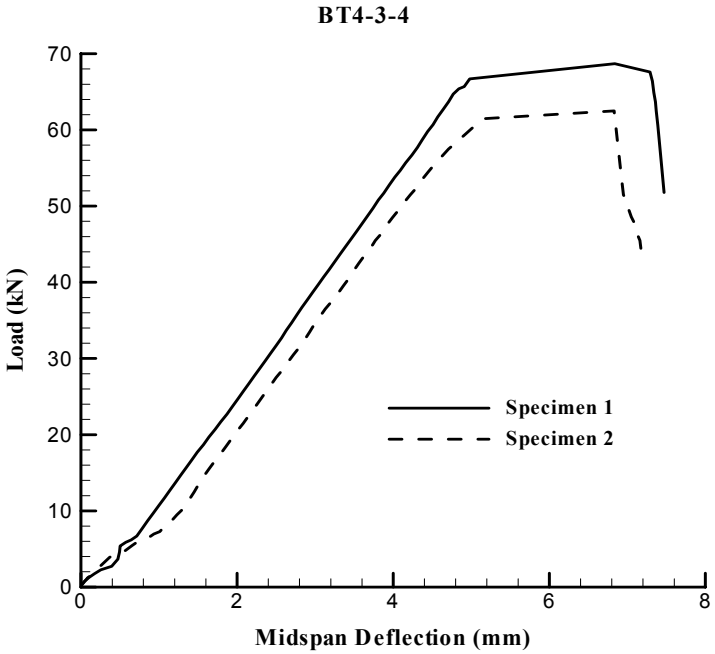

Figure A. 26: Load-midspan deflection plot for two BT4-3-4 specimens

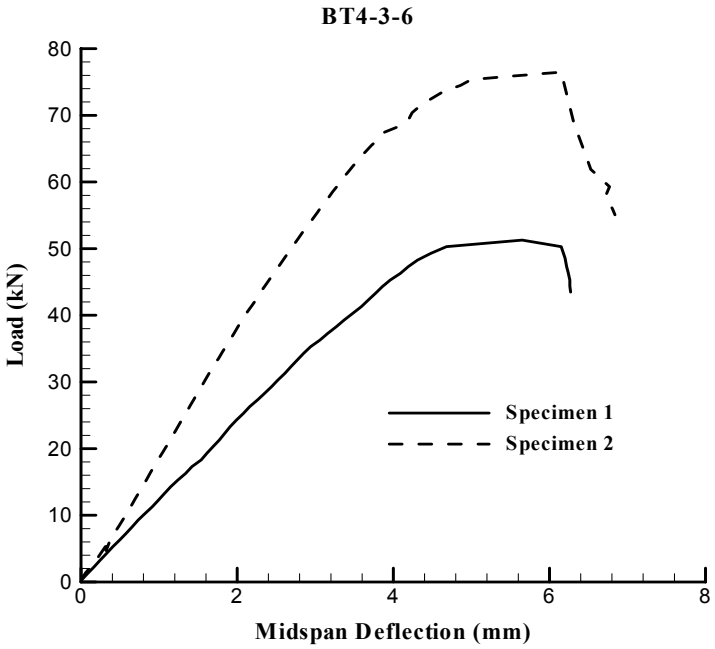

Figure A. 27: Load-midspan deflection plot for two BT4-3-6 specimens

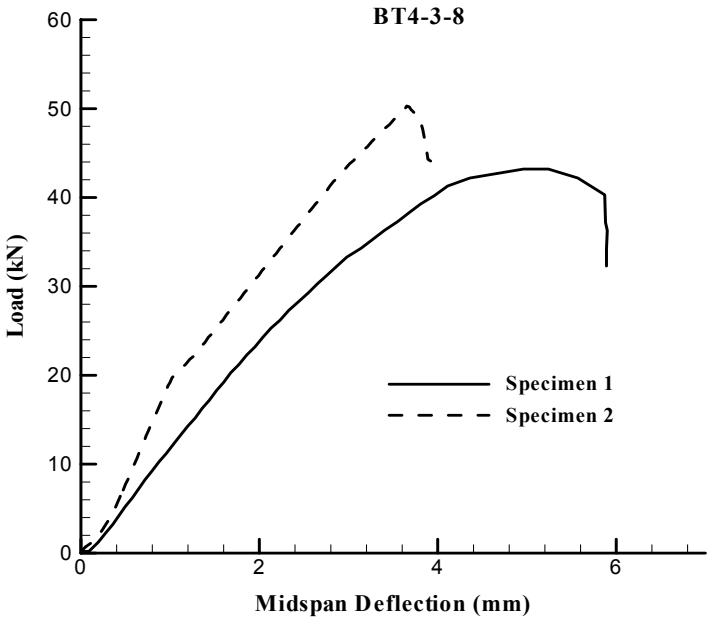

Figure A. 28: Load-midspan deflection plot for two BT4-3-6 specimens

APPENDIX B

Sample Calculations of Theoretical Flexural Strengths of Both Control and Corroded Beams Using Strain Compatibility Analysis

1. CONTROL BEAMS

Case 1: BT1-C

Diameter of tension reinforcement, D = 10 mm

Area of tension reinforcement, $A_s = 2 \times \pi \times \frac{10^2}{4}$ = 157 mm^2

Clear cover to tension reinforcement, C_v = 25 mm

Diameter of hanger bars = 8 mm

Area of the hanger bars, $A_s' = 2 \times \pi \times \frac{8^2}{4}$ = 100.53 mm^2

Compressive strength of the concrete, f'_c = 45.8 MPa

Effective depth, $d = 150 - C_v - \frac{D}{2} = 150 - 25 - \frac{10}{2}$ = 120 mm

Width of the beam, b = 150 mm

CG of hanger bar from top, h = 41 mm

Strain Compatibility and Equilibrium Analysis

The value of the neutral axis depth, *c* is calculated using trial-and-error approach to satisfy strain-compatibility and equilibrium equation. With c = 25.9 mm, from Fig. B.1, $\frac{0.003}{c} = \frac{\varepsilon_{s'}}{(h-c)}$

Hence, strain in the compression steel, $\varepsilon_s' = 0.003 \times \left[\frac{(h-c)}{c}\right] = 0.00175$

The corresponding stress, $f_s' = 0.00175 \times 2 \times 10^5 = 349.81$ MPa (which is less than the yield stress of 8 mm bar, 500 MPa)

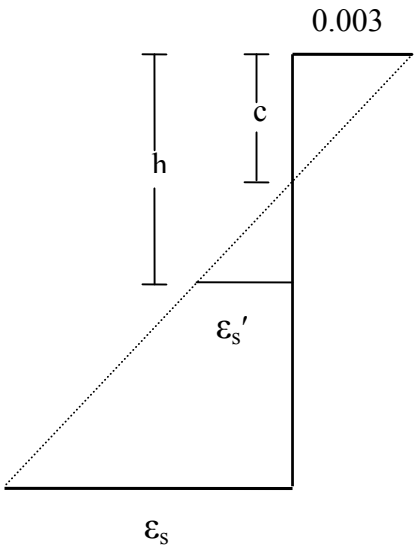

Figure B.1

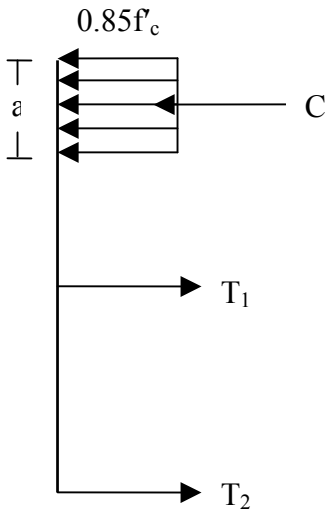

Figure B.2

Also from Fig. B.1, $\frac{0.003}{c} = \frac{\varepsilon_s}{(d-c)}$

Hence, strain in the tension steel, $\varepsilon_s = 0.003 \times \left[\frac{(d-c)}{c}\right] = 0.0109$

The corresponding stress, f_s from the stress strain plot is 546 MPa.

From Fig. B.2,

$T_1 = A_s' f_s' = 100.53 \times 349.81 = 35185.5$N

$T_2 = A_s f_s = 157 \times 546 = 85722$ N

$a = \frac{(T_1 + T_2)}{0.85 f_c' b} = 20.719$ mm

$c = \frac{a}{0.8} = 1.25 \times a = 25.9$ (same as the assumed value of 25.9 mm)

Now, the theoretical flexural strength of control beam,

$M_{th\text{-}uc} = T_1 (h\text{-}a/2) + T_2 (d\text{-}a/2)$

$= 35185.5 (41\text{-}20.719/2) + 85722 (120\text{-}20.719/2)$

$= 10476704.25$ N mm = 10.48 KN-m

Case 2: BT2-C

Diameter of tension reinforcement, $D = 12$ mm

Area of tension reinforcement, $A_s = 2 \times \pi \times 144/4 = 226.1$ mm^2

Clear cover to tension reinforcement, $C_v = 25$ mm

Diameter of hanger bars = 8 mm

Area of the hanger bars, $A_s' = 2 \times \pi \times 64/ 4 = 100.53$ mm^2

Compressive strength of the concrete, $f'_c = 36.3$ MPa

Effective depth, $d = 150 - C_v - D/2$

$= 150 - 25 - 12/2 = 119$ mm

Width of the beam, $b = 150$ mm

CG of hanger bar from top, $h = 41$ mm

Strain Compatibility and Equilibrium Analysis

The value of the neutral axis depth, c is calculated using trial-and-error approach to satisfy strain-compatibility and equilibrium equation. With $c = 37.54$ mm from Fig. B.1, $\frac{0.003}{c} = \frac{\varepsilon_{s'}}{(h-c)}$

Hence, strain in the compression steel, $\varepsilon_s' = 0.003 \times \left[\frac{(h-c)}{c}\right] = 0.000276$

The corresponding stress, $f_s' = 0.000276 \times 2 \times 10^5 = 55.30$ MPa (which is less than the yield stress of 8 mm bar, 500 MPa)

Also from Fig. B.1, $\frac{0.003}{c} = \frac{\varepsilon_s}{(d-c)}$

Hence, strain in the tension steel, $\varepsilon_s = 0.003 \times \left[\frac{(d-c)}{c}\right] = 0.00651$ (which is greater than the yielding strain 0.003, hence considering the yielding strain)

The corresponding stress at yield, f_y from the stress strain plot is 590 MPa.

From Fig. B.2,

$T_1 = A_s' f_s' = 100.53 \times 55.30 = 5559.31$ N

$T_2 = A_s f_s = 226.1 \times 590 = 133399$ N

$$a = \frac{(T_1 + T_2)}{0.85 f_c' b} = 30.04 \text{ mm}$$

$$c = \frac{a}{0.8} = 1.25 \times a = 37.55$$ (which is almost the same as the assumed value of 37.54 mm)

Now, the theoretical flexural strength of control beam,

$M_{th\text{-}uc} = T_1 (h\text{-}a/2) + T_2 (d\text{-}a/2)$

$= 5559.31 (41\text{-}30.04/2) + 133399 (119\text{-}30.04/2)$

$= 14015259$ N mm = 14.02 KN m

2. CORRODED BEAMS

Case 1: BT1-3-6

The reduced cross sectional area of the corroded bar A_s' is calculated using Eq. (4.9) as, $A_s' = A_s (1\text{-}\alpha)^2$

where A_s is the original cross-sectional area of the bar and $\alpha = 2P_r T/D$

From Eq (4.7) the penetration rate, due to corrosion, $P_r = 25/7.85 = 3.185$ cm/year

Corrosion period = 6 days = 0.01644 years and

Diameter of the rebar, D=10 mm = 1 cm

$\alpha = 2 \times 3.185 \times 0.01644 / 1 = 0.105$

Hence the reduced cross sectional area, $A_s' = (2 \times \pi \times 100/ 4)(1\text{-}0.105)^2 = 125.8$ mm^2

Clear cover to tension reinforcement, C_v = 25 mm

Diameter of hanger bars = 8 mm

Area of the hanger bars $A_s'' = 2 \times \pi \times 64/ 4 = 100.53$ mm^2

Compressive strength of the concrete, f'_c = 46.5 MPa

Effective depth, $d = 150 - C_v - D/2 \quad = 150 - 25 - 10/2 = 120$ mm

Width of the beam, b = 150 mm

CG of hanger bar from top, h = 41 mm

Strain Compatibility and Equilibrium Analysis

The value of the neutral axis depth, c is calculated using trial-and-error approach to satisfy strain-compatibility and equilibrium equation. With c = 23.78 mm, from Fig. B.1, $\frac{0.003}{c} = \frac{\varepsilon_{s'}}{(h-c)}$

Hence, strain in the compression steel, $\varepsilon_s' = 0.003 \times \left[\frac{(h-c)}{c}\right] = 0.002172$

The corresponding stress, $f_s' = 0.002172 \times 2 \times 10^5 = 434.4$ MPa (which is less than the yield stress of 8 mm bar, 500 MPa)

Also from Fig. B.1, $\frac{0.003}{c} = \frac{\varepsilon_s}{(d-c)}$

Hence, strain in the tension steel, $\varepsilon_s = 0.003 \times \left[\frac{(d-c)}{c}\right] = 0.01214$

The corresponding stress, f_s from the stress strain plot is 548.6 MPa.

From Fig. B.2,

$T_1 = A_s'' f_s' = 100.53 \times 434.4 = 43670.23$ N

$T_2 = A_s' f_s = 125.8 \times 548.6 = 69014$ N

$a = \frac{(T_1 + T_2)}{0.85 f_c' b} = 19.027$ mm

$c = \frac{a}{0.8} = 1.25 \times a = 23.78$ mm (which is the same as the assumed value of 23.78 mm)

Now, the theoretical flexural strength of corroded beam,

$M_{th\text{-}c} = T_1 (h\text{-}a/2) + T_2 (d\text{-}a/2)$

$= 43670.23 (41\text{-}19.027/2) + 69014 (120\text{-}19.027/2)$

$= 9000138$ N mm $= 9.00$ kN m

LIST OF NOTATIONS

A_s = cross-sectional area area of uncorroded reinforcement

A'_s = cross-sectional area of corroded reinforcement

b = width of beam

C_f = correction factor ($M_{ex,c}/M_{th,c}$)

C_c = $M_{ex,uc}/M_{th,uc}$

C_v = concrete cover thickness

D' = diameter of corroded rebar

D = diameter of uncorroded rebar

d = effective depth of beam

F = Faraday's constant (96487 A-sec)

f'_c = 28-day compressive strength of concrete

f_y = yield strength of reinforcing bar

I_{app} = applied corrosion current density

I_{corr} = actual corrosion current density

$I_{corr}T$ = corrosion activity index

J_r = corrosion rate, i.e. loss of metal per unit surface area per unit time

$M_{ex,\,c}$ = experimental ultimate moment capacity of *corroded* beams

$M_{ex,uc}$ = experimental ultimate moment capacity of *uncorroded* beams

$M_{th,c}$ = theoretical ultimate moment capacity of *corroded* beams

$M_{th,uc}$ = theoretical ultimate moment capacity of *uncorroded* beams

P_r = penetration rate, i.e. reduction in the rebar diameter per unit time

R = percentage residual strength of a corroded beam

T = corrosion duration

W = equivalent weight of steel (27.9 g)

α = metal loss factor = $2P_rT/D$

γ_{st} = density of steel (7.85 g/cm^3)

ρ = percentage weight loss, i.e. degree of corrosion induced through accelerated test

REFERENCES

[1] "As Solid as Concrete," *Middle East Construction*, April/May 1987, pp. 20-21.

[2] Schutt, W. R., "Cathodic Protection of New High- Rise Buildings in Abu-Dhabi," *Concrete International*, May 1992, pp. 45-46.

[3] Page, C. L., and Treadway, K. W. J., "*Aspects of Electrochemistry of steel in concrete- Nature*," Vol. 297, 1982, pp. 109-115.

[4] Concrete Repair Manual, "ACI International, BRE, Concrete society, and International Concrete Repair Institute (ICRI)"; Second edition, Vol. 1, May 2003.

[5] Cabrera, J. G., "Deterioration of Concrete Due to Reinforcement Steel Corrosion," *Cement & Concrete Composites*, 18 (1996), pp. 47-59.

[6] Kimberly, E. K., and Mehta, P. K., "A Critical Review of Deterioration of Concrete Due to Corrosion of Reinforcing Steel", *Proceedings, Fourth CANMET/ACI International conference on Durability of Concrete*, Sydney, Australia, 1997, pp. 535-554.

[7] Morinaga, S., "Prediction of service lives of reinforced concrete buildings based on the corrosion rate of reinforcing steel", *Proceedings, Building Materials and Components*, Brighton, UK, 7-9 November 1990, pp. 5-16.

[8] Dagher, H. J., and Kulendran, S., "Finite element model of corrosion damage in concrete structures," *ACI Structural Journal*, Vol. 89, No. 6, 1992, pp. 699-708.

[9] Bazant, Z. P., "Physical model for steel corrosion in concrete sea structures-application," *ASCE Journal of Structural Division*, Vol. 105, 1979, pp. 1155-1166.

[10] Wang, X. M., and Zhao, H. Y., "*The residual service life prediction of R.C. structures*," Durability of Building Materials and Components 6, Edited by Nagataki S, et al., E & FN Spon, 1993, pp. 1107-1114.

[11] Mangat, P.S., and Elgarf, M.S., "Flexural strength of concrete beams with corroding reinforcement," *ACI Structural Journal*, Vol. 96, No. 1, January-February 1999, pp. 149-158.

[12] Rodriguez, J., Ortega, L.M., and Casal, J., "Load carrying capacity of concrete structures with corroded reinforcement," *Construction and Building Materials*, Vol. 11, No. 4, 1997, pp. 239-248.

[13] Tachibana, Y., Maeda, K. I., Kajikawa, Y., and Kawamura, M., "Mechanical behaviour of RC beams damaged by corrosion of reinforcement", *Third International Symposium on Corrosion of reinforcement in Concrete Construction*, Wishaw, UK, 1990, pp. 178-187.

[14] Townsend, H. E., Cleary, H. J., and Allegra, L., "Breakdown of Oxide films in steel exposure to chloride solutions," *Corrosion- NACE*, Vol 37, 1981, pp. 384-391.

[15] Verbeck, G. J., (1975). "Mechanism of corrosion in concrete," *Corrosion of metals in concrete*, ACI SP –49.

[16] Mehta, P. K., (1993). "*Concrete Structures, Properties and Materials*," Prentice-Hall Inc.

[17] Li, C. Q., "Initiation of Chloride-Induced Reinforcement Corrosion in Concrete Structural Members-Prediction", *ACI Structural Journal*, Vol. 99, No.2, March-April 2002, pp. 133-141.

[18] Li, C. Q., "Initiation of Chloride-Induced Reinforcement Corrosion in Concrete Structural Members-Experimentation", *ACI Structural Journal*, Vol 98 (4), July-August 2001, pp. 502-510.

[19] Tuutti, K., "Corrosion of Steel in Concrete", 1st edition. *Swedish Cement and Concrete Research Institute*, Stockholm, Sweden, 1982.

[20] Amleh, L., and Mirza, S., "Corrosion influence on bond between steel and concrete," *ACI Structural Journal*, Vol. 96, No.3, May-June 1999, pp. 415-423.

[21] Fu, X., and Chung, D. D. L., "Effect of corrosion on the bond between concrete and steel rebar," *Cement and Concrete Research*, Vol. 27, No. 12, 1997, pp. 1811-1815.

[22] Auyeung, Y., Balaguru, P., and Chung, L., "Bond behavior of corroded reinforcement bars," *ACI Materials Journal*, Vol. 97, No. 2, March-April, 2000, pp. 214-220.

[23] Al-Sulaimani, G. J., Kaleemullah, M., Basunbul, I. A., and Rasheeduzzafar., "Influence of corrosion and cracking on bond behaviour and strength of reinforced concrete members," *ACI Structural Journal*, Vol. 87, No.2, March-April 1990, pp. 220-231.

[24] Cabrera, J. G., and Ghoddoussi, P., "The effect of reinforcement corrosion on the strength of the steel/concrete interface", *Proceedings, International Conference on Bond in Concrete*, Riga, Latvia, October 15-17, 1992, pp. 10/11 to 10/24.

[25] Almusallam, A. A., Al-Gahtani, A. S., Aziz, A.R., and Rasheeduzzafar., "Effect of reinforcement corrosion on bond strength," *Construction and Building Materials*, Vol. 10, No.2, 1996, pp. 123-129.

[26] Ravindrarajah, R., and Ong, K., "Corrosion of Steel in Concrete in Relation to Bar Diameter and Cover Thickness", *ACI Special Publication*, Volume 100/4, April 1987, pp. 1667-1678.

[27] Rasheeduzzafar., and Dakhil, F. H., "Field studies on the durability of concrete construction in a high chloride-sulphate environment", *International Journal of Housing Science*, Vol. 4, 1980, pp. 203-232.

[28] Rasheeduzzafar., Dakhil, F. H., and Al-Gahtani, A. S., "Corrosion of reinforcement in concrete structures in the middle east", *Concrete International; American Concrete Institute*, Vol.7, No.9, Sept.1985, pp. 48-55.

[29] Rasheeduzzafar., Dakhil, F. H., and Bader, M. A., "Toward solving the concrete deterioration problem in the Arabian Gulf region", *The Arabian Journal for science and Engineering*, Vol. 11, No.2, 1986, pp. 129-146.

[30] Tarek Uddin, M., Nobuaki, O., Makota, H., and Tsunenori, S., "Effect of crack width and bar types on corrosion of steel in concrete", *Journal of Materials in Civil Engineering*, Vol. 13, No. 3, May/June, 2001, pp. 194-201.

[31] Ting, S.C., and Nowak, A. S., "Effect of Reinforcing Steel Area Loss on Flexural Behavior of Reinforced Concrete Beams," *ACI Structural Journal*, May-June 1991, pp. 309-314.

[32] Uomoto, T., and Misra, S., "Behaviour of concrete beams and columns in marine environment when corrosion of reinforcing bars take place," *ACI Special Publication* SP-109-6, 1988, pp. 127-145.

[33] Huang, R., and Yang, C. C., "Condition Assessment of Reinforced Concrete Beams Relative to Reinforcement Corrosion," *Cement and Concrete Composites*, 19 (1997), pp. 131-137.

[34] Yoon, S., Wang, K., Weiss W. J., and Shah, S. P., "Interaction between Loading, Corrosion, and Serviceability of Reinforced Concrete", *ACI Materials Journal*, Vol. 97, No. 6, November-December 2000, pp. 637-644.

[35] Nokhasteh, M. A., Eyre, J. R., and Mcleish, A., "The effect of reinforcement corrosion on the strength of reinforced concrete members",

Structural Integrity Assessment, Elsevier Applied Science, 1992, pp. 314-325.

[36] Hognestad, E., Hanson, N. W., and McHenry, D., "Concrete stress distribution in ultimate strength design", *Proceedings, American Concrete Institute*, Vol. 52, 1955-56, pp. 455-479.

[37] Aziz, A.R., "*Reduction in bond and the strength of slabs due to corrosion of reinforcement"*, M.S.Thesis, King Fahd University of Petroleum and Minerals, June, 1994.

[38] Jin, W.L., and Zhao, Y. X., "Effect of corrosion on bond behavior and bending strength of reinforced concrete beams", *Journal of Zheijang University (SCIENCE)*, Vol. 2, No. 3, July-September 2001, pp. 298-308.

[39] Escalante, E., Ito, S., and Cohen, M., "Measuring the Rate of Corrosion of Steel in Concrete", *Annual Report NBSIR* 80-2012, National Bureau of Standards, Gaithersburg, Md., March 1980, pp. 1-26.

[40] Escalante, E., Whitenton, E., and Qui, F., "Measuring the Rate of Corrosion of Reinforcing Steel in Concrete", *Final Report NBSIR* 86-3456, National Bureau of Standards, Gaithersburg, Md., Oct. 1986, pp. 1-27.

[41] Stern, M., and Geary, A. L., "Electrochemical polarization, theoretical analysis of the shape of polarization curves", *Journal of Electrochemical Society*, Vol. 104, No. 1, 1957, pp. 56-63.

[42] Andrade, C., and Alonso, C., “On-Site Measurements of Corrosion Rate of Reinforcements”, *Construction and Building Materials,* March, 2001, pp. 171-183.

[43] Millard, S. G., “Corrosion rate measurement of in-situ reinforced concrete structures”, *Proceedings, Institution of Civil Engineers, Structures and Buildings*, Vol. 99, Feb. 1993, pp. 84-88.

[44] ASTM G-1, “*Standard Practice for Preparing, Cleaning and Evaluating Corrosion Test Specimens*”. Annual Book of ASTM Standards, Vol. 01.05, American Society for Testing and Materials, Philadelphia, PA.

[45] Uomoto, T., Tsoji, K, and Kakizawa, T., “Deterioration mechanism of concrete structures caused by corrosion of reinforcing bars”, *Transactions of Japan Concrete Institute*, Vol. 6, 1984, pp. 163-170.

[46] Ijsseling, F. P., "Application of electrochemical methods of corrosion rate determination to system involving corrosion product layers," *British Corrosion Journal*, Vol. 21, No. 2, 1986, pp. 95-101.

[47] Yubun, A., Balaguru, P., and Lan, C., “Bond behavior of corroded reinforcement bars”, *ACI Materials Journal*, Vol. 97, No.2, March-April 2000, pp. 214-220.

[48] Ballim, Y., and Reid, J. C., “Reinforcement corrosion and deflection of RC beams- an experimental critique of current test methods”, *Cement and Concrete Composites*, Vol. 25, 2003, pp. 625-632.

[49] Zhang, P. S., Lu, M., and Li, X.Y., "Mechanical property of rustiness in reinforcement steel", *Industrial Construction*, 25, 1995, pp. 41-44.

[50] Xi, W.L., Li, R., Lin, Z. S., et al., "Experimental studies on the property before and after reinforcement corrosions in basic concrete members", *Industrial Construction*, 27, 1997, pp. 14-18.

[51] Almusallam, A. A., "Effect of degree of corrosion on the properties of reinforcing steel bars", *Construction and Building Materials,* Vol. 15, 2001, pp. 361-368.

VITA

NAME: Syed Ayub Azher

ADDRESS: H.No: 5-2-255, Idgah, Hanamkonda,
Warangal – 506001
Andhra Pradesh, INDIA

E-MAIL: azher_sa@yahoo.com

EDUCATIONAL QUALIFICATIONS

Master of Science in Civil Engineering (Structures)

Sept. 2002 – Jan. 2005

King Fahd University of Petroleum and Minerals, Dhahran, Saudi Arabia

GPA – 3.31/4.0

Bachelor of Engineering (Civil)

Aug. 1998 – Feb. 2001

Osmania University, Hyderabad, India

First Class with Distinction

Diploma in Civil Engineering

Jan. 1994 – June 1996

Government Polytechnic, Warangal, India

First Division with Distinction.